Robert L. Elliott, M.D., Ph.D.
Jonathan F. Head, Ph.D.

Mastology Research Institute
of the
Elliott-Hailey-Head Breast Cancer Research
and Treatment Center
17050 Medical Center Drive, 4th Floor
Baton Rouge LA, 70816

Telephone: (225) 755-3070

FAX: (225) 755-3085

National Toll Free: 1-800-762-5313

e-mail: jhead@ehhbreastca.com

Web Site:

breastoncology.com

MASTOLOGY RESEARCH INSTITUTE
INFRARED IMAGING

Elliott, R.L., Head, J.F., and Werneke, D.K.: Thermography in Breast Cancer: Comparison with Patient Survival, TNM Classification and Tissue Ferritin Concentration. Proc. Amer. Soc. Clin. Oncol. 9:99, 1990

Head, J.F., Shah, U., Elliott, M.C., and Elliott, R.L.: Breast Thermography and Cancer Patient Survival. Thermology 3:277, 1991.

Elliott, R. L., and Head, J.F.: Termografia Mamaria (Tecnica Clinica Valiosa o Despreciable). Focus 3:41-42, 1992.

Head, J.F., Wang, F., and Elliott, R.L.: Breast Thermography Is a Noninvasive Prognostic Procedure That Predicts Tumor Growth Rate in Breast Cancer Patients. Ann New York Acad. Sci. 698:153-158, 1993.

Snyder, W., Wang, C., Wang, F., Elliott, R., and Head, J.: Improving the Resolution of Infrared Images of the Breast. Proc. IEEE Eng. Med. Biol. 18:1058-1059, 1996.

Head, J.F., Lipari, C.A., Wang, F., Davidson, J.E., and Elliott, R.L.: Application of Second Generation Infrared Imaging and Computerized Image Analysis to Breast Cancer Risk Assessment. Proc. IEEE Eng. Med. Biol. 18:1019-1021, 1996.

Head, J.F., Wang, F., Lipari, C.A., and Elliott, R.L.: Breast Cancer Risk Assessment with an Advanced Infrared Imaging System. Proc. Amer. Soc. Clin. Oncol. 16:172, 1997.

Head, J.F., and Elliott, R.L.: Correspondence on Thermography: Its Relation to Pathological Characteristics, Vascularity, Proliferation Rate, and Survival of Patients with Invasive Ductal Carcinoma of the Breast. Cancer 79:186-188, 1997.

Head, J.F., Lipari, C.A., Wang, F., and Elliott, R.L.: Cancer Risk Assessment With a Second Generation Infrared Imaging System. S.P.I.E. 3061:300-307, 1997.

Head, J., Lipari, C., Wang, F., and Elliott, R.: Image Analysis of Digitized Infrared Images of the Breasts from a First Generation Infrared Imaging System. Proc. IEEE Eng. Med. Biol. 19:681-684, 1997.

Elliott, R.L., Wang, F., Lipari, C.A., and Head, J.F.: Application of Second Generation Infrared Imaging to Breast Cancer Risk Assessment. Southeastern Surg. Conference 65:16, 1997.

Luther, D.G., Davidson, J.E., and Head, J.F.: Helmet Mounted Infrared Imaging Combat Casualty System. Adv. Tech. Application Combat Casualty Care: CDROM, 1997.

Luther, D., Davidson, J., Cromer, R., and Head, J.: A Head Mounted Infrared Imager for Treating the Wounded on the Battlefield. Proc. IEEE Eng. Med. Biol. 19:722-724, 1997.

Lipari, C, and Head, J.: Advanced Infrared Image Processing for Breast Cancer Risk Assessment. Proc. IEEE Eng. Med. Biol. 19:673-676, 1997.

Head, J.F., Lipari, C.A., and Elliott, R.L.: Computerized Image Analysis of Digitized Infrared Images of the Breasts from a Scanning Infrared Imaging System. S.P.I.E. 3436:290-294, 1998.

Luther, D.G., Head, J.F., Davidson, J.E., Grenn, M., Hargroder, A.G., and Hubble, K.: A Head Mounted Thermal Imaging System for the Medic. Adv. Tech. Application Combat Casualty Care: CDROM, 1998.

Hargroder, A.G., Davidson, J.E., Luther, D.G., and Head,J.F.: Infrared Imaging of Burn Wounds to Determine Burn Depth. S.P.I.E. 3698:103-108, 1999.

Head, J.F., Lipari, C.A., and Elliott, R.L.: Comparison of Mammography and Breast Infrared Imaging: Sensitivity, Specificity, False Negatives, False Positives, Positive Predictive Value and Negative Predictive Value. Proc. IEEE Eng. Med. Biol. 21: CDROM, 1999.

Head, J.F., Wang, F., Lipari, C.A., and Elliott, R.L.: The Important Role of Infrared Imaging in Breast Cancer: New Technology Improves Applications in Risk Assessment, Detection, Diagnosis and Prognosis. IEEE Eng. Med. Biol. 19:52-57, 2000.

Snyder, W.E., Qi, H., Elliott, R.L., Head, J.F., and Wang, C.X.: Increasing the Effective Resolution of Thermal Images: An Algorithm Based on Mean-field Anealing that Also Removes Noise and Preserves Image Edges. IEEE Eng. Med. Biol. 19:63-70, 2000.

Qi, H., Synder, W.E. Head, J.F., and Elliott, R.L.: Detecting Breast Cancer from Infrared Images by Asymmetry Analysis. Proc. IEEE Eng. Med. Biol. 22:CDROM, 2000.

Li, W., and Head, J.: Infrared Imaging in the Detection and Evaluation of Tumor Angiogenesis. Proc. IEEE Eng. Med. Biol. 22:CDROM, 2000.

Qi, H., and Head, J.F.: Asymmetry Analysis Using Automatic Segmentation and Classification for Breast Cancer Detection in Thermograms. Proc. IEEE Eng. Med. Biol. 23:1347(CDROM), 2001.

Head, J.F., Lipari, C.A., and Elliott, R.L.: Determination of Mean Temperatures of Normal Whole Breast and Breast Quadrants by Infrared Imaging and Image Analysis. Proc. IEEE Eng. Med. Biol. 23:666(CDROM), 2001.

Head, J.F., Lipari, C.A., and Elliott, R.L.: Determination of Mean Temperatures of Normal Whole Breast and Breast Quadrants by Infrared Imaging and Image Analysis. Thermology International 11:145, 2001.

Head, J.F., and Elliott, R.L.: Infrared Imaging: Making Progress in Fulfilling Its Medical Promise (Past, Present and Future Applications of Infrared Imaging in Medicine). **IEEE Eng. Med. Biol.** 21:80-85, 2002.

Head, J.F., Hoekstra, P., Keyserlingk, J., Elliott, R.L, and Diakides, N.A.: Comparison of Breast Infrared Imaging Results by Three Independent Investigators. **Proc. IEEE Eng. Med. Biol.** 25:1125-1128(CDROM), 2003.

Head, J.F., Hoekstra, P., Keyserlingk, J., and Elliott, R.L: Concordance of Scores for Breast Infrared Images by Three Independent Investigators. **S.P.I.E.** In press.

GRANTS AND CONTRACTS

SBIR contract, Phase I, DOD (Army), $100,000/6 months, 7/15/95-1/15/96, Development of Second Generation Thermography with Computerized Image Analysis for Breast Cancer Diagnosis. Principal Investigator: J.F. Head.

SBIR contract, Phase II, DOD (Army), $750,000/2 years.

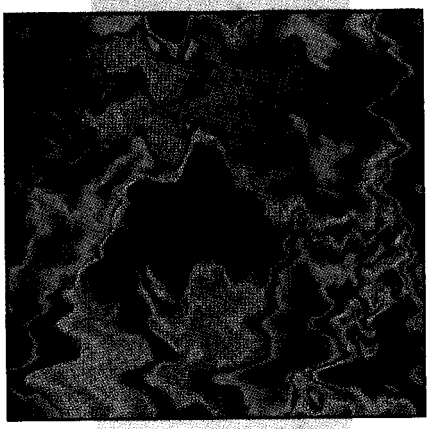

The Important Role of Infrared Imaging in Breast Cancer

New Technology Improves Applications in Risk Assessment, Detection, Diagnosis, and Prognosis

Jonathan F. Head, Fen Wang, Charles A. Lipari, Robert L. Elliott
Medical Thermal Diagnostics, Baton Rouge

Early studies of infrared (IR) imaging of the breast, commonly called thermography in medicine, were initiated in both Europe and the United States in the 1970s and concentrated on the diagnosis of breast cancer. From 1973 to 1981, the National Cancer Institute (USA) sponsored the Breast Cancer Detection Demonstration Projects (BCDDP). These studies were designed to test the role of both IR imaging and mammography in the diagnosis of breast cancer. However, IR imaging was discontinued very early in the study. The premature closing of the IR imaging of the breast in the BCDDP study was due to technical difficulties, lack of training of technical staff, lack of experience in reading by professional staff, lack of standardization of equipment, and lack of interest in this new technology by radiologists.

The closure resulted in there being no clear demonstration of the possible importance of IR imaging in the diagnosis of breast cancer. Other consequences of discontinuation of this part of the study was that no data were collected to compare the diagnostic ability of mammography with IR imaging, to evaluate IR imaging as an indicator of risk of developing breast cancer, or to evaluate this imaging modality as a prognostic indicator in patients with abnormal mammograms who later were surgically biopsied and diagnosed with breast cancer.

After the BCDDP discontinued their study of IR imaging, several studies were published supporting the role of IR imaging as a high-risk marker for breast cancer [1, 2], in the diagnosis of breast cancer [1, 2, 3], and as a prognostic indicator for breast cancer patients [3, 4]. The results reported in this article further support the use of IR imaging in risk assessment, detection, and as a prognostic indicator. We present preliminary evidence showing that the improvements in technology that have been incorporated into second-generation, focal-plane, indium-antimonide detector systems can significantly improve breast IR images.

Methods

The normal and breast cancer patients in the first part of this study were selected from patients who had undergone breast IR imaging as part of their breast examination at the Elliott Mastology Center beginning in 1973. These exams also included mammography and clinical examination. The study included three categories of patients: (1) 126 patients who died of breast cancer during this period and had breast IR imaging within the one-year period leading up to diagnosis of their breast cancer, (2) 100 randomly selected living breast cancer patients who also had IR imaging within the one-year period previous to their diagnosis of breast cancer, and (3) 100 patients who had a variety of mastopathies but had not been diagnosed as having breast cancer during screening. If, during IR imaging examination, asymmetric heat patterns (diffuse heat, focal hot spots, areolar and/or periareolar heat, vessel discrepancy, or edge signs) were noted, the patient was considered at high risk of getting breast cancer or to have a poor prognosis, if already diagnosed. Clinical/pathological staging (tumor size, nodal status, presence of metastasis), age, and location of the cancer were also documented for all these patients, and the results were compared to IR imaging results.

 0739-5175/00/$10.00©2000

A second group of patients, being screened with mammography, also underwent IR imaging of their breasts. During the study, normal and high-risk patients had IR images of their breasts taken with an Inframetrics (North Billerica, MA) scanning mercury-cadmium-telluride detector system (right oblique, left oblique, and frontal views) and recorded as hard-copy photographic images (a color frontal isotherm view, and three black and white views: frontal, left oblique, and right oblique). For comparison, three additional breast views (frontal, right oblique, and left oblique) were recorded with an Amber (Raytheon, Inc., Dallas, TX) focal-plane, indium-antimonide, staring array system. IR images of 220 patients from both the scanning and focal-plane systems were digitized and stored on computer hard disk, thus creating a digitized IR image database for later image analysis.

Results

When the IR imaging results were grouped into the three groups of screened, cancer, and deceased cancer patients, there was a significantly greater percentage of abnormal IR images in breast cancer patients than in women being screened who were at normal or high risk of developing breast cancer (Table 1). There was a 28% incidence of abnormal IR images in screened patients and a significantly greater incidence at diagnosis, 65%, for living breast cancer patients. The 88% incidence of abnormal IR images at diagnosis in the deceased breast cancer patients was also significantly higher than the 65% incidence of breast cancer patients in general. The data in Table 1 show that the increasing incidence of abnormal IR images is significantly related to the likelihood of progression of the disease. Thus, IR imaging results, which are useful for risk assessment, also have prognostic significance.

The prognostic significance of the components of the clinical/pathological staging system has previously been demonstrated in breast cancer patients. In this study, we found that nodal status and presence of metastatic disease were not related to IR imaging results. However, clinical tumor size (diameter of palpable mass), but not pathological tumor size (diameter of cross section of mass after surgical removal), was significantly related to IR findings, which resulted in patients with larger tumors being more likely to have an abnormal IR image (Table 2). Even though patients with larger tumors were more likely to have abnormal IR images, it is important to note that the group of patients with the smallest tumors (T1) also had over 50% abnormal IR images. The age of the patients (less than 50 compared to greater than or equal to 50) and location of the tumor (left compared to right breast) were also found to be independent of and therefore unrelated to IR imaging results.

Table 3 presents the results from 20 cancer patients in this study who had serial IR imaging and had at least one IR image a minimum of one year before being diagnosed with breast cancer. These 20 patients had IR results at diagnosis that are representative of the larger group that they were selected from, in that 50% (10 of 20 patients) had abnormal IR images, which is similar to the 65% (65 of 100 patients) with abnormal IR images from Ta-

Table 1. Breast Infrared Imaging Results for Screened, Cancer, and Deceased Patients

Infrared Imaging Results	Patients		
	Screened	*Cancer*	*Deceased*
Normal	72 72%	35 35%	15 12%
Abnormal	28 28%	65 65%	111 88%
$p < 0.0001$, chi-square analysis for independence			

Table 2. Comparison of Clinical Tumor Size and Infrared Imaging Results

Infrared Imaging Results	Clinical Size Classification		
	T1 (<2cm)	T2 (2-5 cm)	T3 (>5 cm)
Normal	9	14	0
Abnormal	10	31	10
% Abnormal	53	69	100
$p < 0.05$, chi-square analysis for independence			

Table 3. Infrared Imaging Results of Patients Who Had an Infrared Image of Their Breasts at Least One Year Before Diagnosis and at Diagnosis of Breast Cancer

Infrared Image Results at Least One Year Prior to Diagnosis	Infrared Image Results at Diagnosis	
	Normal	Abnormal
Normal	10	3
Abnormal	0	7
$p < 0.005$, chi-square analysis for independence		

Table 4. Length of Time of Follow-Up

Infrared Imaging Results		Number of Patients	Follow-up Time in Months		
>1 Year Before	At Diagnosis		Mean ± SD	Median	Range
Abnormal	Abnormal	7	95 ± 46	87	18-158
Normal	Normal	10	90 ± 30	95	24-123
Normal	Abnormal	3	34 ± 19	24	23-56

Table 5. Comparison of Results from First- and Second-Generation Infrared Imaging Systems			
Second-Generation System	**First-Generation System Subjective Thermographic Diagnostic Classification**		
Infrared Index	Normal	Slightly Abnormal	Abnormal
0	87/220 (39.5%)	12/220 (5.5%)	10/220 (4.5%)
1	23/220 (10.5%)	5/220 (2.3%)	4/220 (1.8%)
2	22/220 (10.0%)	16/220 (7.3%)	10/220 (4.5%)
3	10/220 (4.5%)	1/220 (0.5%)	4/220 (1.8%)
4	5/220 (2.3%)	0/220 (0.0%)	6/220 (2.7%)
5	1/220 (0.5%)	1/220 (0.5%)	3/220 (1.4%)
p = 0.0001, chi-square analysis for independence			

ble 1. All 10 of the patients who had normal IR images at diagnosis had normal IR images at least one year before diagnosis. A large proportion (70%) of the patients who had abnormal IR images at diagnosis had abnormal IR images at least one year prior to diagnosis. A small proportion (30%) of patients with abnormal IR images at diagnosis previously had normal IR images.

The average times between earliest positive or negative IR images and diagnosis are presented in Table 4. The seven patients with abnormal IR images at diagnosis, who also had abnormal IR images at least a year earlier, had abnormal IR images for an average of almost eight years. The 10 patients with normal IR images at diagnosis had normal IR images for an average of seven and a half years. The few patients who changed from normal to abnormal IR images at diagnosis had normal IR images at least 23 months before diagnosis.

In the second part of the study, the second-generation, focal-plane, starring array system was found to produce much higher quality images than the first-generation scanning system. The first decision made was to try to quantitate the six individual asymmetric abnormalities present in the focal-plane images and to create an IR index by adding together the individual scores for each abnormality (small hot spot, score = 1; large hot spot, score = 2; global heat, score = 3; vascular heat, score = 1, 2, 3; areolar heat, score = 1; edge heat, score = 1). The images from the focal-plane starring array had IR indexes that could range from zero to eight, but the highest index computed was five. Previously, scanning IR images were considered abnormal if any of the six asymmetric abnormalities were present, and images that only had a borderline IR asymmetry were called slightly abnormal (three levels of results: normal, slightly abnormal, abnormal).

The IR indexes derived from the second-generation, focal-plane imaging results were compared to the levels of abnormality from the scanning results on the patients being screened for breast cancer (Table 5). Chi-square analysis for independence showed that the two methods produced results that were strongly associated ($p = 0.0001$). The most interesting result was an increase in the sensitivity for asymmetric heat patterns with the focal-plane system: 50.5% (111 of 220) of the patients without breast cancer had abnormal IR images, whereas only 32.7% (72 of 220) of the patients had asymmetric heat patterns with the first-generation scanning system. Analysis of the six asymmetric abnormalities individually (Table 6) showed that most of the increase in sensitivity could be attributed to a significant ($p = 0.0054$) increase in vascular asymmetry from 43 of 218 patients with the scanning system to 70 of 220 with the focal-plane system.

Next, the distribution of the IR index was compared to the levels of abnormality from the scanning images to determine if the increase in sensitivity of the second-generation technology would create small subsets with higher IR indexes that could be used to refine risk assessment. When an IR index of 1 is considered to be so insignificant that a patient's risk of getting breast cancer is not increased, and 2 is considered to only slightly increase risk, then 14.1% (31 of 220) of the patients being screened for breast cancer would be categorized at high risk. On the other hand, 37 of 220 patients had abnormal IR images with the scanning system, which means that 16.8% of the screened patients would be at high risk (Table 5).

Three known risk factors (family history of breast cancer, previous estrogen hormone therapy, and previous breast biopsy) were compared to the IR results from the first-generation scanning and second-generation focal-plane systems (Table 7). None of these risk factors was found to correlate with IR imaging results

Table 6. Distribution of Abnormalities for First- and Second-Generation Infrared Imaging Systems		
Abnormality	**First-Generation System (Scanning)**	**Second-Generation System (Focal Plane)**
Asymmetric Small Focal Hot Spot	41/218 (18.8%)	28/220 (12.7%)
Asymmetric Large Focal Hot Spot	3/218 (1.4%)	35/220 (15.9%)
Asymmetric Global Heat	6/218 (2.8%)	2/220 (0.9%) p = 0.1434
Asymmetric Vascular Heat	43/218 (19.7%)	70/220 (31.8%) p = 0.0054
Asymmetric Areolar Heat	6/218 (2.8%)	14/220 (6.4%)
Asymmetric Edge Heat	1/218 (0.5%)	0/220 (0.0%)

from either system. Therefore, IR imaging results were an independent risk factor in breast cancer. The physician also assigned patients being screened into normal and high-risk categories by subjectively integrating family history, mastopathy, previous use of estrogen hormones, and previous breast biopsy (Table 7). The results of this physician-integrated risk assessment was also not related to the results from either IR imaging system.

The final part of the study was an attempt to apply image processing and computer-vision techniques to produce objective measures of asymmetric heat patterns. Preliminary results showed that comparative pixel statistics (mean, standard deviation, median, minimum, maximum temperatures) could be computed for complete breasts, quadrants of the breast (Fig. 1, schematic; Fig. 2, IR image of breasts), and hot spots.

Discussion

To date, IR imaging of the breast has not been adequately studied for conclusions to be drawn about its role in the detection and treatment of breast cancer. In the BCDDP, IR imaging was originally included in the study, but it was quickly discontinued without collection of the data necessary to determine its value in detection and diagnosis of breast cancer. The high false positive rate (found to be 28% in the present study) of IR imaging compared to mammography in women being screened for breast cancer has always been considered a major drawback. The combination of this high false positive rate with the inability of IR imaging to localize a lesion or tumor (abnormalities found by IR imaging do not define an area that can be surgically biopsied) has been sufficient reason to prevent breast IR imaging from becoming a routine procedure.

The high false positive rate of IR imaging of the breasts does suggest that this technique might be useful in defining a group of patients at high risk for developing breast cancer. Many of the women who are undergoing mammography and IR imaging at our breast clinic are symptomatic, have a family history of breast cancer, or have abnormalities discovered by their primary care physicians. Therefore, their risk exceeds the 10% lifetime risk/occurrence of breast cancer for women in the general population. Gautherie and Gros [1] showed that 38% (298/784) of patients with abnormal IR images were diagnosed with breast cancer in the four-year period following the abnormal IR images. Stark [2] found that 23% of patients with abnormal IR images developed breast cancer within 10 years. In the present study, the significantly ($p < 0.0001$, chi-square analysis for independence) higher percentage (65%) of patients with abnormal IR images at the time of breast cancer diagnosis compared to the 28% rate of abnormal IR images in the screening group of normal and high-risk patients suggests that an abnormal image is a high-risk marker in breast cancer. Of the screened patients, a much higher proportion (approximately a two- to three-fold increase in risk) with abnormal IR images will develop breast cancer, as compared with those with normal images. This suggestion is reinforced by the data in Table 4, where it can be seen that 35% (7/20) of the cancer patients had abnormal IR images 18 to 158 months prior to their diagnosis of breast cancer. These studies all provide strong evidence that breast IR imaging, an inexpensive and completely noninvasive procedure, has an important role in defining a group of women at high risk for breast cancer. These patients at increased risk of developing breast cancer should have mammography, IR imaging, and clinical examination more frequently, in an attempt to diagnose at an earlier and more curable stage.

Infrared imaging results, which are useful for risk assessment, also have prognostic significance.

Since the mid 1980s, breast cancer researchers have been searching for clinical, pathological, and biochemical characteristics that can be integrated to provide a rational basis of selecting node-negative (absence of spread of the breast cancer to the axillary lymph nodes) patients for adjuvant chemotherapy. It is known that breast cancer will not recur (and cause death) in approximately 90% of node-negative patients with tumors less than 2 cm in diameter. However, in the 10% where recurrence occurs, the cancer will be less responsive to chemotherapy than it would have been in the adjuvant setting. IR imaging appears to provide prognostic information that could be used in combination with other clinical, pathological, and biochemical parameters in the selection of those patients for adjuvant chemotherapy. Isard, et al. [4], in a study of 70 breast cancer patients, showed that 30% of patients with abnormal IR images survived five years, compared to 80% of patients with normal IR images. The present study showed that 65% of the breast cancer patients had abnormal IR images, but a significantly ($p < 0.0001$) greater proportion (88%) of those who had died of breast cancer had abnormal IR images. This significantly greater proportion of deceased breast cancer patients with abnormal IR images is further evidence to support IR imaging as a prognostic indicator.

Table 7. Comparison of Results of First- and Second-Generation Infrared Imaging to Known Risk Factors in Breast Cancer

Risk Factors	First-Generation Scanning Infrared Imaging System		Second-Generation Focal-Plane Infrared Imaging System	
	p	n	p	n
Family History	0.3903	213	0.7971	213
Previous Estrogen Therapy	0.5357	210	0.8875	210
Previous Breast Biopsy	0.0747	212	0.3582	212
Physician's Subjective Integration	0.2399	220	0.9522	220

p = probability, n = number of cases compared; chi-square analysis for independence

Although IR imaging of the breast has been shown to have prognostic value, it is important to determine if such results have value independent of other previously identified prognostic indicators. We have previously reported that when IR imaging was done at the same time as diagnostic mammography (prior to diagnostic needle or surgical biopsy for breast cancer) and compared to the size, nodal status, and presence of metastatic disease of the TNM classification system (T, tumor size; N, nodal status; M, presence of metastatic disease), then IR imaging results were only related to clinical tumor size (see Table 2). It is important to note that even though the percentage of patients with abnormal IR imaging increased with increasing tumor size, over 50% (10 of 19) of the patients with small tumors (less than 2 cm in diameter) had abnormal IR images. This finding suggests that the risk of recurrence could be related to IR imaging results even in the group of patients with tumors less than 2 cm in diameter. When looking at all stages of breast cancer, IR imaging results were independent of nodal status, but we do not, as yet, have enough Stage I (a tumor less than 2 cm in diameter, negative lymph nodes, and free of metastatic disease) patients to analyze IR imaging results for disease-free and overall survival in relation to adjuvant chemotherapy. Head, et al. [3], also showed that IR imaging results were unrelated to age, tumor location (right or left breast), and estrogen and progesterone receptor status. Many more patients will have to be analyzed to determine if IR imaging is an independent and useful prognostic indicator. We feel that this would be a worthwhile pursuit considering the small cost and noninvasive nature of IR imaging.

The growth rate of breast cancers, determined by measuring the change in diameter of breast tumors over time and by calculating tumor volume doubling times, has been shown to be one of the best predictors of disease-free and overall survival and therefore is a good prognostic indicator. However, the clinician is rarely able to follow a growing tumor in individual patients over a long enough period of time to determine the volume doubling time. It will be necessary to find a more practical method of approximating growth rate or other more easily determined prognostic indicators that are highly correlated to and dependent on it. Tumor growth rate [5], tumor ferritin concentration [3], proliferation index by flow cytometry [3], and semiquantitation of the proliferation-associated antigen Ki-67 in frozen sections by immunocytochemistry [3] have all been shown to be related to IR imaging results. The correlation of growth rate and these proliferation-related parameters with IR imaging results suggests that a breast cancer patient with an abnormal IR image has a higher probability of having a fast-growing tumor with increased blood flow to it and its immediately surrounding tissue. This increased blood flow is necessary to bring the nutrients required to maintain the growth rate of fast-growing tumors and is probably responsible for the IR abnormalities observed. The most remarkable aspect of IR imaging is that these abnormalities often precede mammographic abnormalities associated with breast cancer by years and sometimes even decades [1, 2]. We therefore believe that the higher metabolic rate of faster-growing tumors and the associated increase in local vascularization causes most of the abnormalities seen in the IR image of breast cancer patients. Since faster-growing tumors are known to have a poorer prognosis, their association with abnormal IR imaging results offers significant prognostic value for breast cancer patients.

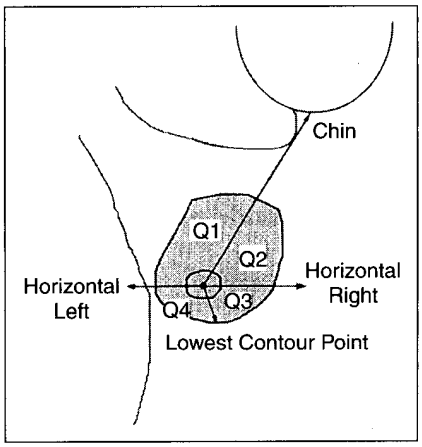

1. Guidelines for breast quadrants.

2. Abnormal infrared image of the breasts.

Comparison of IR images from the first-generation scanning IR imaging systems to the results from a second-generation IR imaging system clearly showed the higher quality of the images from the newer technology. The improvement was due to the greater thermal sensitivity, greater number of elements, and greater dynamic range of the focal-plane, staring array imager. The proportion of patients determined to be at increased risk of breast cancer is probably a little high and therefore yields lower specificity, as determined with the second-generation IR system. However, the strength of using an IR index is not in the overall proportion of patients who are at increased risk, but with its ability to create a series of groups of patients with semiquantitative increasing risk. This grading can be done by adjusting the weight of the different asymmetric IR abnormalities used in creating the IR index. In future studies, we will be able to address the independent values of the six IR abnormalities and to create an index where each will be appropriately weighted. This process of weighing the independent variables, the different asymmetric IR abnormalities, is not possible with the three-level subjective analysis used with the scanning IR system.

In this study, the lack of association between IR imaging results and known risk factors in patients being screened for breast cancer confirms that IR results are independent of known risk factors. Therefore, in light of the evidence [1, 2, 3] showing a strong association of asymmetric IR abnormalities with a high risk of getting breast cancer, it can be concluded that such images are a significant independent risk factor for breast cancer.

The objective measurements from our initial image analysis need to be done on a larger database of focal-plane images to determine their utility. Hopefully, by removing the subjectivity of current image-analysis methods, there will be an improvement in risk assessment, detection, and treatment of breast cancer. Methods of analysis of the breast IR images need to be developed that reduce perspective distortions that are inherent to imaging of three-dimensional shapes and also to overcoming the lack of ideal body symmetry due to both natural asymmetry and also the spatial orientation of the imager to the subject. Finally, the whole analysis must be automated, as highly interactive analysis is not conducive to the typical practice of medicine.

Conclusions

The role of IR imaging in breast cancer risk assessment, detection, diagnosis, and prognosis has not been fully determined. The use of IR imaging for detection and diagnosis of breast cancer is limited by an inability to localize the tumor. Therefore, IR imaging can only be used to complement mammography and physical exam in the detection and diagnosis of breast cancer.

IR imaging does have an important role in screening for breast cancer risk assessment. The evidence presented in this article further demonstrates that women with abnormal IR images are at increased risk, approaching 30%, of developing breast cancer. These high-risk patients should be followed closely with IR imaging, mammography, and clinical examination in order to detect their cancers early, when there is a higher probability of cure. IR imaging also has prognostic value for breast cancer patients. Further study in Stage I breast cancer patients is needed to see if IR imaging results can be integrated with the results of other prognostic indicators, when deciding whether to give adjuvant chemotherapy. Additional studies are needed to better define the role of improved second-generation IR imaging instrumentation and computer-assisted image-analysis techniques.

Acknowledgments

Partial financial support was provided by the Breast Foundation, Baton Rouge, LA, and through a SBIR contract with the Army Night Vision Laboratory. We are also indebted to Raytheon for kindly lending us an Amber IR imaging system for this study.

Jonathan F. Head is the director of research at the Mastology Research Institute of the Elliott Mastology Center and director of research and development of Medical Thermal Diagnostics in Baton Rouge, LA. He obtained his B.S. in zoology from Syracuse University, his M.A. in biology from Brooklyn College of CUNY, and his Ph.D. in biology from Fordham University. He was in the Division of Cell Biology of Naylor Dana Institute for Disease Prevention of the American Health Foundation, NY (1974-1978); the Department of Immunology at Cornell University Medical School, NY (1978); the Department of Pediatrics at Mt. Sinai Medical School, NY (1978-1987); and the director/department head of tumor cell biology at the Center for Clinical Sciences, International Clinical Laboratories, TN (1986-1988). In 1988, he moved to Baton Rouge, LA, to become president of the Mastology Research Institute and is both the director of research and director of the clinical laboratory. He has appointments in the Department of Biochemistry at Tulane University School of Medicine and the Department of Physical Sciences at Delta State University.

Fen Wang was born in Xingjiang, China, and graduated from Beijing Medical University in 1984. After medical school he completed a surgical residency in China. As an exchange scholar he went to Essen University Medical School, Germany, for three years and studied applications of infrared imaging in medicine, specifically the human female breast. He received a Ph.D. from Essen University after finishing his dissertation. In 1991 he joined the Mastology Research Institute of the Elliott Mastology Center in Baton Rouge, LA. His cancer research activities include growing primary tissue culture from breast cancer tissue for cancer vaccinations, investigating the complexes of chemotherapeutic agents bound to human transferring for cancer patient chemotherapy, and the study of iron metabolism in cancer cells. After finishing a one-year surgical residency at the University of South Alabama Medical Center in Mobile, AL, he is now doing a radiation oncology residency at the Kansas University Medical Center in Kansas City, MO.

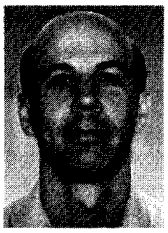

Charles A. Lipari received the B.S. and M.S. in electrical engineering from the University of S.W. Louisiana in 1975 and 1978, respectively. In 1989 he received his Ph.D. in electrical engineering from Louisiana State University in Baton Rouge. He worked as a digital systems engineer for Texas Instruments from 1978 to 1984, where he was part of a design team developing array processor technology for seismic signal processing. Before returning to an academic career, he worked for Thermalscan Inc., where he was chief engineer for the development of a pavement image processing system for surveying distress in road beds. In 1990, he joined Arizona State University, where he is now an assistant professor in the Department of Electronic and Computer Engineering Technology. He is currently working on projects to develop an image-processing system for the recognition of breast cancer using infrared imaging. Other interests include the use of reconfigurable computing elements for high-speed image processing and computer vision.

Robert L. Elliott was born in Greenville, MS, in 1936. He received his M.D. from the University of Mississippi School of Medicine in 1961. He did a residency in general and thoracic surgery from 1961 to 1967 at the University of Mississippi School of Medicine and did a traineeship in electron microscopy at Washington University during his residency. He was in private practice of general and thoracic surgery from 1967 to 1973 in Anniston, AL. In 1974, he moved to Baton Rouge, LA, and founded the Elliott Mastology Center, which consists of the Breast Clinic and the Mastology Research Institute. He received his Ph.D. from LaSalle University in 1994. He limits his practice to the areas of prevention, early diagnosis, treatment, and research of diseases and cancer of the breast.

Address for Correspondence: Dr. Jonathan Head, Mastology Research Institute, 8221 Kelwood Drive, Baton Rouge, LA 70806. Tel: +1 225 927 2256. Fax: +1 225 927 3772. E-mail: emcmri@iamerica.net.

References

1. **Gautherie M, and Gros CM:** Breast thermography and cancer risk prediction. *Cancer* 45: 51-56, 1980.

2. **Stark AM:** The value of risk factors in screening for breast cancer. *Eur J Cancer* 11: 147-150, 1985.

3. **Head JF, Wang F, and Elliott RL:** Breast thermography is a noninvasive prognostic procedure that predicts tumor growth rate in breast cancer patients. *Ann NY Acad Sci* 698: 153-158, 1993.

4. **Isard HJ, Sweitzer CJ, and Edelstein GR:** Breast thermography: A prognostic indicator for breast cancer survival. *Cancer* 62: 484-488, 1988.

5. **Gautherie M:** Thermography of breast cancer: Measurement and analysis of the *in vivo* temperature and blood flow. *Ann NY Acad Sci* 335: 383-413, 1982.

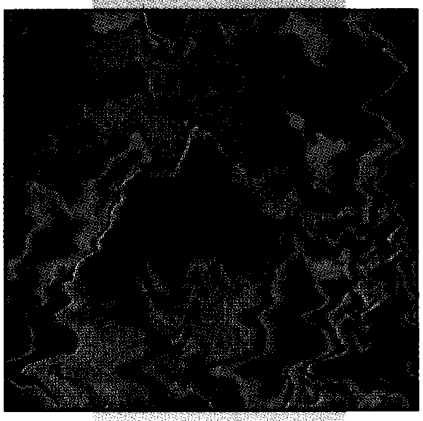

Increasing the Effective Resolution of Thermal Infrared Images

An Algorithm Based on Mean-Field Annealing that Also Removes Noise and Preserves Image Edges

Wesley E. Snyder[1], Hairong Qi[2], Robert L. Elliott[3], Jonathan F. Head[3], Cliff X. Wang[4]

[1]Center for Advanced Computing and Communication, North Carolina State University

[2]Electrical and Computer Engineering Dept. University of Tennessee - Knoxville

[3]Elliott Mastology Center, Baton Rouge

[4]Ascend Communication, Columbus

Thermal infrared (TIR) imaging is recognized as the most efficient technique for the study of skin temperature distribution. Many studies have been performed that show the anticipated normal pattern of temperature in a thermal image [1]. In specific diseases, characteristic changes can be measured from target anatomical sites. In this way, objective noninvasive investigations can be of diagnostic value [15]. TIR imaging of the breast for breast cancer risk assessment is an example.

Clearly, the efficacy of TIR is greater for surface or shallow lesions and for perfusion difficulties such as peripheral vascular occlusive disease, particularly deep venous thrombosis, in which TIR is 79% sensitive and 84% specific [16]. Surprisingly, even deep lesions of the breast induce abnormalities in skin temperature that can be detected by TIR. Anbar [1] argues that such abnormalities are due to nitric oxide (NO)-induced increases in perfusion throughout the breast, including near the skin, and not due to hypervascularization of the tumor itself. Studies of breast cancer diagnosis using TIR have shown sensitivities from 62% to 88% [6, 18, 19]. The current sensitivity of X-ray mammography is still below 85% [14], with most of the difficulty occurring in women with dense breasts (about 25% of the tested population) [13].

Acknowledging that TIR may not be sufficiently mature to be considered a diagnostic tool for breast cancer, some researchers [7, 10] have asked the question of whether an abnormal TIR image of the breast can be used for risk assessment [11]. They compared abnormal TIR with three other risk factors: family history of breast cancer, previous estrogen hormone therapy, and previous breast biopsy. None of these risk factors was found to correlate with the TIR result and therefore may be considered independent risk factors. Furthermore, TIR, when treated as a risk factor, was found to have excellent prognostic capability.

Although TIR imaging possesses the advantages of being noninvasive, risk free, and considerably less expensive, it suffers the disadvantage of a lack of resolution due to blur compounded by rather high levels of noise. A maximum a-posteriori probability (MAP) image restoration

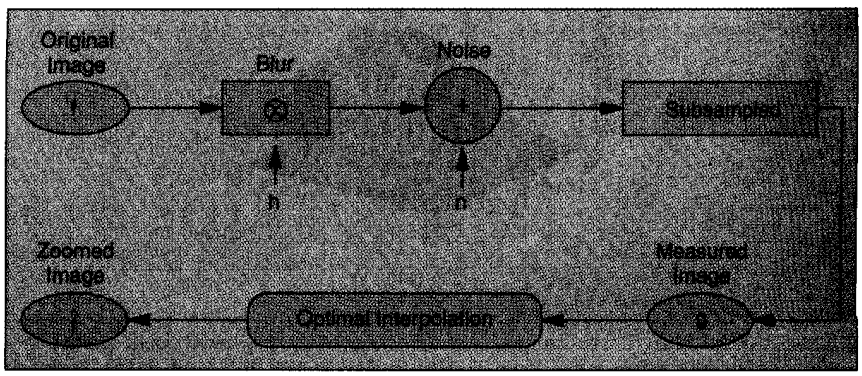

1. System model of image corruption and reconstruction.

0739-5175/00/$10.00©2000IEEE

philosophy is proposed in this article to solve this problem of resolution. The objective is three-fold: to increase the resolution of the measured image by using a type of 2:1 zooming; to remove the noise; and simultaneously to preserve the detail of features, including, in particular, the sharpness of edges.

Mathematical Approach

A system model is first constructed to simulate the image-formation process and the image-reconstruction process. Then, the problem of increasing the resolution is formulated into an optimization problem using the approach of mean-field annealing (MFA).

System Model Construction

Figure 1 explains the system model under the current study. In this model, image f (resolution $2N \times 2N$) is first blurred by the point-spread function (PSF) (h) and then corrupted by noise (n). The resulting blurred, noisy image is subsampled (2:1) to produce the measured image g (resolution $N \times N$).

The algorithm proposed in this article reverses this process. That is, once we know the measured image g, the system PSF h, and the noise model n, we can determine an estimate $\hat{f}$ (resolution $2N \times 2N$) of image f, from the subsampled image g. An optimal interpolation algorithm is pursued to make $\hat{f}$ as close to f as possible. Before going into the problem formulation, we first analyze, hypothetically, the degradation that the measured image suffers.

To estimate the PSF that produces the image blur, a single point source of heat was imaged at five different points in the field of view by making small changes in the camera angle (Fig. 2). The totally different shapes displayed from the five pictures show us that the blur is space variant. Optimal estimation of the PSF is beyond the scope of this article.

To exploit the noise model, we select a homogeneous area from the original image and analyze its histogram. Figure 3 shows the histograms from two relatively homogeneous areas in an original image, both of which are approximately Gaussian.

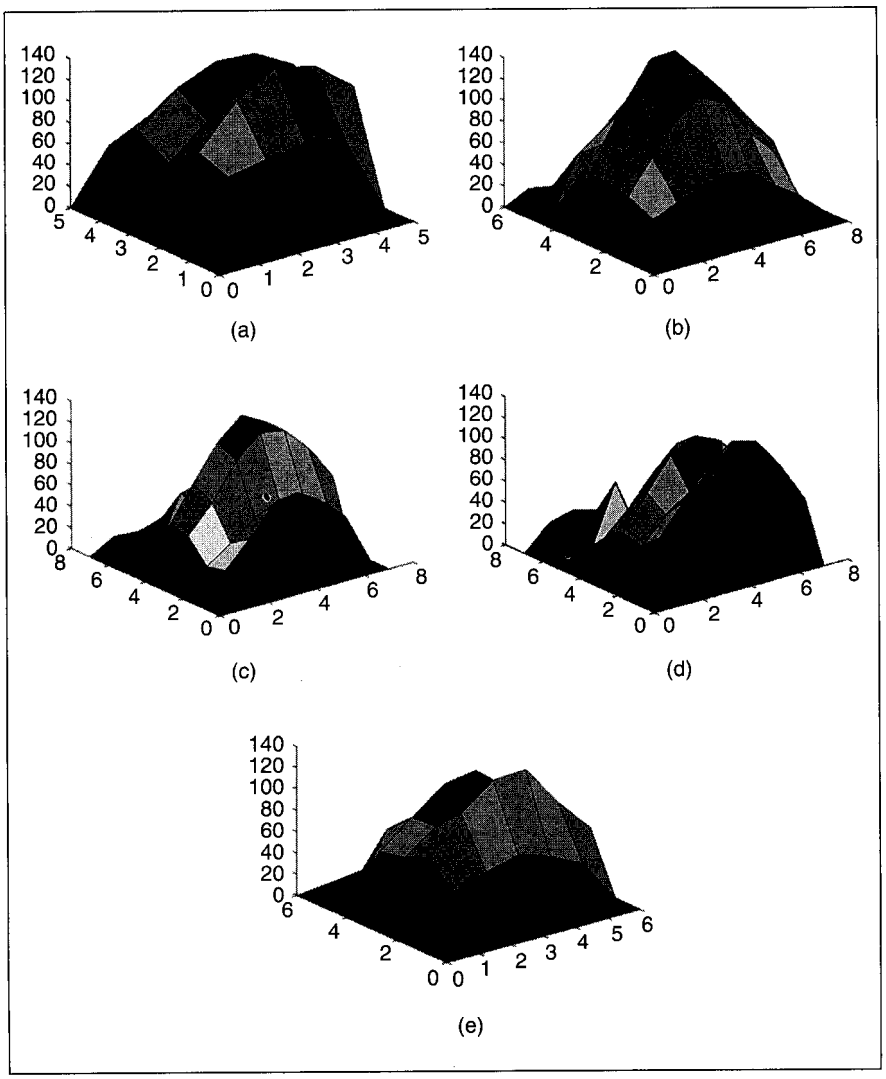

2. Space-variant blur. Three-dimensional drawings of the captured single point source of heat with different camera angles. (a) Upper-left, (b) upper-right, (c) center, (d) lower-left, and (e) lower-right.

Problem Formulation

The problem of TIR image reconstruction with increased resolution can be posed as an optimization problem. We state our optimization as follows: Given the subsampled measured image g, we seek the zoomed image f that maximizes the a-posteriori conditional probability $p(f|g)$. According to Bayes' rule, the a-posteriori conditional probability can be written as:

$$p(f|g) = \max_f \frac{p(g|f)P(f)}{P(g)} \quad (1)$$

where the denominator $P(g)$ is independent of f and therefore does not affect the maximization process. Taking the logarithm of both sides of Eq. (1), we then obtain the objective function:

$$\log p(f|g) = \max_f (\log p(g|f) + \log P(f)) \quad (2)$$

We denote as the *noise term* the part that involves the conditional probability $p(g|f)$ and depends on the blur and the noise process, and we denote as the prior term the a-priori probability $P(f)$, which is independent of the measured image.

Noise Term

We have determined that the noise in the thermal image is approximately Gaussian and that the blur is space variant. Without losing generality, we can assume that the Gaussian is zero mean with variance σ^2. In the experiments, we use a single 5×5 convolution kernel at all points in the image, instead of a space-variant nonisotropic kernel to model the blur, which is effectively a space-invariant assumption. Future work will take spatial variation of the PSF into account.

From the model constructed in Fig. 3, we know that the difference between the original image f and the measured image g can only be due to the noise. Since the

noise is an independent Gaussian function with zero mean and variance σ^2, the conditional probability $p(g|f)$ can be written as:

$$p(g|f) = \prod_{i,j} \frac{1}{\sqrt{2\pi}\sigma} \times \exp\left(-\frac{((f \otimes h)_{i,j} - g_{i,j})^2}{2\sigma^2} \right) \quad (3)$$

where $f \otimes h$ denotes a 5×5 sum of products (local convolution) centered at point (i, j).

Taking the logarithm of Eq. (3) and changing the sign allows one to convert the maximization of the conditional probability to the minimization of a summation, which is what we called the noise term H_n:

$$H_n = \sum_{i,j} \frac{((f \otimes h)_{i,j} - g_{i,j})^2}{2\sigma^2}. \quad (4)$$

In the case of 2:1 zooming, the measured pixels exist on every other row and every other column, so the summation is only taken over pixels where g is measured.

Prior Term

Unlike the noise term, the prior term incorporates only the knowledge of the properties of image f. One typical property that f should have is smoothness. We use a penalty function to express the prior term H_p, which penalizes the noise but not the edges. Considerable literature [2, 5, 8, 12] has shown that the upside-down Gaussian function in Fig. 4 produces noise removal without blur of edges.

Based on this property, we derive the prior term:

$$H_p = -\sum_{i,j} \left(\frac{\beta}{T} \right) \exp\left(-\frac{(\nabla f)^2_{i,j}}{2T^2} \right) \quad (5)$$

where β is a constant weight selected dependent on the noise variance and ∇f is an edge operator specific to the problem at hand, operating in the vicinity of pixel (i, j). Usually, the edge operator is implemented as a convolution with a symmetric edge operator kernel r. We note that if ∇f is zero for the neighborhood of each pixel, the prior term is maximally negative. The "temperature" T will be gradually reduced over the iterations of the algorithm to T_{final}, which is a problem-dependent constant property of the expected scenes that specifies the "steepness" or maximum expected value of the edge operator between regions. It is important to point out that this form of the prior is bounded, which restricts the amount of blurring for the edges in the image.

Since TIR images have features of varying intensity and may be separated by roof edges, we use a *piecewise linear prior model* that preserves roof edges well [4]. The piecewise linear model can be implemented by a second derivative operator such as a Laplacian or a quadratic variation. We choose the quadratic variation because this form is never negative, making the edge more stable [Eq. (6)].

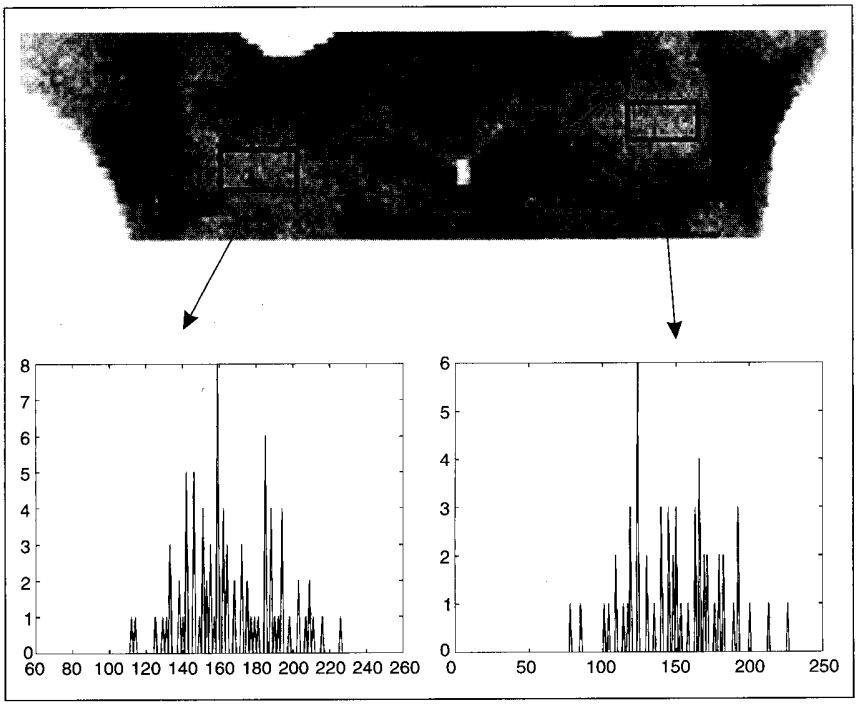

3. Gaussian noise (histograms of two homogeneous areas in a thermal image are Gaussian).

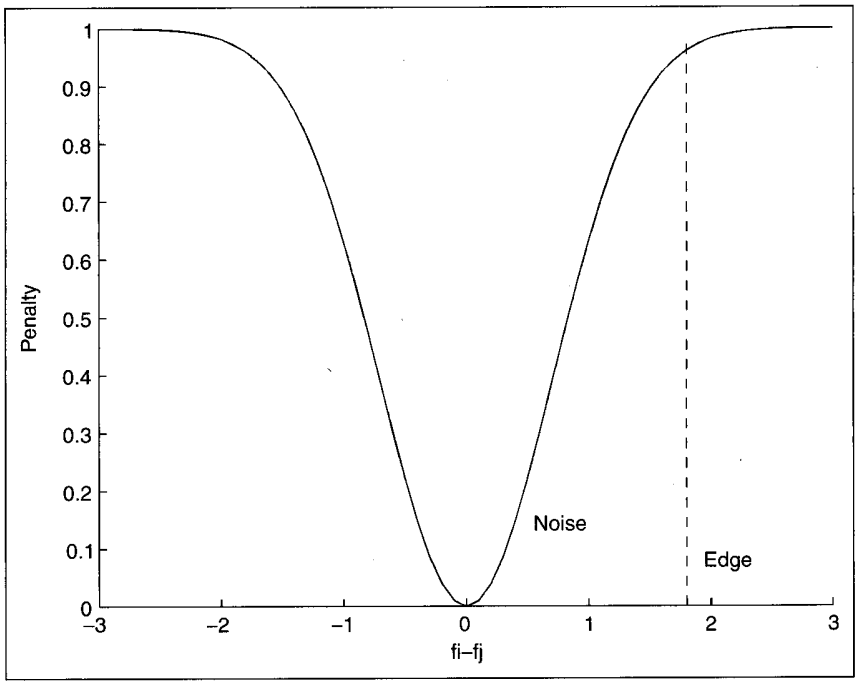

4. Estimated penalty function for the prior term. The horizontal axis is the difference in brightness of adjacent pixels.

The quadratic variation operator can be estimated by convolving with three kernels h_{xx}, h_{yy}, and h_{xy} [Eq. (7)]:

$$(\nabla f)^2_{i,j} = \left(\frac{\partial^2 f}{\partial x^2}\right)^2 + \left(\frac{\partial^2 f}{\partial y^2}\right)^2 + 2\left(\frac{\partial^2 f}{\partial x \partial y}\right)^2 \tag{6}$$

$$h_{xx} = \frac{1}{\sqrt{6}}\begin{bmatrix} 0 & 0 & 0 \\ 1 & -2 & 1 \\ 0 & 0 & 0 \end{bmatrix},$$

$$h_{yy} = \frac{1}{\sqrt{6}}\begin{bmatrix} 0 & 1 & 0 \\ 0 & -2 & 0 \\ 0 & 1 & 0 \end{bmatrix},$$

$$h_{xy} = \frac{1}{\sqrt{6}}\begin{bmatrix} -1 & 0 & 1 \\ 0 & 0 & 0 \\ 1 & 0 & -1 \end{bmatrix}. \tag{7}$$

Optimization by Mean-Field Annealing

With the noise term and the prior term, the objective function can be written as $H = H_n + H_p$, and f is pursued such that H can reach its minimum. To solve this optimization problem, we use the MFA technology [3, 4]. MFA follows a particular methodology (the mean-field approximation) to derive a minimization method that will combine *gradient descent* and annealing to find the global minimum. We consider the noise term and the prior term separately.

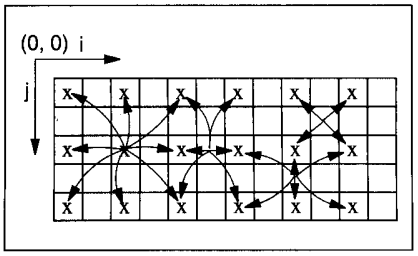

5. Four distinct cases in the reverse convolution of Eq. (8), as indicated by the centers of the four clusters: (1) when *i* and *j* are both even, (2) when *i* is even but *j* is odd, (3) when *i* is odd but *j* is even, and (4) when *i* and *j* are both odd (*x* indicate pixels with a measurement).

An initial estimate of the image and an initial temperature T_{initial} must be made at the start of the annealing process. In the case of 2:1 zooming, since three-quarters of the pixels do not have any corresponding measurements, we use linear interpolation to estimate the initial values of those pixels.

The partial derivative of H with respect to $f_{i,j}$ is required in order to perform the gradient descent component of the MFA optimization, resulting in:

$$\frac{\partial H_n}{\partial f_{i,j}} = \frac{((f \otimes h)_{i,j} - g_{i,j}) \otimes h_{rev}}{\sigma^2} \tag{8}$$

$$\frac{\partial H_p}{\partial f_{i,j}} = \left(\frac{\beta}{T^3}\right) \cdot \left(\left((f \otimes r)\exp\left(-\frac{(f \otimes r)^2}{2T^2}\right)\right)_{i,j} \otimes r_{rev}\right) \tag{9}$$

where the terms h_{rev} and r_{rev} denote the kernels h and r, with elements reversed about the origin of the kernel, respectively. When performing the reverse convolution in Eq. (8), four distinct cases (Fig. 5) need to be identified, since convolution can only be taken over pixels in g where they are measured.

The gradient descent then can be carried out as:

$$f^{k+1}_{i,j} = f^k_{i,j} - \alpha \frac{\partial H}{\partial f_{i,j}} \tag{10}$$

where α is the step size, and

$$\frac{\partial H}{\partial f_{i,j}} = \frac{\partial H_n}{\partial f_{i,j}} + \frac{\partial H_p}{\partial f_{i,j}}.$$

See [20] for details on the selection of step size.

The annealing minimization process starts with large T and gradually reduces the temperature over time. This process avoids most local minima and produces an optimal reconstructed image with increased resolution based on the knowledge of blur, noise, and the a-priori model of the image. This is the *optimal interpolation* that adopts MFA technology.

Experiments and Results

Fifteen studies were acquired, with three breast TIR images in each study. In order to increase the blood flow to the skin, patients were cooled for 10 min in a 68° room and then moved into a 72° room to be imaged. An Inframetrics 600M scanner, which uses a scanning mirror for image acquisition, was used. The images include five patients with normal TIR breast images, five patients who were normal but had abnormal TIR breast images (therefore were at high risk for breast cancer), and five patients with breast cancer confirmed positive by biopsy. All the images were zoomed using the above optimal interpolation algorithm and two other conventional zooming methods (pixel replication and linear interpolation [9]).

Experiments were carried out on both synthetic images and real images. This article shows the comparison results based on one synthetic image and one real image. More results are presented in [20] and at our website [17].

Performance Evaluation Based on Synthetic Image

The simplest synthetic image is the checkerboard. We created a checkerboard

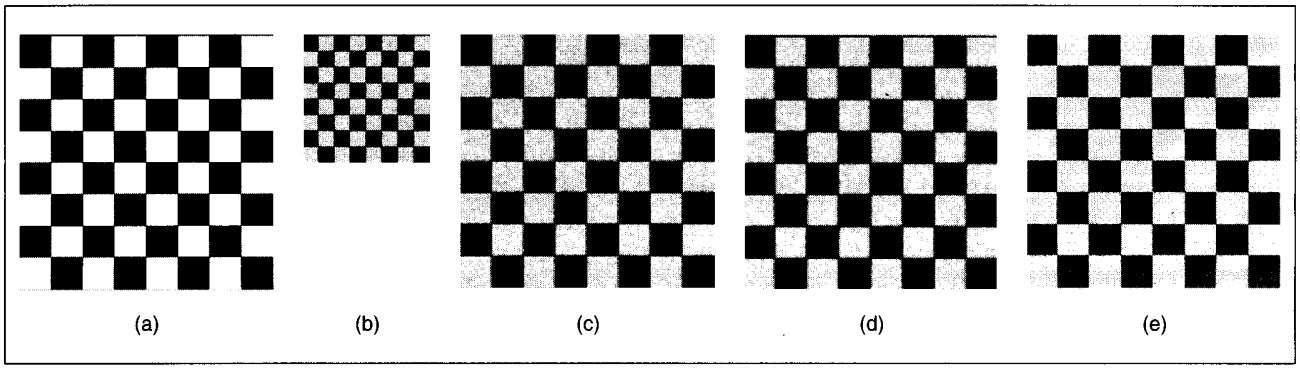

6. Results from checkerboard images. (a) Original image, (b) subsampled measured image, (c) zooming by pixel replication, (d) zooming by linear interpolation, and (e) zooming by optimal interpolation.

pattern of 64 squares with a resolution of 256×256, with intensity levels of 100 and 200. The original image was blurred by a 3×3 Gaussian kernel, corrupted by zero-mean stationary Gaussian noise with a signal-to-noise ratio (SNR) of 24 dB, and subsampled to create the measured image. Figure 6 shows the original synthetic image, the subsampled measured image, and the zoomed images from the three zooming algorithms.

To quantitatively compare the performance of the three zooming algorithms, we used histograms, difference images, and the mean-square error (MSE) to do the analyses.

Figure 7 shows the histograms of the three zoomed images. From the histogram distributions, we can see that the optimal interpolation generates a much more favorable result in comparison with the other two, with a distribution having two narrow sharp peaks corresponding to the original binary image. In contrast, the image zoomed by pixel replication has two side peaks that are due to blur at the edge in addition to the two main peaks. Linear interpolation (Fig. 7, center) cannot correct the blur and there is a continuous gray-level distribution between two peaks.

The difference image is another way to detect if the zoomed images have kept most of the characteristics of the original and have removed much noise. If so, the difference image should be much like a plain surface with only noise on it. Figure 8 is the difference images obtained by subtracting the zoomed image from the original clear image.

MSE is computed by taking the average of the summation of squared errors/difference. Figure 9 is a comparison of MSE values under different SNR. We can see that optimal interpolation always has the smallest MSE. The MSE curve from optimal interpolation tends to increase slower than those from pixel replication and linear interpolation.

Performance Evaluation Based on TIR Images

From the comparison results based on the synthetic image, we observe that the optimal interpolation has better performance than the other two algorithms. Figure 10 presents one of the TIR images, its subsampled version, and the images zoomed by the three algorithms mentioned above. One can see that the image zoomed by MFA has less noise than that

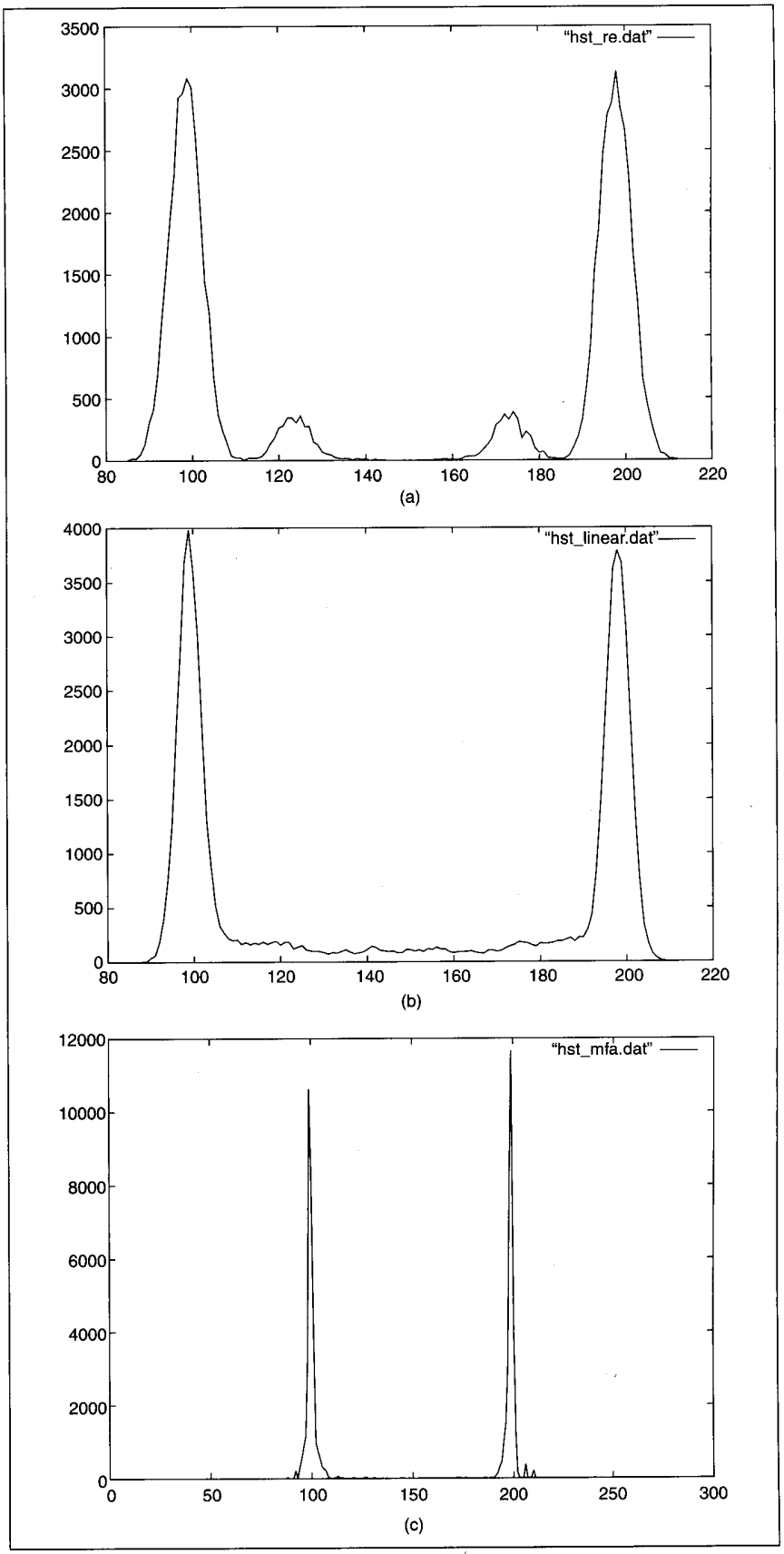

7. Histogram distributions of the three zoomed images. (a) Pixel replication, (b) linear interpolation, and (c) optimal interpolation.

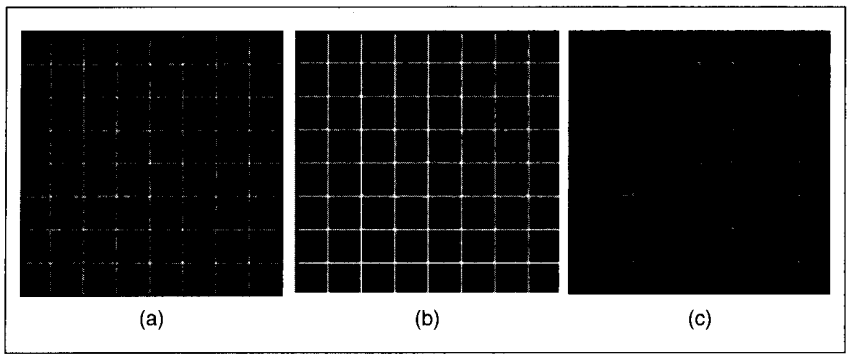

8. Difference images between the zoomed images and the original image. (a) Pixel replication, (b) linear interpolation, and (c) optimal interpolation.

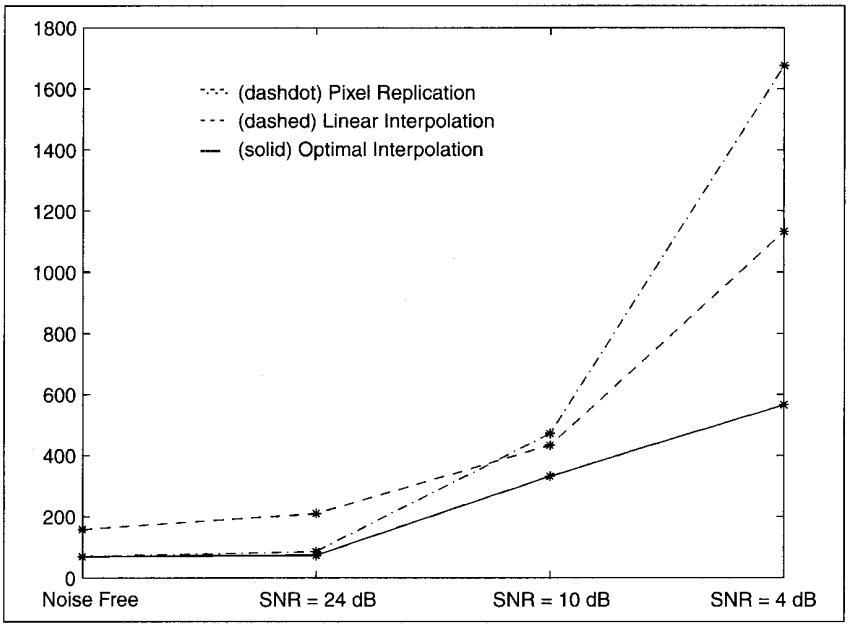

9. MSE from the three difference images with different SNRs.

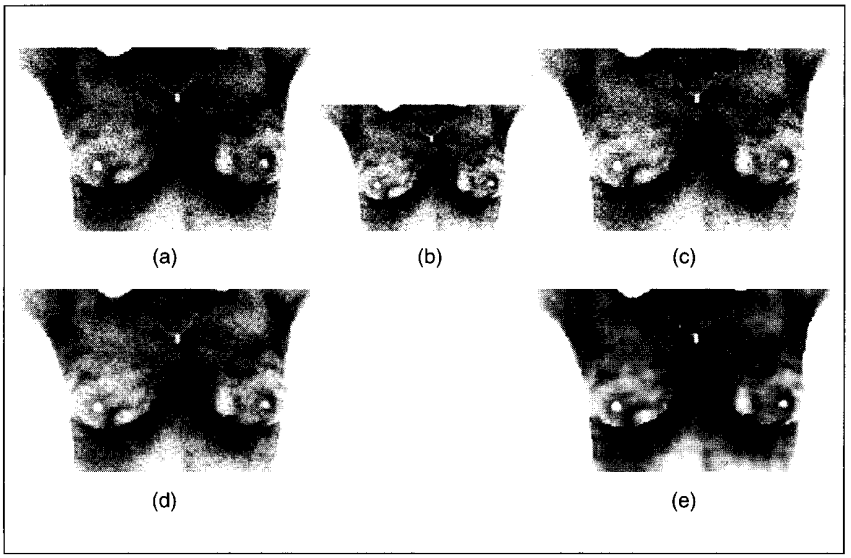

10. Results from TIR images. (a) Original image, (b) subsampled measured image, (c) zooming by pixel replication, (d) zooming by linear interpolation, and (e) zooming by optimal interpolation.

from pixel replication or linear interpolation. While the noise is removed to a great extent, MFA performs better in preserving the detail characteristics of the original image, especially the sharp edges.

To compare the results quantitatively, we used two methods: row/column profile comparison and difference images. We did not use histograms in this test image because the original image does not possess the obvious characteristics as from the checkerboard.

The row/column profile comparison draws the intensity profiles with respect to the same row/column of the three zoomed images. This method can discern in great detail how each zooming algorithm preserves the characteristics of the original image, and how much noise can be removed. Figure 11 displays the intensity profiles of the four images in Fig. 10 at row 40 and column 120, respectively. It is clear that the profiles from optimal interpolation [Fig. 11(d) and (h)] are much smoother than the others, while at the same time restoring the features of the original profile very well.

Figure 12 shows the difference between the zoomed images and the original. We can see that (c) possesses the best effect.

Conclusion

We proposed to use the optimal interpolation algorithm to increase the resolution of TIR images by a factor of 2. The algorithm is based on MAP, which estimates the missing data based on the measured image. The quality of the estimation is formulated into an objective function, where MFA is used to solve the optimization problem. The optimal interpolation algorithm is compared with pixel replication and linear interpolation. From the comparison results, both quantitatively and qualitatively, we claim that the optimal interpolation algorithm performs better, especially with increasing noise. It can increase the image resolution, while at the same time reducing noise and preserving the edges of the original image.

Wesley E. Snyder is professor and director of the Center for Advanced Computing and Communication at North Carolina State University. He received his B.S. in electrical engineering at North Carolina State University (1968) and his M.S. and Ph.D. in electrical engineering

from the University of Illinois in 1971 and 1975, respectively. His research interests include image processing and analysis. His best-known work concerns pattern recognition with applications to robot vision, and recent efforts involve implementing computer vision algorithms in neural networks and medical image processing. Snyder is also an adjunct professor of radiology at the Bowman Gray School of Medicine, where he directs research in computer processing of images from computed tomography, ultrasound, position emission tomography (PET), and magnetic resonance imaging (MRI).

Hairong Qi received her Ph.D. in computer engineering from North Carolina State University in 1999, her B.S. (1992) and M.S. (1995) in computer science at Northern JiaoTong University, Beijing, P.R. China. She is currently an assistant professor in the Department of Electrical and Computer Engineering at the University of Tennessee, Knoxville. Her major research areas are image restoration, global optimization, content-based image retrieval, and digital mammography.

Robert L. Elliott was born in Greenville, MS, in 1936. He received his M.D. from the University of Mississippi School of Medicine in 1961. He did a residency in general and thoracic surgery from 1961 to 1967 at the University of Mississippi School of Medicine and did a traineeship in electron microscopy at Washington University during his residency. He was in private practice of general and thoracic surgery from 1967 to 1973 in Anniston, AL. In 1974, he moved to Baton Rouge, LA, and founded the Elliott Mastology Center, which consists of the Breast Clinic and the Mastology Research Institute. He received his Ph.D. from LaSalle University in 1994. He limits his practice to the areas of prevention, early diagnosis, treatment, and research of diseases and cancer of the breast.

Jonathan F. Head is the director of research at the Mastology Research Institute of the Elliott Mastology Center and director of research and development of Medical Thermal Diagnostics in Baton Rouge, LA. He obtained his B.S. in zoology from Syracuse University, his M.A. in biology from Brooklyn College of CUNY, and his Ph.D. in biology from Fordham University. He was in the Division of Cell Biology of Naylor Dana Institute for Disease Prevention of the American Health Foundation, NY (1974-1978); the Department of Immunology at Cornell University Medical School, NY (1978); the Department of Pediatrics at Mt. Sinai Medical School, NY (1978-1987); and the director/department head of tumor cell biology at the Center for Clinical Sciences, International Clinical Laboratories, TN (1986-1988). In 1988, he moved to Baton Rouge, LA, to become president of the Mastology Research Institute and is both the director of research and director of the clinical laboratory. He has appointments in the Department of Biochemistry at Tulane University School Medicine and the Department of Physical Sciences at Delta State University.

Cliff X. Wang received his B.S. in electrical engineering from Zhejiang University, China, in 1983; his M.S. in biomedical engineering from Akron University, OH, in 1992; and his Ph.D. in computer engineering from North Carolina State University in 1996. He has worked at various engineering positions at Gould Electronics Inc., Bowman Gray School of Medicine, and IBM. He is currently working for Ascend Communication on internetworking projects. He has published over 16 technical papers, and he filed for five patents during his employment with IBM.

Address for Correspondence: Wesley E. Snyder, Center for Advanced Computing and Communication, North Carolina State University, Box 7914, Raleigh, NC 27695-7914. Tel: +1 919 515 5114. Fax: +1 919 515 2285. E-mail: wes@eos.ncsu.edu.

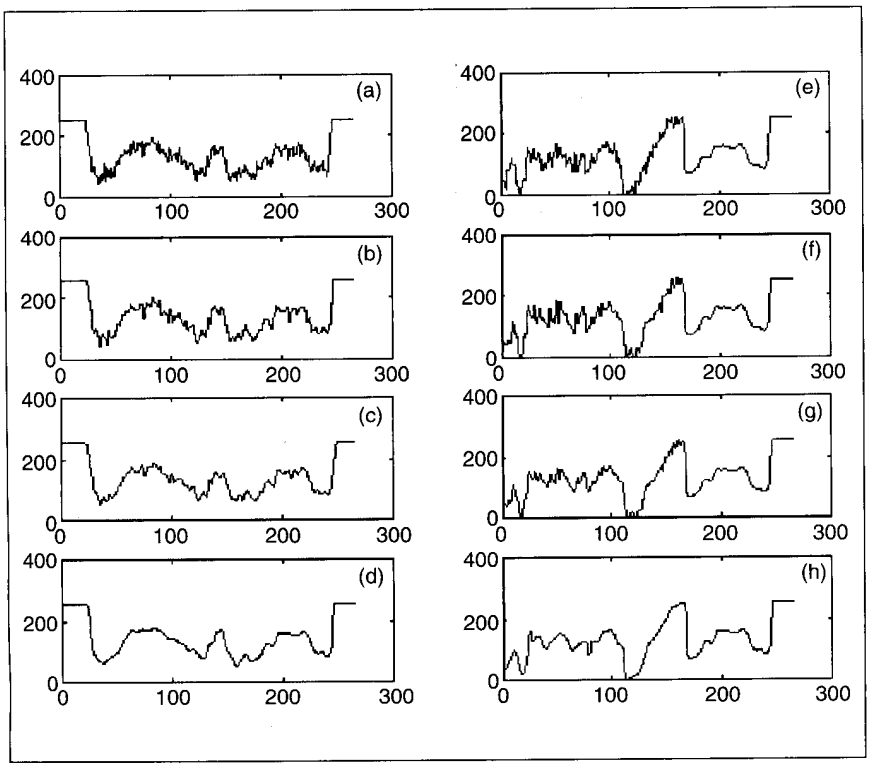

11. Intensity profile. Left is from row 40, right is from column 120. (a), (e) from original image; (b), (f) from pixel replication; (c), (g) from linear interpolation; (d), (h) from optimal interpolation.

References

1. **Anbar M:** *Quantitative Dynamic Telethermometry in Medical Diagnosis and Management.* Boca Raton, FL: CRC Press, 1994.

2. **Besag J:** On the statistical analysis of dirty pictures. *J R Statist Soc B* 48(3): 259-302, 1986.

3. **Bilbro G, Mann R, Miller T, and Snyder W:** Optimization by mean field annealing. In: *Ad-*

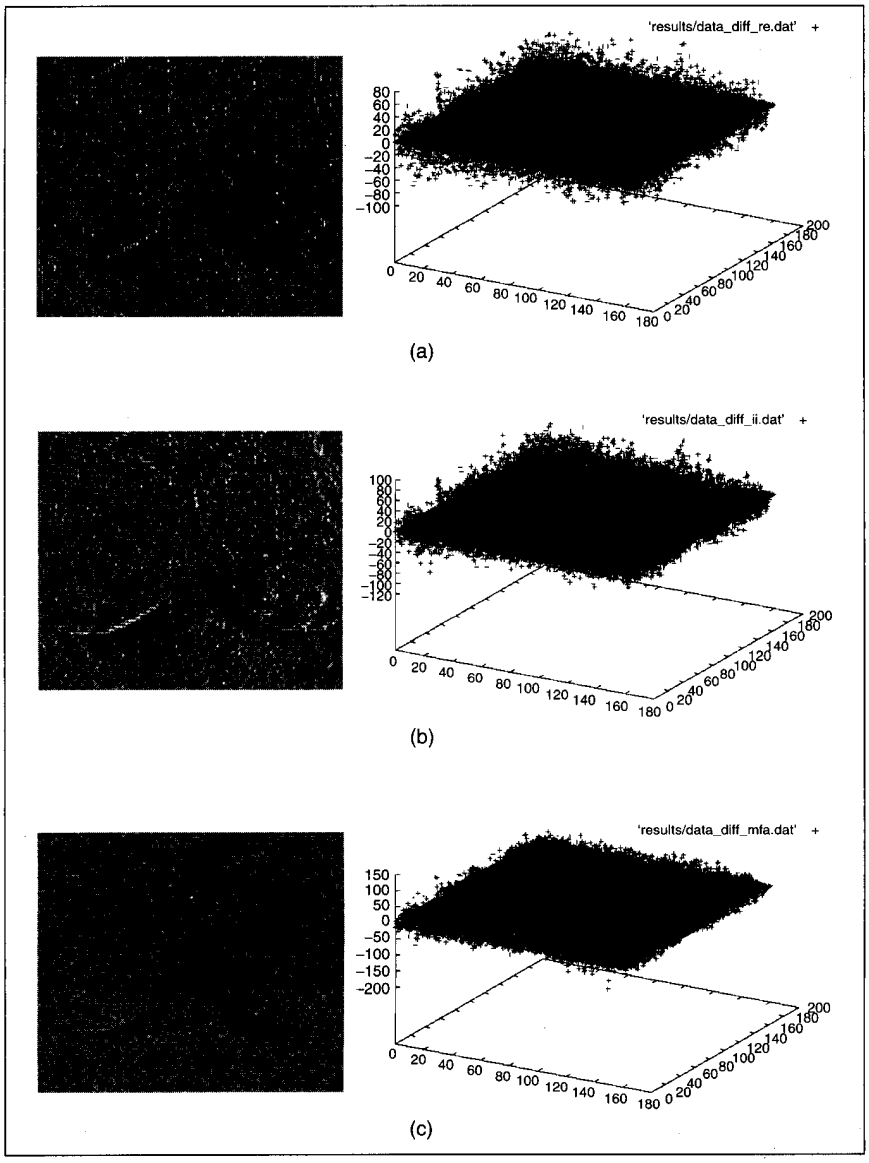

12. Difference images and their range representations from: (a) pixel replication, (b) linear interpolation, and (c) optimal interpolation.

vances in Neural Information Processing Systems. Vol 1. San Mateo, CA: Morgan Kaufmann Publishers, pp. 91-98, 1989.

4. **Bilbro G and Snyder W:** Range image restoration using mean field annealing. In: *Advances in Neural Information Processing Systems*. Vol. 1. San Mateo, CA: Morgan Kaufmann Publishers, pp. 594-601, 1989.

5. **Blake A and Zisserman A:** *Visual Reconstruction*. Cambridge, MA: MIT Press, 1987.

6. **Bothmann GA and Kubli F:** Plate thermography in the assessment of changes in the female breast. 2. Clinical and thermographic results. (Ger) *Fortschr Med* 102: 390-393, 1984.

7. **Gautherie M, Yahyai A, Dehlinger S, De Prins J, and Walter J:** Computerized chronothermodynamic breast examinations under ambulatory conditions. *Chronobiol Int* 7: 239-243, 1990.

8. **Geman S and McClure D:** Bayesian image analysis: An application to single photon emission tomography. *Proc Statistical Comp Sect*, Am Statistical Association, Washington DC, pp. 12-18, 1985.

9. **Gonzalez R and Woods R:** *Digital Image Processing*. Reading MA: Addison-Wesley, 1987.

10. **Head J, Wang F, and Elliott R:** Breast thermography is a noninvasive prognostic procedure that predicts tumor growth rate in breast cancer patients. *Ann NY Acad Sci* 698: 153-158, 1993.

11. **Head J, Lipari C, Wang F, Davidson J, and Elliott R:** Application of second generation infrared imaging with computerized image analysis to breast cancer risk assessment. *Proc 18th Annual Int Conf IEEE Engineering in Medicine and Biology Society* 18(5): 2093-2094, Amsterdam, Netherlands, 1996.

12. **Hebert T and Leahy R:** A generalized EM algorithm for 3D Bayesian reconstruction from Poison data using Gibbs priors. *IEEE Trans Med Imaging* 8(2): 194-202, June 1989.

13. **Jackson VP, Hendrick RE, Feig SA, and Kopans DB:** Imaging of the radiographically dense breast. *Radiology* 188: 297-301, 1993.

14. **Perre CI, de Hooge P, Hustinx PA, and Muller JW:** Ultrasonographic study of the palpable breast tumor is very useful. (Dut) *Ned Tijdschr Geneeskd* 137: 2374-2377, 1993.

15. **Ring F:** Criteria for thermal imaging in medicine. *Proc 17th Annual Conf IEEE Engineering in Medicine and Biology Society and 21st Canadian Medical and Biological Engineering Conf* 17(2): 1697-1698, Montreal, Canada, 1995.

16. **Soini IH:** Thermography in suspected deep venous thrombosis of lower leg. *Eur J Radiol* 5: 281-284, 1985.

17. http://www4.ncsu.edu/eos/users/w/wes/homepage/superresolution.html.

18. **Usuki H, Takashima S, Saeki H, and Moriwaki S:** Thermographic diagnosis of breast disease. (Jpn) *Gan No Rinsho* 32: 958-960, 1986.

19. **Usuki H:** Evaluation of the thermographic diagnosis of breast disease - Relation of thermographic findings and pathologic findings of cancer growth. (Jpn) *Nippon Gan Chiryo Gakkai Shi* 23: 2687-2695, 1988.

20. **Wang CX:** Optimal image interpolation using optimal method. Ph.D. dissertation, North Carolina State University, 1996.

PROCEEDINGS REPRINT

SPIE—The International Society for Optical Engineering

Reprinted from

Infrared Technology and Applications XXIII

20–25 April 1997
Orlando, Florida

Volume 3061

Cancer risk assessment with a second generation infrared imaging system

Jonathan F. Head, Charles A. Lipari, Fen Wang, and Robert L. Elliott

Medical Thermal Diagnostics, LA Business & Technology Center, Baton Rouge, LA 70803

ABSTRACT

Infrared imaging of the breasts for breast cancer risk assessment with a second generation Amber indium antimonide focal plane staring array system was found to produce images superior to a first generation Inframetrics scanning mercury cadmium telluride system. The second generation system had greater thermal sensitivity, more elements in the image and greater dynamic range, which resulted in a greater ability to demonstrate asymmetric heat patterns in the breasts of women being screened for breast cancer. Chi-square analysis for independence of the results from 220 patients with both the scanning and focal plane infrared imaging systems demonstrated that the results from the two systems were strongly associated with each other (p=.0001). However, the improved image from the second generation focal plane infrared imaging system allowed more objective and quantitative visual analysis, compared to the very subjective qualitative results from the first generation infrared imaging system. The improved image also resulted in an increase in the sensitivity for asymmetric heat patterns with the second generation focal plane system and yielded an increase in the percentage of patients with an abnormal asymmetric infrared image of the breasts from 32.7% with the scanning system to 50.5% with the focal plane system. The greater sensitivity and resolution of the digitized images from the second generation infrared imaging system has also allowed computer assisted image analysis of both breasts, breast quadrants and hot spots to produce quantitative measurements (mean, standard deviation, median, minimum and maximum temperatures) of asymmetric infrared abnormalities.

Keywords: thermography, infrared imaging, breast cancer, focal plane array, risk assessment

1. INTRODUCTION

Early studies of infrared imaging of the breast concentrated on its ability to detect and diagnose breast cancer. Mammography and infrared imaging, commonly called thermography in medicine, were compared for detection and diagnostic ability in the United States during the Breast Cancer Detection and Demonstration Projects between 1973 and 1981, but infrared imaging was discontinued after only a few years. Collection of infrared images of the breast was discontinued because of the poor quality of the infrared images being collected. The poor quality of the images was a result of the lack of standardization of instrumentation, the lack of trained technical personnel to maintain high quality infrared imaging, and the lack of trained radiologists to interpret the infrared images. Unfortunately the collection of infrared image was abandoned before enough data could be collected to be analyzed for significance in terms of detection and diagnosis. Further no risk assessment or prognostic significance information for infrared imaging was generated from the Breast Cancer Detection and Demonstration Projects.

Beginning in the 1980s studies supporting the use of infrared imaging in breast cancer risk assessment[1,2,3] began to be published. Gautherie and Gros[1] in a study of 58,000 patients found 784 patients with normal physical, mammographic and ultrasound findings who had abnormal infrared images of the breasts. Of these 784 patients 298 (38%) were diagnosed with breast cancer within 4 years, and this was the first compelling evidence that asymmetric infrared abnormalities of the breasts is a high risk marker for breast cancer. Stark[2] followed with a second study in 1985 which demonstrated that 23% (346 of the 1499 women with abnormal infrared images of the breast, while screening a total of 11,249 women) of the women with abnormal infrared images of the breast were diagnosed with cancer within the next ten years. This study further showed that women with abnormal infrared images of their breasts had a higher incidence of breast cancer (23%) than nulliparitous women (8.1%) or women with a family history of breast cancer (8.6% with either

SPIE Vol. 3061 • 0277-786X/97/$10.00

one or two first degree relatives). Although women with breast biopsies containing extensive hyperplasia and atypia had a 30% to 50% incidence of breast cancer in this study[2] there were only 34 women who had previous breast biopsies, and this is too small a number of woman at risk to allow major changes in incidence through prevention or intervention.

Although several studies have been reported supporting the application of infrared imaging for risk assessment in breast cancer, there still remained an unacceptably high false positive rate (women with an asymmetric infrared abnormality and a normal mammogram) of about 25% for infrared imaging of the breasts. This high false positive rate was due to the low quality of the first generation infrared imaging technology and the very subjective qualitative visual analysis of the results. We believe that the application of second generation infrared imaging systems, with greater sensitivity, improved resolution and the ability to do sophisticated real time computer assisted image analysis of the digitized images of breast heat patterns, should yield standard, reproducible qualitative and quantitative results, that will be applicable to risk assessment, detection, diagnosis and prognosis of breast cancer. Thus, the present study was undertaken to determine if improvements in infrared technology that have been incorporated into the second generation focal plane staring array Amber infrared imaging system can improve the images used for risk assessment in breast cancer.

2. MATERIALS AND METHODS

We recorded 3 breast views (right lateral, left lateral and frontal views) of 220 patients with the Amber focal plane staring array infrared imaging system at the Elliott Mastology Center. The 3 images were digitized and stored on computer hard disk during the study period. We independently analyzed the same 220 patients with the Inframetrics scanning infrared imaging system (right lateral, left lateral and frontal views) using hard copy photographic images (color frontal view and the three black and white views comparable to the Amber digitized images) of the patients that were being screened with mammography and routinely undergoing infrared imaging of their breasts during the study.

The first methodological decision we made, concerning infrared data analysis, was to try to quantitate the asymmetric abnormalities that were present in the Amber images (Table 1). Previously, with the Inframetrics system, we called

TABLE 1
SCORING OF RESULTS FORM THE INFRAMETRICS AND AMBER SYSTEMS

ABNORMALITY	INFRAMETRICS SYSTEM SCORE	AMBER SYSTEM SCORE
ASYMMETRIC SMALL FOCAL HOT SPOT	YES OR NO	0, 1
ASYMMETRIC LARGE FOCAL HOT SPOT	YES OR NO	0, 2
ASYMMETRIC GLOBAL HEAT	YES OR NO	0, 3
ASYMMETRIC VASCULAR HEAT	YES OR NO	0, 1, 2, 3
ASYMMETRIC AREOLAR HEAT	YES OR NO	0, 1
ASYMMETRIC EDGE HEAT	YES OR NO	0, 1

breast infrared images abnormal if any of the six asymmetric abnormalities were definitely present. Inframetrics images that only had a borderline infrared abnormality were called slightly abnormal (3 levels of results: normal, slightly abnormal, abnormal). For the Amber data we created a quantitative index by adding together the individual scores (Table 1) for the six possible asymmetric abnormalities (small hot spot, large hot spot, global heat, vascular heat, areolar heat and edge heat). The Amber Index could therefore range from 0 to 8 but the highest Amber Index that we computed was five.

3. RESULTS

Table 2 presents a comparison of the features of the Amber and Inframetrics imaging systems. The Amber system produced a much better image because of the focal plane staring array that contained far greater elements, and increase in dynamic range from 8 to 12 bits/element and an increase in thermal sensitivity from 100mK to 25mK. In addition the Amber image was outputed in a digital format that lends itself to image analysis.

TABLE 2
COMPARISON OF FEATURES BETWEEN THE INFRAMETRICS AND AMBER SYSTEMS

INFRAMETRICS SYSTEM	AMBER SYSTEM
First Generation	Second Generation
Scanning Mercury Cadmium Telluride Detector	Indium Antimonide Focal Plane Array
Liquid Nitrogen Cooler	Stirling Cycle Cooler
175 Elements/Line @Line Rate: 7866Hz RS-170/NTSC	256 x 256 Elements - Staring Array
Dynamic Ratings: 8 Bits/Element	Dynamic Range: 12 Bits/Element
Thermal Sensitivity: 100mK@30°C	Thermal Sensitivity: 25 mK@30°C
Spectral, Range: 8-12 Microns	Spectral Range: 3-5 Microns
External Calibration	Internal Calibration
Video Output: Analog	Video Output: Either Digital or Analog

The first comparison (Table 3) we made on the normal and high risk patients being screened for breast cancer was to

TABLE 3
COMPARISON OF INFRARED RESULTS WITH THE INFRAMETRICS AND AMBER SYSTEMS

AMBER SYSTEM	INFRAMETRICS SYSTEM		
AMBER INDEX	NORMAL	SLIGHTLY ABNORMAL	ABNORMAL
0	87/220 (39.5%)	12/220 (5.5%)	10/220 (4.5%)
1	23/220 (10.5%)	5/220 (2.3%)	4/220 (1.8%)
2	22/220 (10.0%)	16/220 (7.3%)	10/220 (4.5%)
3	10/220 (4.5%)	1/220 (0.5%)	4/220 (1.8%)
4	5/220 (2.3%)	0/220 (0.0%)	6/220 (2.7%)
5	1/220 (0.5%)	1/220 (0.5%)	3/220 (1.4%)

p=.0001, chi-square analysis for independence

determine if the results from the second generation Amber infrared imaging system differed from the results from the Inframetrics system. Chi-square analysis for independence showed that the two methods produced results that were not independent and therefore were strongly associated (p=.0001). The most interesting result was that there appeared to be an increase in the sensitivity for picking up asymmetric heat patterns with the Amber system, as 50.5% (111 of 220 patients without breast cancer) had abnormal infrared imaging, whereas only 32.7% (72 of 220 patients) had asymmetric heat patterns with the Inframetrics system. Analysis of the six asymmetric abnormalities individually (Table 4) showed

TABLE 4
DISTRIBUTION OF ABNORMALITIES FOR INFRAMETRICS AND AMBER INFRARED IMAGING SYSTEMS

ABNORMALITY	INFRAMETRICS SYSTEM	AMBER SYSTEM
ASYMMETRIC SMALL FOCAL HOT SPOT	41/218 (18.8%)	28/220 (12.7%)
ASYMMETRIC LARGE FOCAL HOT SPOT	3/218 (1.4%)	35/220 (15.9%)
ASYMMETRIC GLOBAL HEAT	6/218 (2.8%)	2/220 (0.9%) p=.1434
ASYMMETRIC VASCULAR HEAT	43/218 (19.7%)	70/220 (31.8%) p=.0054
ASYMMETRIC AREOLAR HEAT	6/218 (2.8%)	14/220 (6.4%)
ASYMMETRIC EDGE HEAT	1/218 (0.5%)	0/220 (0.0%)

that most of the increase in sensitivity could not be attributed to the small and insignificant (p=.1434) increase in small hot spots, large hot spots and global heat from 22.9% (50 of 218 patients) with the Inframetrics system to 29.5% (65 of 220 patients) with the Amber system. However there was a significant increase (p=.0054) in vascular asymmetry from 19.7% (43 of 218 patients) with the Inframetrics scanning system to 31.8% (70 of 220 patients) with the Amber focal plane system.

Two known risk factors (family history of breast cancer and previous breast biopsy) were compared to the infrared imaging results from the Inframetrics scanning and Amber focal plane systems. Neither of these risk factors were found to correlate with the infrared imaging results and therefore infrared imaging results were found to be an independent risk factor in breast cancer. Women being screened for breast cancer, who come from a family with a history of breast cancer, are at 2- to 5-fold increased risk of developing breast cancer, if one or more first degree female relatives (mother, sister or daughter) have had breast cancer. In this study women were divided into two risk categories by either the presence or absence of a family history of breast cancer and compared by group to the results of their breast infrared imaging. When patients' results from infrared imaging, either levels determined by analysis of Inframetrics infrared imaging (Table 5) or the Amber Index (Table 6), were compared to patients' family history of breast cancer, it was found that there was no relationship between having a family history of breast cancer and having an abnormal asymmetric infrared pattern of the breasts. So it seems that an abnormal infrared image is a high risk marker for breast cancer that is independent of family history of breast cancer.

TABLE 5
INFRAMETRICS SYSTEM RESULTS BY FAMILY HISTORY OF BREAST CANCER

INFRAMETRICS SYSTEM	RISK ASSESSMENT	
	NORMAL (NO FAMILY HISTORY)	HIGH (FAMILY HISTORY)
NORMAL	80/213 (37.6%)	64/213 (30.0%)
SLIGHTLY ABNORMAL	21/213 (9.9%)	12/213 (5.6%)
ABNORMAL	17/213 (8.0%)	19/213 (8.9%)

p=.3903, chi-square analysis for independence

TABLE 6
AMBER SYSTEM RESULTS BY FAMILY HISTORY OF BREAST CANCER

AMBER SYSTEM	RISK ASSESSMENT	
AMBER INDEX	NORMAL (NO FAMILY HISTORY)	HIGH (FAMILY HISTORY)
NORMAL (0)	57/213 (26.8%)	49/213 (23.0%)
SLIGHTLY ABNORMAL (1,2)	45/213 (21.1%)	32/213 (15.0%)
ABNORMAL (>2)	16/213 (7.5%)	14/213 (6.6%)

p=.7971, chi-square analysis for independence

The second risk factor that we looked at was previous breast biopsy. It has been clearly shown in studies done by other investigators that patients who have had one or more previous breast biopsies are at increased risk of being diagnosed with breast cancer. This increased risk of developing breast cancer, that has been associated with having had a previous breast biopsy, is probably due to the ability of mammography to detect not only invasive cancerous lesions but also noninvasive cancerous lesions and benign lesions (such as atypical hyperplasia and microcalcifications) that put woman at increased risk of developing breast cancer. In other words, mammographic abnormalities, that lead to open surgical biopsy, are highly associated with invasive carcinomas and further are often caused by precursors of invasive carcinoma that put woman at increased risk of developing breast cancer. These abnormalities that are present in mammograms are probably also the cause of abnormal infrared images in breast cancer screening and at diagnosis of breast cancer. The Inframetrics analysis (Table 7) showed that there was a trend (p=.0747, chi-square analysis for independence) towards patients with abnormal infrared images of the breast having breast biopsies. This trend was not confirmed (p=.3582, Table 8) when the infrared images were digitized and saved with the Amber infrared system and the Amber Index compared to the history of breast biopsy.

Digitization of the higher quality infrared Amber images allowed quantitation of infrared abnormalities by computer assisted image analysis. The location of cancer in the breast is not random and each quadrant of the breast has been shown to have its own rate of occurrence with the upper outer quadrant containing the greatest proportion of tumors. Therefore, we devised a computer analysis method that would quadrant the breast by a defined reproducible method. In all the digital images a line is drawn from the chin to the nipple, then a second line is drawn to the lowest contour of the breast, and finally a third and forth line are drawn horizontally to the left and right margins of the breast (Figure 1). The

same is done for both the right and left breast and we determine the mean, standard deviation, median, minimum and maximum temperatures for each quadrant of the breast. Then these quantitative measurements were compared between the left and right breast to quantitate asymmetric infrared abnormalities.

TABLE 7
INFRAMETRICS SYSTEM RESULTS BY HISTORY OF PREVIOUS BREAST BIOPSY

INFRAMETRICS SYSTEM	RISK ASSESSMENT	
	NORMAL (NO PREVIOUS BIOPSY)	HIGH (PREVIOUS BIOPSY)
NORMAL	116/212 (54.7%)	28/212 (13.2%)
SLIGHTLY ABNORMAL	24/212 (11.3%)	9/212 (4.2%)
ABNORMAL	22/212 (10.4%)	13/212 (6.1%)

p=.0747, chi-square analysis for independence

TABLE 8
AMBER SYSTEM RESULTS BY HISTORY OF PREVIOUS BIOPSY

AMBER SYSTEM	RISK ASSESSMENT	
AMBER INDEX	NORMAL (NO PREVIOUS BIOPSY)	HIGH (PREVIOUS BIOPSY)
NORMAL (0)	84/212 (39.6%)	22/212 (10.4%)
SLIGHTLY ABNORMAL (1,2)	58/212 (27.4%)	18/212 (8.5%)
ABNORMAL (>2)	20/212 (9.4%)	10/212 (4.7%)

p=.3582 chi-square analysis for independence

FIGURE 1
GUIDELINES FOR BREAST QUADRANTS

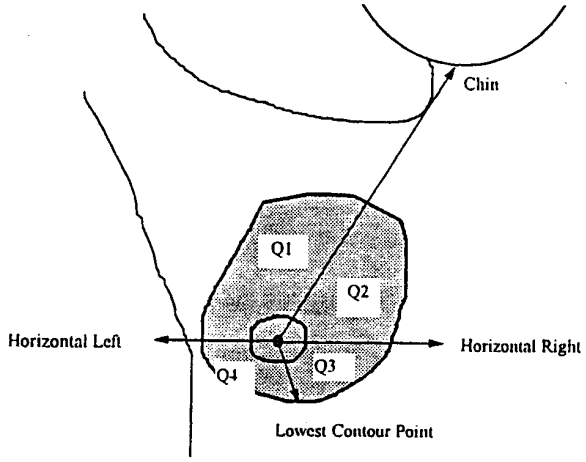

4. DISCUSSION

Infrared imaging of the breast for breast cancer risk assessment with a second generation focal plane staring array system was found to produce images superior to a first generation scanning system. The second generation system had greater thermal sensitivity, more elements in the image and a greater dynamic range, which resulted in a greater ability to demonstrate asymmetric heat patterns in the breasts of women being screened for breast cancer. Comparison of the infrared images from the two systems showed that the 12 bit Amber image was better than the 8 bit Inframetrics image, but the digitized images that were stored on the hard drive were not as good in either case as the analog output from either system. The 16 bit capacity of the Amber system will probably be needed in order for the quality of the recalled digitized image to reach that of the analog output, and for image analysis to reach its full potential. However we did conclude that the second generation Amber infrared images both analog and digital are better for medical applications than the first generation Inframetrics Images.

The improved imaging of the second generation infrared system increased the proportion of women with abnormal breast infrared images in a group of women being screened for breast cancer, and also allowed more objective and quantitative visual analysis, compared to the very subjective qualitative results of the first generation infrared system. Eventually we hope to demonstrate that the application of a simple index (the summation of a semiquantitation of asymmetric hot spots, global heat, vascularity, areolar heat and edge heat) and an appropriate cut-off level can decrease the high false positive rate to an acceptable level. This will require us to determine what types, levels or combination of types and levels of asymmetric abnormalities are most predictive of risk of developing breast cancer. The Amber Index seems to be more suited to this purpose, than the 3 levels of results from the Inframetrics system, because there are many levels (0 to 8 levels) with the Amber Index and we actually had 6 levels of the Amber Index. In this study 50% (111 of 220) of the patients were found to have some infrared abnormality of the breasts, when an Amber Index of zero was considered normal, but if an index of one is considered to be such a small abnormality that a patient's risk of developing breast cancer is not significantly increased, then approximately 36% (79 of 220) of the patients being screened for breast cancer would be categorized as high risk individuals. If an amber index of two is considered insignificant then 14% (31 of 220) of the patients being screened for breast cancer would have sufficiently abnormal infrared images to be at increased risk of developing breast cancer. We feel that 14% would be approximately the proportion of patients in our study group that would be at increased risk of developing breast cancer and therefore an index greater than two would put a patient at increased risk of developing breast cancer. However, a clinical follow-up study will be needed to determine how well we have delineated the women at high risk of developing breast cancer. From Table 3 it can also be seen that the patients, who are determined to be at increased risk of developing breast cancer, are different with the two systems, as 16 patients who have completely normal breast infrared images with the Inframetrics system had abnormal images (Amber Index greater than 2) with the Amber system and 24 other patients with normal Amber images (Amber Index less than or equal to 2) were abnormal with the Inframetrics system. Thus 18% (40 of 220) of the patients had significantly different infrared imaging results with the two systems and we are presently doing clinical follow-up studies to determine if the Amber Index is a better predictor of risk of developing breast cancer than the previous results with the Inframetrics system.

In the past the major shortcoming of infrared imaging of the breast has been its high false positive rate which is typically between 1/4 and 1/3 of women being screened for breast cancer. This seemingly high false positive rate is partly due to mammographers calling all abnormal infrared images of the breast false positives in woman with normal mammograms, instead of being considered at high risk of developing breast cancer -- mammographers have not accepted that an abnormal infrared image is an early predictor of breast cancer. Even though women with an abnormal infrared image of their breasts is very prevalent in the screening population and this would therefore require many high risk women to be followed at shorter intervals with mammography and clinical breast exam, the fact that approximately 25% of the women with abnormal infrared images will develop breast cancer warrants its inclusion in all breast cancer screening programs. We also believe that further improvements in infrared imaging systems and analysis, such as the Amber Index, will eventually allow the clinician to better define infrared abnormalities of the breast that translate into increased risk of breast cancer and therefore decrease the high false positive rate of infrared imaging of the breast.

Patients found to have abnormal infrared images during screening for breast cancer have previously been shown to be at higher risk of developing breast cancer[1,2,3]. This study has clearly shown that the presence of an abnormal infrared image in patients being screened by mammography for breast cancer is a high risk marker independent of the commonly used high risk markers of family history and previous breast biopsy. The improvement in risk assessment that could be

achieved by integrating infrared image analysis with family history and previous breast biopsy results could have significant impact on the selection of patients for breast cancer prevention studies. For example, in hormonal intervention studies with the antiestrogen tamoxifen the addition of infrared imaging results to the other parameters presently used to select patients for these hormonal therapy prevention study might define a group of women at high enough risk of developing breast cancer to warrant the extension of hormonal therapy intervention from only postmenopausal women to both premenopausal and postmenopausal women. This extension to premenopausal women would be possible because of an increase in the therapeutic index of the hormone prevention therapy, caused by decreasing the number of women treated (higher risk women being treated) and therefore increasing the proportion of women that benefit from the hormonal therapy, while the side effects and toxicities remain the same.

The greater sensitivity and resolution of the digitized images of the second generation infrared system has allowed image analysis of total breasts, breast quadrants and hot spots to produce mean, standard deviation, median, minimum and maximum temperatures. This will allow future analysis to be both quantitative and objective as opposed to the subjective qualitative analysis that has been the standard in the past for infrared imaging of the breasts.

In conclusion we believe that infrared imaging of the breast should be an integral part of any breast cancer screening program due to its value as an independent risk factor for breast cancer and its value as a prognostic indicator[4]. The use of improved second generation focal plane staring array infrared technology for breast cancer detection, diagnosis and as a high risk and prognostic indicator should lead to both earlier detection of breast cancer, thus increasing the overall survival of breast cancer patients, and aid in determining which node negative breast cancer patients should receive adjuvant chemotherapy. Continued development of objective computer assisted analysis methods of infrared images of the breast, that compare quantitative thermal parameters of the right and left breasts, will eventually eliminate the problems inherent in the presently used subjective qualitative analysis methods. Accomplishment of these goals should significant decrease the morbidity, mortality and overall cost of therapy for breast cancer patients.

ACKNOWLEDGEMENTS

This work was supported by a SBIR contract with the Army Night Vision Laboratory. We are also indebted to Raytheon for kindly lending us an Amber infrared imaging system for this study.

REFERENCES

1. M. Gautherie and C. M. Gros, "Breast thermography and cancer risk prediction", *Cancer* **45**, pp. 51-56, 1980.
2. A. M. Stark, "The value of risk factors in screening for breast cancer", *Eur. J. Cancer* **11**, pp. 147-150, 1985.
3. J. F. Head, F. Wang and R. L. Elliott, "Breast thermography is a noninvasive prognostic procedure that predicts tumor growth rate in breast cancer patients", *Ann. N. Y. Acad. Sci.* **698**, pp. 153-158, 1993.
4. H. J. Isard, C. J. Sweitzer and G. R. Edelstein, "Breast thermography: A prognostic indicator for breast cancer survival", *Cancer* **62**, pp. 484-488, 1988.

Further author information -
J.F.H.(correspondence): Email: thermal@premier.net; Telephone: 504-388-4245, 800-349-3970; Fax: 504-388-3975

Reprinted from Breast Cancer: From Biology to Therapy
Volume 698 of the *Annals of the New York Academy of Sciences*
November 30, 1993

Breast Thermography Is a Noninvasive Prognostic Procedure That Predicts Tumor Growth Rate in Breast Cancer Patients

JONATHAN F. HEAD, FEN WANG,
AND ROBERT L. ELLIOTT

The Elliott Mastology Center
1770 Physicians Park Drive
Baton Rouge, Louisiana 70816

INTRODUCTION

The Breast Cancer Detection and Demonstration Projects (BCDDP) that were carried out by the American Cancer Society and National Cancer Institute (USA) between 1973 and 1981 evaluated breast thermography as a diagnostic procedure for breast cancer. From the results of the BCDDP study the American Radiology Society concluded that thermography was ineffective as a diagnostic procedure in breast cancer. However, with the abandonment of breast thermography in the United States further large-scale studies to determine its value in predicting the risk of breast cancer and as a prognostic indicator were not pursued. This study demonstrates the prognostic significance of breast thermography for the breast cancer patient and further relates the thermal characteristics of the breast to the growth rate of the breast cancer patient's tumor.

MATERIAL AND METHODS

Two groups of patients were chosen to do the two parts of this study. The first group consisted of 126 deceased breast cancer patients (all women who had died of causes other than breast cancer were eliminated from the study), 100 randomly selected surviving breast cancer patients, and 100 randomly selected normal or noncancer patients, all of whom had undergone breast thermography in conjunction with mammography and clinical examination as part of their breast examination at The Elliott Mastology Center since 1973. The second group consisted of breast cancer patients that had thermography,

clinical/pathological staging, and laboratory testing of known prognostic indicators done since the beginning of 1989. Thermography was interpreted as abnormal when asymmetric heat patterns (focal hot spots, areolar and/or periareolar heat, vessel discrepancy, diffuse global heat, or thermographic edge signs) were found during routine thermographic exam. In the process of clinical/pathological staging the following information was obtained: tumor size (clinical and pathological), nodal status (clinical and pathological), presence of metastatic disease, age and location of tumor (left or right breast). Laboratory testing included the determination of the following prognostic indicators: estrogen and progesterone receptors by both the DCC-cytosol (DuPont; Billerica, MA) and immunocytochemical (Abbott Laboratories; Abbott Park, IL) methods, tumor tissue ferritin (Hybritech Inc.; San Diego, CA), ploidy and cell cycle analysis (S, G_2M) by flow cytometry, and Ki-67 by immunocytochemical method (Cell Analysis Systems; Lombardi, IL).

RESULTS AND DISCUSSION

In TABLE 1 are presented the results of thermography by patient disease status. Patients without cancer that came through the clinic for routine breast exams including clinical exam, thermography, and mammography had a high false-positive rate of 28%, when the results of thermography were compared to mammography. However, these false positives occurred in a population that is at a higher risk than the normal risk of approximately 10%. Gautherie and Gros,[1] and Stark[2] have shown that this group of patients with abnormal thermograms are at significantly higher risk for breast cancer, with occurrence rates of 38% (298/784) in the 4-year period following thermography and 23% (346/1499) in the 10-year period following thermography, respectively.

The prognostic significance of thermography is also demonstrated in TABLE 1, as the 126 deceased patients included a significantly higher proportion (88%) of patients with abnormal thermograms than the 65% for surviving cancer patients, a large proportion of which should have been cured by stan-

TABLE 1. Thermographic Results for Normal, Cancer, and Deceased Cancer Patients

Thermographic Results	Patients		
	Normal	Cancer	Deceased
Normal	72	35	15
	72%	35%	12%
Abnormal	28	65	111
	28%	65%	88%

NOTE: $p < 0.0001$, chi-square analysis for independence.

dard surgery, radiotherapy, and chemotherapy. This is in agreement with a study of 70 patients by Isard *et al.*[3] that clearly demonstrated the prognostic significance of thermography in breast cancer: 30% five-year survival of patients with abnormal thermograms compared to 80% survival with normal thermograms.

To determine if thermographic findings are an independent prognostic indicator, comparisons were made to the components of the TNM classification system. No significant differences were found in the pathological size of the tumor, clinical nodal status, pathological nodal status (number or % of positive nodes) between patients with normal and abnormal thermograms. There were not enough patients with extension of tumor to chest wall or skin, or with metastatic disease to evaluate thermography in relationship to these prognostic indicators. Breast cancer patients with abnormal thermograms had significantly ($p = 0.006$) larger tumors clinically than patients with normal thermograms. TABLE 2 shows the distribution of these patients' thermographic results by clinical size classification and clearly shows the increase in the percentage of patients with abnormal thermograms as the tumor size increases by T classification, so that all patients in this study with T3 tumors (tumors with diameters greater than 5.0 cm in diameter) had abnormal thermograms. Also, it is interesting to note that 53% (10/19) of patients with T1 tumors (less than 2.0 cm in diameter) had abnormal thermograms. Additional studies will be needed to determine if thermography is an effective prognostic indicator for stage I patients (54% of stage I patients had abnormal thermograms), and to see if thermography is useful in determining which stage I patients should be treated with adjuvant chemotherapy. Thermographic results were found to be unrelated to other information of prognostic significance (age, menopausal status, estrogen receptor status, and progesterone receptor status).

A correlation between the growth rate of tumors and their metabolic heat pattern has been demonstrated, and this results in patients with faster-growing tumors being more likely to have abnormal breast thermograms.[4] In TABLE 3 are the growth rate–related tissue ferritin concentrations for patients with normal and abnormal thermograms. There was a significantly higher ($p =$

TABLE 2. Chi-Square Analysis for Independence of Clinical Tumor Size and Thermographic Results

Thermographic Results	Clinical Size Classification		
	T1	T2	T3
Normal	9	14	0
Abnormal	10	31	10
% Abnormal	53	69	100

NOTE: $p = 0.0323$, chi-square analysis for independence.

TABLE 3. Comparison of Proliferation-Related Parameters to Thermographic Results

	Thermographic Results		
	Normal	Abnormal	Significance
Ferritin	762 ± 620 (21)[a]	1512 ± 2027 (50)	$p = 0.021$[b]
Ploidy, % diploid	41 (7/17)	41 (9/22)	NS[c]
S-phase			
Diploid or aneuploid	2.90 ± 0.94 (11)	6.05 ± 4.13 (20)	$p = 0.004$[b]
Diploid and aneuploid	4.18 ± 2.27 (11)	9.35 ± 5.96 (20)	$p = 0.002$[b]
S-phase + G_2M-phase			
Diploid or aneuploid	5.63 ± 3.35 (11)	10.45 ± 6.65 (20)	$p = 0.012$[b]
Diploid and aneuploid	7.63 ± 4.15 (11)	14.65 ± 7.61 (20)	$p = 0.002$[b]

[a] Mean ± standard deviation (number of patients).
[b] Probability from Student's *t*-test.
[c] NS, not significant; chi-square analysis for independence.

0.021) concentration of ferritin in the tumors from patients with abnormal thermograms, which supports the concept that patients with abnormal thermograms have faster-growing tumors and poorer prognosis.[5] Ploidy analysis by flow cytometry showed no relationship to thermographic findings. Both the percent of cells in DNA synthesis (S-phase) and the percent of cells dividing (proliferative index = % S-phase + % G_2M-phase) were strongly associated with thermographic results (TABLE 3), and this was true when the S-phase and proliferative index were calculated by two different methods. In one method the percentages of S-phase and G_2M-phase cells were determined either from the diploid or aneuploid population, whereas in the second method the percentages from both the diploid and aneuploid populations were added together in aneuploid tumors. The results of immunocytochemical determination of Ki-67, a third method for determining cell proliferation,[6] are found in TABLE 4. The expression of this proliferation-associated antigen is related to thermographic results: patients with abnormal thermograms had a significantly higher proportion of tumors that were highly proliferative (greater Ki-67 expression). The association of all three of these proliferation-related prognostic indicators with thermographic results suggests that thermography is a noninvasive prog-

TABLE 4. Chi-Square Analysis of Ki-67 and Thermographic Results

Thermographic Results	Ki-67	
	Low	High
Normal	8	2
Abnormal	3	8

NOTE: $p = 0.021$, chi-square analysis for independence.

nostic procedure that is able to predict the growth rate of breast tumors, and could be useful for determining which stage I breast cancer patients would benefit from adjuvant chemotherapy.

SUMMARY

Our recent retrospective analysis of the clinical records of patients who had breast thermography demonstrated that an abnormal thermogram was associated with an increased risk of breast cancer and a poorer prognosis for the breast cancer patient. This study included 100 normal patients, 100 living cancer patients, and 126 deceased cancer patients. Abnormal thermograms included asymmetric focal hot spots, areolar and periareolar heat, diffuse global heat, vessel discrepancy, or thermographic edge sign. Incidence and prognosis were directly related to thermographic results: only 28% of the noncancer patients had an abnormal thermogram, compared to 65% of living cancer patients and 88% of deceased cancer patients. Further studies were undertaken to determine if thermography is an independent prognostic indicator. Comparison to the components of the TNM classification system showed that only clinical size was significantly larger ($p = 0.006$) in patients with abnormal thermograms. Age, menopausal status, and location of tumor (left or right breast) were not related to thermographic results. Progesterone and estrogen receptor status was determined by both the cytosol-DCC and immunocytochemical methods, and neither receptor status showed any clear relationship to the thermographic results. Prognostic indicators that are known to be related to tumor growth rate were then compared to thermographic results. The concentration of ferritin in the tumor was significantly higher ($p = 0.021$) in tumors from patients with abnormal thermograms (1512 ± 2027, $n = 50$) compared to tumors from patients with normal thermograms (762 ± 620, $n = 21$). Both the proportion of cells in DNA synthesis (S-phase) and proliferating (S-phase plus G_2M-phase, proliferative index) were significantly higher in patients with abnormal thermograms. The expression of the proliferation-associated tumor antigen Ki-67 was also associated with an abnormal thermogram. The strong relationships of thermographic results with these three growth rate–related prognostic indicators suggest that breast cancer patients with abnormal thermograms have faster-growing tumors that are more likely to have metastasized and to recur with a shorter disease-free interval.

REFERENCES

1. GAUTHERIE, M. & C. M. GROS. 1980. Breast thermography and cancer risk prediction. Cancer **45:** 51–56.
2. STARK, A. M. 1985. The value of risk factors in screening for breast cancer. Eur. J. Cancer **11:** 147–150.

3. ISARD, H. J., C. J. SWEITZER & G. R. EDELSTEIN. 1988. Breast thermography: A prognostic indicator for breast cancer survival. Cancer **62:** 484–488.
4. GAUTHERIE, M. 1980. Thermography of breast cancer: Measurement and analysis of *in vivo* temperature and blood flow. Ann. N.Y. Acad. Sci. **335:** 383–413.
5. WEINSTEIN, R. E., B. H. BOND & B. K. SILBERGER. 1982. Tissue ferritin concentration in carcinoma of the breast. Cancer **50:** 2406–2409.
6. BACUS, S. S., R. GOLDSCHMIDT, D. CHIN, G. MORAN, D. WEINBERG & J. W. BACUS. 1989. Biological grading of breast cancer using antibodies to proliferating cells and other markers. Am. J. Pathol. **135:** 783–792.

APPLICATION OF SECOND GENERATION INFRARED IMAGING WITH COMPUTERIZED IMAGE ANALYSIS TO BREAST CANCER RISK ASSESSMENT

Jonathan F. Head, Ph.D., Charles A. Lipari, Ph.D., Fen Wang, M.D., Ph.D., James E. Davidson, B.Ar. and Robert L. Elliott, M.D., Ph.D., Medical Thermal Diagnostics, LBTC, South Stadium Drive, Baton Rouge, LA 70803-6100, USA Telephone: 504-388-4245 FAX: 504-388-3975

ABSTRACT

Infrared imaging of the breast for breast cancer risk assessment with a second generation focal plane staring array system was found to produce images superior to a first generation scanning system. The second generation system had greater thermal sensitivity, more elements in the image and greater dynamic range, which resulted in a greater ability to demonstrate asymmetric heat patterns in the breasts of women being screened for breast cancer. The improved imaging of the second generation infrared system allowed more objective and quantitative visual analysis, compared to the very subjective qualitative results of the first generation infrared system. The greater sensitivity and resolution of the digitized images of the second generation infrared system also allowed image analysis of total breasts, breast quadrants and hot spots to produce mean, standard deviation, median, minimum and maximum temperatures.

KEY WORDS: Thermography, Infrared Imaging, Breast Cancer, Risk Assessment, Diagnosis

INTRODUCTION

Early studies of infrared (IR) imaging of the breast concentrated on its ability to diagnose breast cancer. Mammography and IR imaging, commonly called thermography in medicine, were compared for diagnostic ability during the Breast Cancer Detection and Demonstration Projects (USA) between 1973 and 1981, but IR imaging was discontinued after only a few years and no risk assessment or prognostic information was collected. Beginning in 1980 studies supporting the use of IR imaging in breast cancer risk assessment [1, 2, 3] and prognosis [3, 4] began to appear. The present study was designed to determine whether the improvements in IR technology that have been incorporated into the second generation focal plane indium antimonide detector IR imaging systems can improve the images used in breast cancer risk assessment.

METHODS

Patients at The Elliott Mastology Center (Baton Rouge, LA), who were being screened with mammography for breast cancer, underwent IR imaging of their breasts as part of their breast cancer risk assessment. During the study normal and high risk patients had IR images of their breasts taken with an Inframetrics scanning mercury cadmium telluride detector IR imaging system (right lateral, left lateral and frontal views) and recorded as hard copy photographic images (a color frontal isotherm view and three black and white views: frontal, left lateral and right lateral). For comparison 3 additional breast views (frontal, right lateral and left lateral) were recorded with an Amber focal plane indium antimonide staring array IR imaging system. IR images of 220 patients from both the scanning and focal plane systems were digitized and stored on computer hard disk, thus creating a digitized IR image database for later image analysis.

RESULTS

The focal plane array system produced much higher quality images than the scanning system. However the focal plane system often placed a great proportion of the patient's IR heat pattern beyond the upper limit of the heat range being recorded and thus blacked out the patient (black is hot in medical applications). The blacking out occurred because the averaging window for determining the temperature range had too much cool background when imaging thin patients. The first decision made was to try to quantitate the six individual asymmetric abnormalities that were present in the focal plane images and then to create an IR index by adding together the individual scores for each abnormality (small hot spot, score=1; large hot spot, score=2; global heat, score=3; vascular heat, score=1,2,3; areolar heat, score=1; edge heat, score=1). The focal plane images had IR indexes that ranged from 0 to 8 but the highest index computed was five. Previously, scanning IR images were abnormal if any of the six asymmetric abnormalities were present, and images that only had a borderline IR asymmetry were called slightly abnormal (3 levels of results: normal, slightly abnormal, abnormal).

The IR indexes derived from the second generation focal plane imaging results were compared to the levels of abnormality from the scanning results on the patients being screened for breast cancer. Chi-square analysis for independence showed that the two methods produced results that were strongly associated ($p=.0001$). The most interesting result was an increase in the sensitivity for asymmetric heat patterns with the focal plane system. as 50.5% (111 of 220) of the patients without breast cancer had

abnormal IR images, whereas only 32.7% (72 of 220) of the patients had asymmetric heat patterns with the scanning system. Analysis of the six asymmetric abnormalities individually showed that most of the increase in sensitivity could be attributed to a significant (p=.0038) increase in vascular asymmetry from 43 of 218 patients with the scanning system to 70 of 220 with the focal plane system. Next the distribution of the IR index was compared to the levels of abnormality from the scanning images to determine if the increase in sensitivity of the second generation technology would create small subsets with higher IR indexes that could be used to refine risk assessment. When an IR index of 1 is considered to be so insignificant that a patient's risk of getting breast cancer is not increased and 2 is considered to only slightly increase risk, then 14.1% (31 of 220) of the patients being screened for breast cancer would be categorized as high risk individuals. On the other hand 37 of 220 patients had abnormal IR images with the scanning system and this would mean that 16.8% of the screened patients would be at high risk.

Three known risk factors (family history of breast cancer, previous estrogen hormone therapy and previous breast biopsy) were compared to the IR results from the scanning and focal plane systems. None of these risk factors were found to correlate with the IR imaging results and therefore IR imaging results were found to be an independent risk factor in breast cancer. The physician also assigned patients being screened for breast cancer into normal and high risk categories by subjectively integrating family history, mastopathy, previous use of estrogen hormones and previous breast biopsy. The results of this physician integrated risk assessment was also not related to the IR imaging results.

The final part of the study was an attempt to apply image processing and computer vision techniques to produce objective measures of asymmetric heat patterns present in second generation IR images employed in breast cancer risk assessment. Preliminary results showed that comparative pixel statistics (mean, standard deviation, median, minimum, maximum temperatures) could be computed for complete breasts, quadrants of the breast and hot spots.

DISCUSSION

The improved image of the second generation IR imaging system was due to the greater thermal sensitivity, greater number of elements and greater dynamic range of the focal plane array imager. The one major drawback encountered in this study was blacking out of patients and this will be corrected in the future by adjusting the center of the temperature range (set at either 7.5 or 10°C) of the focal plane imager to optimally take in the temperature range of the patients. This procedure for temperature focusing has been routinely used with scanning IR imagers and has worked very well in breast cancer risk assessment.

The proportion of patients at increased risk of breast cancer is probably still a little high with the second generation IR system, but the strength of the IR index is not in the overall proportion of patients that are at increased risk but with its ability to create different groups of patients at increased risk by adjusting the weight of the different abnormalities being inputted into the index. Future studies will be able to address the independent value of the 6 abnormalities and to create an index where the value of each abnormality will be appropriately weighted. This process of weighing the value of independent variables is not possible with the 3 level subjective analysis used with the scanning system.

In this study the lack of association between IR imaging results and known risk factors in patients being screened for breast cancer confirms that IR results are independent of known risk factors. Therefore, in light of the evidence [1, 2, 3] showing a strong association of asymmetric IR abnormalities of the breasts with a high risk of getting breast cancer, it can be concluded that abnormal IR images are a significant independent risk factor for breast cancer.

The comparative measurements resulting from the initial image analysis need to be done on a large database of focal plane images to determine their utility. Hopefully by removing the subjectivity of the present analysis and by providing additional information to the physician there will be an improvement in risk assessment by IR imaging. Models for the analysis of the breast IR images need to be developed that reduce perspective distortions that are inherent to imaging of 3 dimensional shapes and also to overcome the lack of ideal body symmetry due both to the natural asymmetry of the human body and also the spatial orientation of the imager to the subject. Finally the whole analysis must be automated, as highly interactive analysis is not conducive to the typical practice of medicine.

ACKNOWLEDGEMENTS

Financial support was provided through a SBIR contract with the Army Night Vision Laboratory. We are also indebted to Raytheon for kindly lending us an Amber infrared imaging system for this study.

REFERENCES

1. Gautherie M, Gros CM. Breast thermography and cancer risk prediction. *Cancer* 1980;**45**:51-6.
2. Stark AM. The value of risk factors in screening for breast cancer. *Eur J Cancer* 1985;**11**:147-50.
3. Head JF, Wang F, Elliott RL. Breast thermography is a noninvasive prognostic procedure that predicts tumor growth rate in breast cancer patients. *Ann N Y Acad Sci* 1993;**698**:153-8.
4. Isard HJ, Sweitzer CJ, Edelstein GR. Breast thermography: A prognostic indicator for breast cancer survival. *Cancer* 1988;**62**:484-8.

DETERMINATION OF MEAN TEMPERATURES OF NORMAL WHOLE BREAST AND BREAST QUADRANTS BY INFRARED IMAGING AND IMAGE ANALYSIS

J.F. Head[1], C.A. Lipari[2], R.L. Elliott[1]
[1]Mastology Research Institute, Baton Rouge, LA, USA
[2]Arizona State University East, Mesa, AZ, USA

Abstract-**In clinical testing it is standard to determine the normal range, and then to determine if a test can differentiate normal from diseased patients. Now with the advent of uncooled staring array digital infrared imaging systems (Prism 2000; Bioyear Group, Houston, TX) and image analysis, numerical results (mean temperatures of the whole breast and quadrants of the breast) can be used to determine the normal range and cutoff temperatures for risk assessment and detection of breast cancer. In this study we determined mean temperatures of whole breast and breast quadrants of women being screened for breast cancer. The mean temperatures for the right breast, left breast, right upper outer quadrant (UOQ), Left UOQ, right upper inner quadrant (UIQ), left UIQ, right lower outer quadrant (LOQ), left LOQ, right lower inner quadrant (LIQ), and left LIQ were 32.79, 32.65, 32.60, 32.46, 32.91, 32.69, 32.28 32.12, 33.29,and 33.00°C, respectively. Temperature differences were calculated between the right and left breasts and quadrants, and temperature differences greater than 0.5°C for whole breasts and 1.00°C for breast quadrants were considered asymmetric and abnormal. This resulted in 4 (17%) patients with differences in whole breast temperatures and 3 (13%) patients with quadrant differences from the 23 screened patients. These results are consistent with our previous results with both objective image analysis and subjective visual analysis (15% of screened patients have asymmetric breast infrared patterns). Further objective infrared measurements in breast cancer patients are needed to determine the sensitivity and specificity of this objective method for risk assessment and detection of breast cancer.**

Keywords - **Breast cancer, infrared imaging, cancer detection, risk assessment, image analysis**

I. INTRODUCTION

Infrared imaging in breast cancer has been around since the early 1970s, but was not widely accepted because of the lack of large clinical trials to prove its utility. In recent years the availability to the civilian sector of infrared systems with high thermal sensitivity, focal plane staring arrays, and digital output, that can be exported to a personal computer for image analysis, has caused many investigators to re-evaluate infrared imaging in breast cancer. This renaissance of infrared imaging in breast cancer has again focused on the ability of infrared imaging to contribute to breast cancer detection [1] but other areas such as risk assessment [2-7], breast cancer prognosis [8-10] and the monitoring of antihormone and chemotherapy have also been investigated.

The ability to export data as a two dimensional array of radiometric temperatures, that represent numerically the information that is displayed in the pictorial images, combined with the ability to designate areas within the arrays, has allowed computer assisted image analysis. Thus medical researches, often working with algorithms developed in the military for target recognition, are able to develop and test a wide variety of methods for their applicability to medical problems and specifically breast cancer.

Although much research has already been done to determine what an abnormal asymmetric infrared image of the breast means in terms of breast cancer risk assessment, detection, prognosis and therapeutic response, there has not been adequate determination of what is a normal breast infrared image. This is true for individual breasts or when two breasts are compared to each other for asymmetry. Therefore this study was undertaken to determine what are the temperature parameters of the breasts of normal women and this was done by using a group of women being screened for breast cancer who did not have breast cancer.

II. METHODOLOGY

Twenty-three women being screened for breast cancer by infrared imaging, physical exam, mammography and ultrasound (when appropriate) were included in this study. Three infrared images of each patient's breasts were taken with a Prism 2000 infrared imaging system (Bioyear Group, Houston, TX). The three black and white views of both breasts with black being hot included front, right oblique and left oblique views. The front view was also rendered in a colorized isotherm for improved viewing and size determination of breast areas with asymmetric increased heat.

The digital infrared images and the associated temperatures were exported for additional analysis. Proprietary software was used to access the radiometric information that is included with each image. For each patient the mean, standard deviation, minimum, median and maximum temperatures were determined for each breast and these quantitative parameters were compared between the two breasts in order to find temperature asymmetry. Then each breast was divided into quadrants (upper outer, upper inner, lower outer and lower inner) by drawing a line from each nipple to the chin, lines horizontally left and right from the nipple to the edge of the breast, and a line from the nipple to the lowest contour of the breast. Quantitative temperature parameters (mean, standard

TABLE 1
TEMPERATURES OF BREAST AREAS

BREAST AREA	BREAST AREA MEAN TEMPERATURE (°C)		DIFFERENCE IN TEMPERATURE BETWEEN TWO BREAST AREAS
	RIGHT	LEFT	
WHOLE BREAST	32.79	32.65	+0.14
UPPER OUTER QUADRANT	32.60	32.46	+0.14
UPPER INNER QUADRANT	32.91	32.69	+0.22
LOWER OUTER QUADRANT	32.28	32.12	+0.16
LOWER INNER QUADRANT	33.29	33.00	+0.29

deviation, minimum, median, maximum temperatures) were determined for each quadrant of both the right and left breasts. Then temperature comparisons were made between the quadrants of the right and left breasts, and among the quadrants of each individual breast.

III. Results

The mean temperatures of the two breasts (see Table 1) in this population of women being screened for breast cancer were 32.79°C for the right breast and 32.65°C for the left breast, and the two breasts were not significantly different by Student's t-test. Also there was no significant difference between the mean quadrant temperatures between the right and left breasts. There seems to be a trend toward higher temperatures on the right side (See Table 1) with the whole breast and all four quadrants of the breast having slightly higher temperatures for the right breast. However the difference for the whole breasts is less that 0.25°C, and for the breast quadrants is less than 0.50°C.

We then decided to use a 0.50°C difference between the right and left whole breasts in mean temperatures as the cutoff for asymmetry of the breast temperature, and therefore patients with greater than a 0.50°C difference between breasts would be at increased risk of having or getting breast cancer. For the quadrants we used a cutoff of 1.00°C difference to put the women being screened for breast cancer at increased risk. Using these cutoffs we found that 4 (17%) of the patients had asymmetric whole breast temperatures and 3 (13%) had asymmetric quadrant breast temperatures.

IV. Discussion

Infrared imaging in medicine has failed to reach its full potential due to a variety of reasons, but two of the most important reasons are the lack of sensitivity of the infrared imagers and the lack of objective analysis of the temperature data present in the images. Within the past five years state of the art focal plane staring array infrared imaging systems with true digital output have become available for medical applications. This has allowed the medical research community the opportunity to process the digital radiometric information from the infrared images [11-13] and to develop and test algorithms based on objective measurements obtained from image analysis of the digital data.

One of advantages of using objective numerical criteria to describe asymmetric abnormalities is that it allows the determination of what is normal by the same objective numerical criteria. Thus if a breast infrared image is analyzed by several readers at different locations the results will be the same, and this is not true of subjective visual analysis. An additional advantage of the easy export of the digital radiometric information is that test sets can be developed and easily analyzed by any available algorithm that can use digital numerical information. Therefore civilian medical researchers can develop and apply new algorithms, while many of the algorithms already developed by the military for target recognition can also be tested.

In the present study we have used a previously developed analysis method [14,15] to determine several numerical parameters of the whole breast and quadrants of the breast, and further to compare the numerical results (temperatures) from the right and left breasts. The mean whole breast temperatures from a group of 23 control women (normal without diagnosed breast cancer) did not significantly differ between the right (32.79°C) and left (32.65°C) breasts. There also was no significant difference between the comparable quadrants of the right and left breasts (See Table 1). However the right breast whole temperature and four quadrant temperatures (range 32.28°C to 33.29°C) were all slightly greater (range 0.14°C to 0.29°C) than those found for the left breast (range 32.12°C to 33.00°C). The lower inner quadrants had the highest temperatures of all the quadrants (33.29°C right and 33.00°C left), and this is probably due to heat from the heart.

Several conclusions can be drawn from this study when viewed in the context of our preliminary data on screened patients with and

without breast cancer. Our previous studies [14,15] have looked at numerical breast infrared data from very small groups of women and suggested that increases of 0.50°C for whole breast would be the best cutoff to distinguish asymmetry that would best differentiate normal from breast cancer. In the present study on a different data set of only noncancer patients we again found that the differences between the right and left whole breasts and all four quadrants are less than 0.50°C and therefore differences greater than this would be associated with high risk, breast cancer and poor prognosis of breast cancer patients. Due to the higher differences (0.14 to 0.29°C for quadrants compared to 0.14°C for whole breast) we chose to use a 1.00°C cutoff for quadrants. This again reflects well on our previously reported cutoffs, but the cutoffs presented here will be more useful in clinical practice as they are simpler than the ones used in our previous algorithms.

When using the objective cutoffs, that are similar to the cutoffs previously found to both improve sensitivity and specificity over subjective visual infrared image analysis by lowering both the false positive and false negative rate [16], in this study, we were able to define a subgroup of women with asymmetric breast heat patterns. This resulted in 17% (4 of 23) of the women, who were screened by infrared imaging for breast cancer, being found to have abnormal asymmetric whole breast mean temperatures, and 13% (3 of 23) of these women being found to have abnormal asymmetric quadrant mean temperatures. This suggests that these cutoffs may function well to distinguish in an objective manner the women at increased risk of getting breast cancer or who already have breast cancer, from women at reduced or normal risk of getting or having breast cancer.

V. Conclusion

The use of infrared imaging with state of the art focal plane staring array infrared systems, that can export digital images for computer assisted analysis of radiometric information, has only recently become available for medical application. The application of these new state of the art infrared imaging systems to breast cancer risk assessment, detection, prognosis and monitoring of therapy must be further investigated and developed before it will become widely accepted in clinical practice. The future promises the development of objective parameters, based on numerical analysis, which will eliminate the very subjective visual analysis presently done by physicians. This could possibly remove the long learning curve for medical infrared interpretation as well as diminish the inherently variable results from subjective visual analysis.

Acknowledgment

Partial financial support was provided by the Breast Foundation, Baton Rouge, LA.

References

[1] Keyserlingk JR, Ahlgren PD, Yu E, Belliveau N, and Yassa M: Functional infrared imaging of the breast. *IEEE Eng Med Biol Mag* 19:30-41, 2000.

[2] Head JF, Lipari CA, Wang F, Davidson JE, and Elliott RL: Application of second generation infrared imaging and computerized image analysis to breast cancer risk assessment. *Proc IEEE Eng Med Biol* 18:1019-1021, 1996.

[3] Head JF, Wang F, Lipari CA, and Elliott RL: Breast cancer risk assessment with an advanced infrared imaging system. *Proc Amer Soc Clin Oncol* 16:172, 1997.

[4] Head JF, Lipari CA, Wang F, and Elliott RL: Cancer risk assessment with a second generation infrared imaging system. *SPIE* 3061:300-307, 1997.

[5] Elliott RL, Wang F, Lipari CA, and Head JF: Application of second generation infrared imaging to breast cancer risk assessment. *Southeastern Surg Conference* 65:16, 1997.

[6] Lipari C, and Head J: Advanced infrared image processing for breast cancer risk assessment. *Proc IEEE Eng Med Biol* 19:673-676, 1997.

[7] Head JF, Wang F, Lipari CA, and Elliott RL: The important role of infrared imaging in breast cancer: New technology improves applications in risk assessment, detection, diagnosis and prognosis. *IEEE Eng Med Biol Mag* 19:52-57, 2000.

[8] Elliott RL, Head JF, and Werneke DK: Thermography in breast cancer: Comparison with patient survival, TNM classification and tissue ferritin concentration. *Proc Amer Soc Clin Oncol* 9:99, 1990.

[9] Head JF, Shah U, Elliott MC, and Elliott RL: Breast thermography and cancer patient survival. *Thermology* 3:277, 1991.

[10] Head JF, Wang F, and Elliott RL: Breast thermography is a noninvasive prognostic procedure that predicts tumor growth rate in breast cancer patients. *Ann New York Acad Sci* 698:153-158, 1993.

[11] Snyder W, Wang C, Wang F, Elliott R, and Head J: Improving the resolution of infrared images of the breast. *Proc IEEE Eng Med Biol* 18:1058-1059, 1996.

[12] Snyder WE, Qi H, Elliott RL, Head JF, and Wang CX: Increasing the effective resolution of thermal images: An algorithm based on mean-field annealing that also removes noise and preserves image edges. *IEEE Eng Med Biol Mag* 19:63-70, 2000.

[13] Qi H, Synder WE, Head JF, and Elliott RL: Detecting breast cancer from infrared images by asymmetry analysis. *Proc IEEE Eng Med Biol* 22:CDROM, 2000.

[14] Head J, Lipari C, Wang F, and Elliott R: Image analysis of digitized infrared images of the breasts from a first generation infrared imaging system. *Proc IEEE Eng Med Biol* 19:681-684, 1997.

[15] Head JF, Lipari CA, and Elliott RL: Computerized image analysis of digitized infrared images of the breasts from a scanning infrared imaging system. *SPIE* 3436:290-294, 1998.

[16] Head JF, Lipari CA, and Elliott RL: Comparison of mammography and breast infrared imaging: Sensitivity, specificity, false negatives, false positives, positive predictive value and

negative predictive value. *Proc IEEE Eng Med Biol* 21: CDROM, 1999.

IMAGE ANALYSIS OF DIGITIZED INFRARED IMAGES OF THE BREASTS FROM A FIRST GENERATION INFRARED IMAGING SYSTEM

Jonathan F. Head, Charles A. Lipari, Fen Wang and Robert L. Elliott
Medical Thermal Diagnostics, LBTC, South Stadium Drive, Baton Rouge, LA 70803-6100
E-mail: thermal@premier.net

ABSTRACT

Infrared imaging, often called thermography in medicine, of the breasts has been shown to be of value in risk assessment, detection, diagnosis and prognosis of breast cancer. However, infrared imaging has not been widely accepted for a variety of reasons, including the lack of standardization of the subjective visual analysis method. The subjective nature of the standard analysis makes it difficult to achieve equivalent results with different equipment and different interpreters of the infrared patterns of the breasts. Therefore, this study was undertaken to develop more objective methods of analysis of infrared images of the breasts by creating objective semiquantitative and quantitative analysis of computer assisted image analysis determined mean temperatures of whole breasts and quadrants of the breasts. When using objective quantitative data on whole breasts (comparing differences in means of left and right breasts), semiquantitative data on quadrants of the breast (determining an index by summation of scores for each quadrant), or summation of quantitative data on quadrants of the breasts there was a decrease in the number of abnormal patterns (positives) in patients being screen for breast cancer and an increases in the number of true positives in the breast cancer patients. It is hoped that the decrease in positives in women being screened for breast cancer will translate into a decrease in the false positives but larger numbers of women with longer follow-up will be needed to clarify this. Also a much larger group of breast cancer patients will need to be studied in order to see if there is a true increase in the percentage of breast cancer patients presenting with abnormal infrared images of the breast with these objective image analysis methods.

KEYWORDS: Thermography, Infrared Imaging, Breast Cancer, Risk Assessment, Image Analysis

INTRODUCTION

Infrared imaging of the breast, usually referred to as thermography in medicine, has been shown to be efficacious in risk assessment [1,2,3] and prognostic determination in breast cancer [3,4]. Infrared imaging has also been shown to be a useful in conjunction with mammography and ultrasound for the detection and diagnosis of breast cancer. However, the subjective visual analysis of asymmetric abnormalities in infrared images of the breast for risk assessment, detection, diagnosis and prognosis in breast cancer has hindered acceptance of this technology as it has been very difficult to standardize and to learn the subjective analysis method. Therefore it has been very difficult to obtain reproducible results among investigators and clinicians, who are determining the presence or absence of asymmetric infrared abnormalities of the breasts. The introduction of digital output in a variety of both proprietary and standard formats has allowed image analysis by both proprietary image capturing cards and software, and also standard image capturing formats. Standard imaging formats that can export standard files are more useful as they can be submitted to a variety of commercially available image analysis software that are very good at target identification and for creating automated image analysis programs.

Although early attempts at standardizing the analysis procedure of analogue exported images by creating scoring systems by which patients could be categorized in term of risk, detection, diagnosis and prognosis were a great improvement that allowed highly trained thermographers to detect and semiquantitate the infrared abnormalities, they were still quite subjective. These semiquantitative results were quite reproducible by highly trained thermographers, but training was still quite an involved and time consuming experience. The present study is an attempt to totally automate the process so that thermographers can look at an infrared image of the breasts and combine the information that is subjectively processed by their minds with quantitative numerical data derived from image analysis of digitized images that were derived from the analogue output. Eventually we hope to develop an image analysis method that will eliminate the highly subjective nature of the present day infrared image reading by thermographers with an automated procedure that will only require qualified thermographers to over-read the image analysis results.

METHODS

Infrared images from 13 patients (10 women without breast cancer, 5 with normal infrared patterns and 5 with abnormal infrared patterns, and 3 breast cancer patients, 1 with a normal infrared pattern and 2 with abnormal infrared patterns) were taken with a first generation, liquid nitrogen cooled, scanning mercury cadmium telluride detector, Inframetrics 500M infrared imaging system with an 8 bit

dynamic range, 100 mK sensitivity@30° and a spectral range of 8-12 microns. Although there was proprietary software, we chose to export the digitized images in a TIF file and used customized image analysis software to derive quantitative data on infrared patterns that previously had been subjectively visually analyzed by an expert thermographer. For each patient the mean, standard deviation, minimum, median and maximum temperature was determined for each breast and comparisons were made between the two breasts. Then, each breast was divided into upper outer, upper inner, lower outer and lower inner quadrants (Figure 1) by drawing lines on the infrared images

FIGURE 1
GUIDELINES FOR BREAST QUADRANTS

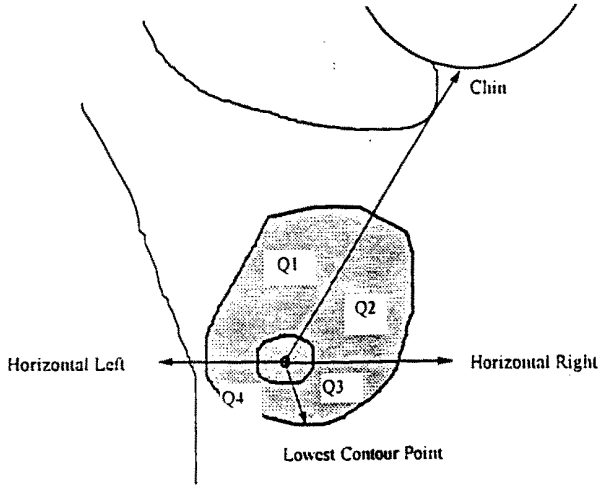

from the chin of the patient to each nipple and then two horizontal lines left and right to the edge of the breast and finally a forth line to the lowest contour of the breast. Again the mean, standard deviation, minimum, median and maximum temperatures were determined for each quadrant of both breasts, and comparative statistics were generated between the left and right breasts.

Three objective quantitative methods of determining asymmetric abnormalities of the breast were developed. The first method (Method 1) compared the difference in mean temperature between the right and left breasts and if this mean temperature was equal to or greater than 0.50°C then the patient was considered to have an abnormal asymmetric breast infrared heat pattern. The second method (Method 2) involved calculating a score based on addition of scores to create an index, if the mean temperature of a quadrant was 0.50 to 1.00°C higher than the same quadrant of the opposite breast then a score of 0.5 is assigned, and when a quadrant has a mean temperature that is greater than 1.00°C higher then a score of 1.0 is assigned. An index is created by adding together the scores for the comparisons of all four quadrants and the index can have a value from 0.0 to 4.0. For purposes of this study patients with an index greater than 1.0 were considered to have abnormal asymmetric breast infrared heat patterns. The third method was the simple addition of the mean differences of the quadrants comparing the left and right breasts and absolute differences greater than 1.00 were considered to represent abnormal asymmetric infrared patterns. Comparison of the results from these three objective determinations of asymmetry of infrared heat patterns of the breasts were then compared to the subjective results of an expert thermographer.

RESULTS

Figure 2 shows the quadrants of the breasts of a patient (patient #1 in Table 1) with a normal infrared heat pattern of the breasts and Figure 3 shows a patient (patient #2 in Table 1) with a highly abnormal asymmetric infrared heat pattern of the breasts. In both Figures 2 and 3 the quadrant

FIGURE 2
NORMAL INFRARED PATTERN IN PATIENT BEING SCREENED FOR BREAST CANCER

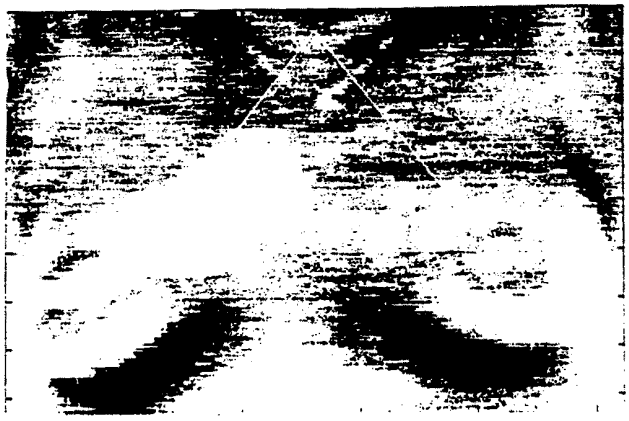

FIGURE 3
ABNORMAL INFRARED PATTERN IN PATIENT BEING SCREENED FOR BREAST CANCER

lines have been overlaid on the actual digitized infrared

TABLE 1
SUBJECTIVE AND OBJECTIVE DETERMINATION OF ASYMMETRIC INFRARED ABNORMALITIES IN PATIENTS BEING SCREEN FOR BREAST CANCER

PATIENT #	SUBJECTIVE	METHOD 1 (°C)	METHOD 2 (INDEX)	METHOD 3 (°C)
1N[a]	N[b]	-0.42	1.0	-1.00
2N	L+	**-1.30**[c]	**3.5**	**-8.68**
3N	N	+0.33	1.0	+0.94
4N	N	+0.20	0.0	+0.74
5N	L+	+0.10	1.0	-0.46
6N	N	-0.26	0.0	-0.60
7N	L+	-0.24	0.5	-0.56
8N	L+	**-0.79**	**2.0**	**-2.95**
9N	N	-0.28	0.0	-0.87
10N	L+	-0.45	**1.5**	-0.88
11CA	N	+0.10	0.5	+0.36
12CA	R+	**+0.59**	**1.5**	**+1.99**
13CA	N	**+0.65**	**1.5**	**+2.60**

[a]N, normal patient; CA, breast cancer patient
[b]N, normal infrared breast pattern; L+, abnormal left infrared breast pattern; R+, abnormal right infrared breast pattern
[c]bold numbers signify abnormal values for infrared images

images from the patients with normal and abnormal infrared images of their breasts. The patient in Figure 2 with the normal infrared heat pattern has vascularity demonstrated in both breasts but they are approximately equivalent, as there are no major asymmetries in either breast. The patient in Figure 3 has a generally hotter (black is hot) left breast with periareolar heat and a large hot spot on the outer quadrants, and vascular asymmetry on the inner quadrants.

Table 1 presents the results from the subjective whole breast analysis, quantitative whole breast analysis (Method 1), semiquantitative quadrant analysis (Method 2) and quantitative quadrant analysis (Method 3) of the 13 patients in this study. While doing the subjective analysis the thermographers were not sure if patient 9 had a normal or a slightly abnormal left breast and for patient 11 there was some uncertainty whether the right breast was abnormal. When the objective quantitative Method 1 was used, that compared the difference in mean temperature between the two breasts, there was a decrease from 50% abnormal infrared patterns in the 10 patients being screened for breast cancer (chosen to be half normal and half abnormal) by 3 so that only 20% (2 of 10) of the patients being screened for breast cancer had abnormal asymmetric heat patterns of the breasts. Both the objective semiquantitative Method 2 and quantitative Method 3, decreased the abnormal asymmetric infrared images in the patients being screened for breast cancer to 3 patients (a 20% decrease in the positive rate for this group of patients). In the 3 breast cancer patients one of the three patients with a normal infrared pattern by subjective analysis was found to have an abnormal infrared pattern by all three objective analysis methods.

DISCUSSION

The subjective method of determining whether an asymmetric infrared abnormality of the breasts is significant, that is presently being utilized by most physicians, is hard to learn, and not adequately reproducible. In a previous study [5] we attempted to use a semiquantitative method of determining when an asymmetric infrared heat pattern of the breasts was sufficiently different to be called abnormal. Although this method seemed to produce a greater

continuum of abnormalities through the creation of an abnormality index from 1 to 8 (summation of scores that reflected the severity of hot spots, global heat, vascularity, areolar/periareolar heat and edge sign), it still had major shortcomings. The method required highly trained thermographers to rate the abnormalities and the exact cut-off index for abnormal was not obvious or easy to determine. Further it would be almost impossible to create a computer assisted analysis program that could do this analysis without subjective input by a highly qualified thermographer.

The present study used a computer assisted image analysis program that presently requires significant operator interaction but will be made operator independent. We believe that eventually whole breast or quadrant temperature differences will be inputed into one of the three methods of analyses presented in this paper, or some other method of analysis, and that the subjective methods presently used by thermographers will be replaced by an objective method of analysis. Initially the results from objective analysis will probably be used as another piece of information in the present subjective analysis, but, if successful, the results of the whole breast or quadrant image analysis should become the most important information used in determining whether patients, being screened for breast cancer or presenting with breast cancer, have abnormal asymmetric infrared patterns of their breasts.

Image analysis for determination of mean temperatures of the whole breast or quadrants of the breast, followed by a simple method of numerical analysis and finally the application of numerical cut-offs for a normal range of temperature difference was also undertaken in this study to determine if this type of analysis could decrease the high false positive rate found in women being screened for breast cancer with infrared imaging. The results from this study show that all three objective methods, based on image analysis for temperature differences in either whole breast or quadrant comparisons, significantly reduced the number of patients being screened for breast cancer with abnormal asymmetric infrared heat patterns. The two methods (Methods 1 and 3), where 0.50°C and 1.00°C are the normal cut-offs for whole breast and summation of quadrant differences, respectively, seem to be very promising methods of analysis and could easily transform the infrared pattern analysis from a subjective visual analysis into a purely objective quantitative analysis. One somewhat surprising finding in this study was the increase in the number of patients with breast cancer that had positive infrared patterns of the breast. Although these objective quantitative results suggest that their application will reduce the number of false positives in women being screened for breast cancer with infrared imaging, while also increasing the true positive rate for women found to have breast cancer during screening with infrared imaging, larger studies must be undertaken to better clarify if the objective methods are better than the subjective methods and, if the objective methods are better, then which objective method is the best.

ACKNOWLEDGEMENT

Partial financial support was provided through a SBIR contract with the Army Night Vision Laboratory.

REFERENCES

1. Gautherie M, Gros CM. Breast thermography and cancer risk prediction. *Cancer* 1980;**45**:51-6.
2. Stark AM. The value of risk factors in screening for breast cancer. *Eur J Cancer* 1985;**11**:147-50.
3. Head JF, Wang F, Elliott RL. Breast thermography is a noninvasive prognostic procedure that predicts tumor growth rate in breast cancer patients. *Ann N Y Acad Sci* 1993;**698**:153-8.
4. Isard HJ, Sweitzer CJ, Edelstein GR. Breast thermography: A prognostic indicator for breast cancer survival. *Cancer* 1988;**62**:484-8.
5. Head JF, Lipari CA, Wang F, Elliott RL. Cancer risk assessment with a second generation infrared imaging system. *Proc Int Soc Optical Eng* 1997; In press.

PROCEEDINGS OF SPIE REPRINT

SPIE—The International Society for Optical Engineering

Reprinted from

Infrared Technology and Applications XXV

5–9 April 1999
Orlando, Florida

Volume 3698

Infrared imaging of burn wounds to determine burn depth

Andrew G. Hargroder[a], James E. Davidson[b], Donald G. Luther[b], and Jonathan F. Head[b]

[a]Baton Rouge General Regional Burn Center, Baton Rouge, LA 70806
[b]Medical Thermal Diagnostics, Baton Rouge, LA 70803

ABSTRACT

Determination of burn wound depth is at present left to the surgeons visual examination. Many burn wounds are obviously, by visual inspection, superficial 2° burns or true 3° burns. However, those burn wounds that fall between the obvious depth burns are difficult to assess visually, and therefore wound depth determination often requires waiting 5 to 7 days postburn. Initially, 10 burn patients underwent infrared imaging at various times during the evaluation of their burn wounds. These patients were followed to either healing or skin grafting. The infrared images were then reviewed to determine their accuracy in determining the depth of the wound. Infrared imaging of burn wounds with focal plane staring array midrange infrared systems appears promising in determination of burn depth one to two days postburn. This will allow clinical decisions regarding operative or nonoperative intervention to be made earlier, thus decreasing hospital stays and time to healing.

Keywords: thermography, infrared imaging, injuries, burns, wound healing

1. INTRODUCTION

Determination of burn depth in some burn patients can be difficult. Often 5-7 days are required before a decision is made as to whether the burn will heal or surgical intervention will be necessary. This delay prolongs patient discomfort, increases the need for wound care and dressing changes, and increases hospital stay.

Over the years several techniques (fluorescein dye flow studies, ultrasound, and laser doppler imaging) have been investigated as means of early determination of burn depth. None of these techniques have been proven to be beneficial. In Europe infrared imaging was also investigated[1-3] for the determination of burn depth but was not sufficiently studied to prove the utility of infrared imaging for this purpose.

Using more sensitive infrared equipment that produces infrared images with greater resolution, we undertook the collection of preliminary infrared images. Results from analysis of these digitized infrared images were compared and combined with the visual evaluation by the burn surgeon to determine if infrared images would be useful in early determination of burn depth.

2. MATERIALS AND METHODS

2.1. Patients

The burns from 10 burn patients were recorded with a camcorder for later visual comparison to images recorded with a video recording of infrared images of the burn made within the first seven days after the patients received the burn trauma. In one patient no infrared digital images were stored so the patient's infrared data could not be analyzed. For two patients complete patient information has not been obtained. One patient's infrared data was not analyzable as she had burns to her feet and we did not know what is the normal infrared pattern of the foot. Also her other foot was bandaged and was not available for comparison. This left us with 6 patients with 16 separate burns for infrared analysis.

Part of the SPIE Conference on Infrared Technology and Applications XXV
Orlando, Florida • April 1999 SPIE Vol. 3698 • 0277-786X/99/$10.00

2.2. Infrared images

Infrared images were taken with an Amber imaging system: indium antimonide focal plane staring array (256 x 256 elements) radiometer, Stirling cycle cooler, dynamic range of 12 bits/element, thermal sensitivity of 25 mK@30°C, spectral range 3-5 microns, internal calibration, and both analog and digital output. Color isotherms were generated with 2°F ranges for skin temperature analysis, which consisted of comparing the temperature of the surround unburned area to the lowest temperature within the burned area.

3. RESULTS

Figure 1 shows both the visual picture and infrared isotherm image of the right forearm of patient G.W. and the relative severity of the burn and the 8.7°F decrease in temperature that occurs at the center of the burn, respectively. These visual results and infrared isotherms are representative of the images obtained in all the burn patients. Figure 2 graphically demonstrates the decrease in temperature associated with deep second and third degree burns, as each line connects the temperature surrounding a burn with the lowest temperature within the burn. In Table 1 are the results from all the patients who had isotherm analysis performed on their digitized infrared images. It is obvious that patients with deep second and third degree burns have a significant decrease in the temperature at the surface of their burns within hours of sustaining the burn and that this decrease in temperature was maintained for up to seven days. However L.W.2 did have a second degree burn on his right forearm that was actually increased in temperature at day seven.

The average skin temperature of the unburned area surrounding a burned area (excluding face, fingers and toes) was 90.1 ± 1.7 (15 burns), and the average temperature of the area of lowest temperature of the burns was 84.3 ± 3.0 (14 burns, excludes the second degree burn on L.W.2, that had a 3.9°F increase over surrounding unburned skin). The burned areas had significantly ($p<.0001$, paired t-test) lower temperatures. Patient W.J. had a facial burn that required skin grafting of the right side of the face, and this side was 10.6°F colder (basal temperature of the face was a much higher 97.7°F).

4. DISCUSSION

In this study we demonstrated that patients with burns that require monitoring for 5 to 7 days in order to determine whether they are deep second degree or true third degree burns, have a significant decrease in the surface temperature of the burned areas from 90.1 to 84.3°F. We divided the patients' burns into three groups: burns whose dept could not be initially determined but after monitoring were found to be second degree, burns whose depth could not be initially determined but after monitoring were found to be third degree, and burns that were initially third degree. The mean$\pm$SD temperature differences of the burns from the surrounding normal nonburned skin were -3.9 ± 5.0 ($n=5$), -5.8 ± 2.3 ($n=9$) and -7.4 ($n=2$) for these three types of burns, respectively. This shows that there is a greater decrease in skin temperature of burns as they get deeper and require skin grafting. We believe that the destruction of the vasculature under the third degree burns caused the dramatic decrease in temperature on the surface of these wounds. However, the maintenance of blood flow to the area of the deep second degree burns allows healing and inflammatory responses that maintain the surface temperature or even increase it.

Some authors[2,3] have expressed concern that evaporation from burns can introduce an evaporative cooling artefact, and that this can be corrected by covering the wound with a water impermeable polyvinylchloride film. We did not do this but we do feel this should be investigated in future studies. Also we need to determine temperature differences in a wider range of second degree burns and in obvious third degree burns in order to better quantify the increasing temperature loss associated with increasing depth of burn. Further we must develop the best method with greatest utility of analyzing the digitized infrared images taken at presentation or within the first 2 to 3 days postburn, and integrate the infrared results with the burn surgeons visual evaluation to produce an accurate way of determining which burns should be grafted. We believe, that by integrating early objective determination of which burns require skin grafts into the patient's treatment plan, we could greatly improve and shorten the treatment of burn

patients. However many more burn patients will have to be studied before an infrared method is work out that can become a routine part of burn analysis.

5. ACKNOWLEDGEMENTS

Partial support was provided through a SBIR contract with the Army Night Vision Laboratory.

6. REFERENCES

1. R.P. Cole, S.G. Jones, and P.G. Shakespeare, "Thermographic assessment of hand burns", *Burns* **16**, pp. 60-63, 1990.
2. R.P. Cole, P.G. Shakespeare, H.G. Chissell and S.G. Jones, "Thermographic assessment of burns using a nonpermeable membrane as wound covering", *Burns* **17**, pp. 117-122, 1991.
3. M.I. Liddington and P.G. Shakespeare, "Timing of the thermographic assessment of burns", *Burns* **22**, pp. 26-28, 1996.

Further author information -
J.F.H.(correspondence): Email: emcmri@iamerica.net; Telephone: 225-927-2256; Fax: 225-927-3772
A.G.H.: Telephone: 225-687-4703; Fax: 225-687-4704

Figure 1

VISUAL PHOTOGRAPHIC (UPPER) AND INFRARED (LOWER) IMAGES OF G.W.'s RIGHT FOREARM BURN

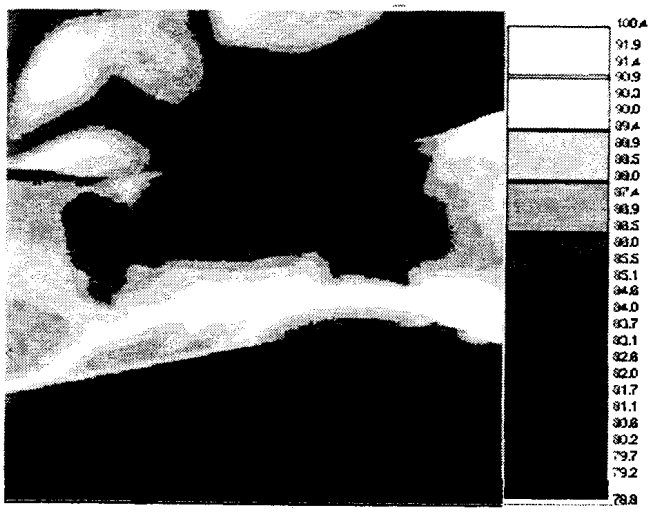

Figure 2

NORMAL ADJACENT SKIN AND BURN TEMPERATURE

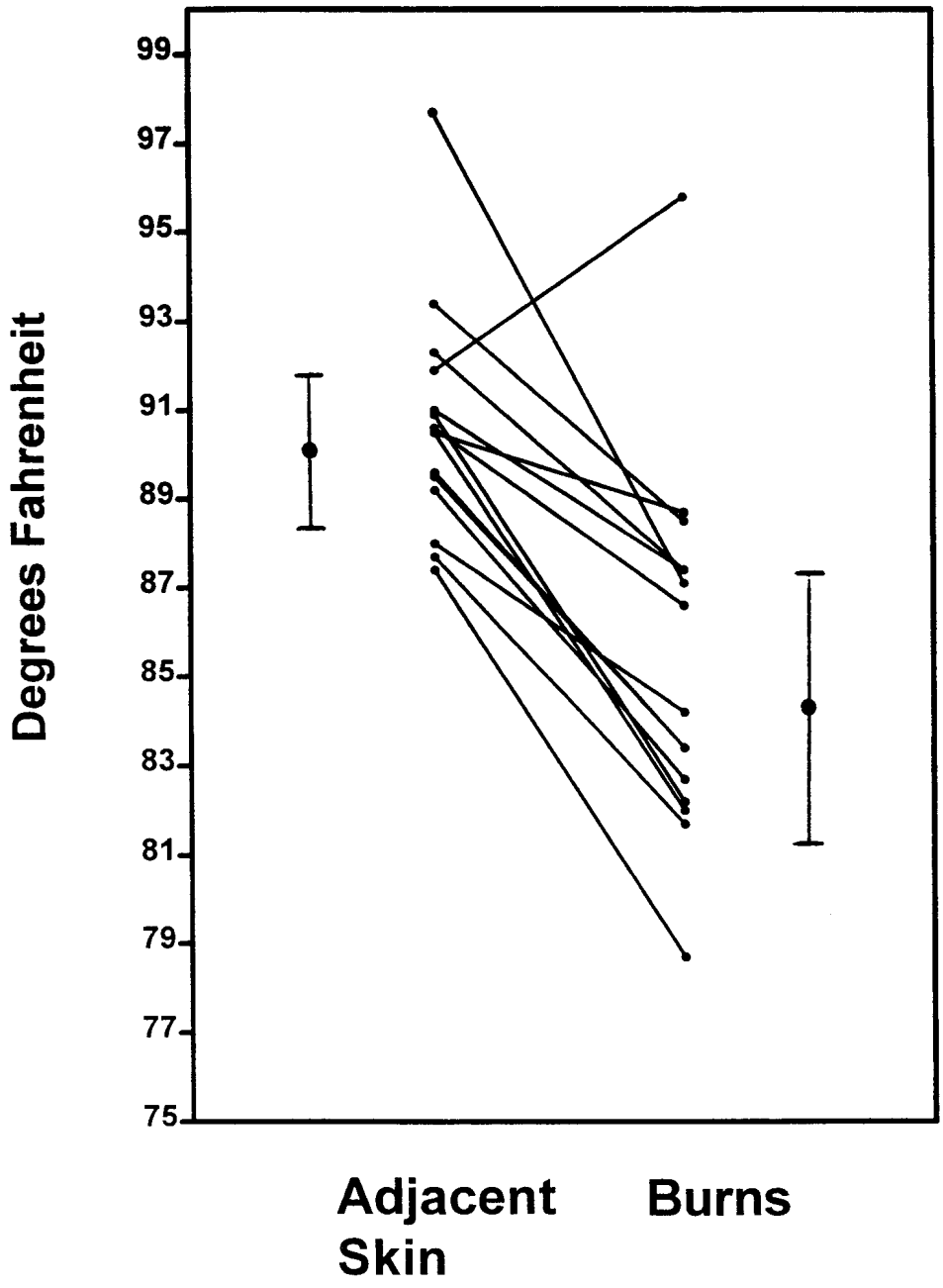

Table 1

BURN PATIENT DATA

PATIENTS INITIALS	BURN SITE	DAYS POST BURN	INITIAL 2ND/3RD	5-7 DAYS 2ND/3RD	GRAFT	ADJACENT SKIN TEMP. (°F)	BURN TEMP. (°F)	TEMP. DELTA (°F)
G.W.	rt forearm	0	3rd	3rd	Y	87.4	78.7	-8.7
	lt forearm		3rd	3rd	Y	87.7	81.7	-6.0
	rt thigh		2nd/3rd	2nd	N	89.2	82.7	-6.5
	lt thigh		2nd/3rd	2nd	N	89.2	82.7	-6.5
L.B.	lt hand	1	2nd/3rd	3rd	Y	92.3	87.4	-4.9
L.G.	lt hand	1	2nd/3rd	3rd	Y	91.0	87.4	-3.6
L.W.1	abdomen	3	2nd/3rd	3rd	Y	89.5	83.4	-6.1
	rt thigh		2nd/3rd	3rd	Y	90.6	86.6	-4.0
	lt thigh		2nd/3rd	3rd	Y	88.0	84.2	-3.8
	rt forearm		2nd/3rd	2nd	N	90.9	82.2	-8.7
	lt forearm		2nd/3rd	2nd	N	90.5	88.7	-1.8
L.W.2	rt ankle	7	2nd/3rd	3rd	Y	89.6	83.4	-6.2
	lt ankle		2nd/3rd	3rd	Y	90.5	82.0	-8.5
	rt forearm		2nd/3rd	2nd	N	91.9	95.8	+3.9
	lt thigh		2nd/3rd	3rd	Y	93.4	88.5	-4.9
W.J.	face	0	2nd/3rd	3rd	Y	97.7 (lt)	87.1 (rt)	-10.6

Asymmetry Analysis Using Automatic Segmentation and Classification for Breast Cancer Detection in Thermograms

Hairong Qi[1] , Jonathan F. Head[2]

Abstract— **Thermal infrared imaging has shown effective results as a diagnostic tool in breast cancer detection. It can be used as a complementary to traditional mammography. Asymmetry analysis are usually used to help detect abnormalities. However, in infrared imaging, this cannot be done without human interference. This paper proposes an automatic approach to asymmetry analysis in thermograms. It includes automatic segmentation and pattern classification. Hough transform is used to extract the four feature curves that can uniquely segment the left and right breasts. The feature curves include the left and the right body boundary curves, and the two parabolic curves indicating the lower boundaries of the breasts. Upon segmentation, unsupervised learning technique is applied to classify each segmented pixel into certain number of clusters. Asymmetric abnormalities can then be identified based on pixel distribution within the same cluster. Both segmentation and classification results are shown on images captured from Elliott Mastology Center.**

Keywords— **asymmetry analysis, breast cancer detection, thermogram, Hough transform, pattern classification, unsupervised learning**

I. Introduction

Making comparisons between contralateral images are routinely done by radiologists. When the images are relatively symmetrical, small asymmetries may indicate a suspicious region. This is the underlying philosophy in the use of asymmetry analysis for mass detection in breast cancer study [2]. Unfortunately, due to various reason like short of radiologists, fatigue, carelessness, or simply because of the limitation of human visual system. these small asymmetries might not be easy to detect. Therefore, it is important to design an automatic approach to eliminate human factors.

There have been a few papers addressing techniques for asymmetry analysis of mammograms [2], [7], [8], [9], [10], [11]. [3], [5] recently analyzed the asymmetric abnormalities in infrared images. In their approach, the thermograms are segmented first by operator. Then breast quadrants are derived automatically based on unique point of reference, i.e. the chin, the lowest, rightmost and leftmost points of the breast. In an earlier paper we published [6], Hough transform is used to segment the image, and curvature analysis is proposed to identify the abnormalities. This paper extends our work on using Hough transform for segmentation. New experimental results are provided. Instead of using curvature analysis which is very sensitive to noise, this paper describes a pattern classification approach which uses unsupervised learning to identify abnormalities. k-means algorithm is applied on the segmented images.

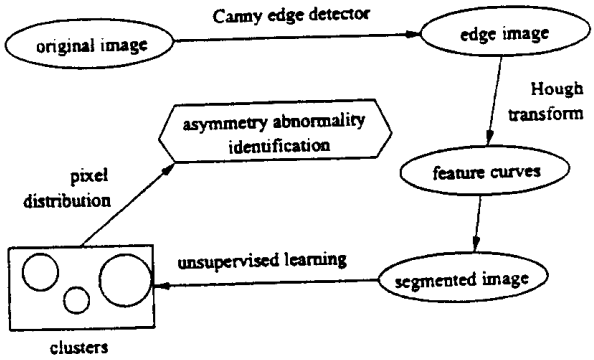

Fig. 1. Procedure of automatic asymmetry analysis of thermogram.

Testing images are obtained using the Inframetrics 600M camera, with a thermal sensitivity of 0.05^0K.

II. Approach

Figure 1 is a block diagram of the five procedures involved in the proposed approach: (1) *Edge image* detection by Canny edge detector; (2) *Feature curve* extraction including the left and right body boundary curves, and the two lower boundaries of the breasts. Hough transform is used to detect the parabolic shaped lower breast boundaries; (3) *Segmentation* based on the intersection of the two parabolic curves and the line formed by the two armpits; (4) *Pattern classification* using unsupervised learning to group each pixel of the segments into certain clusters; and (5) *Pixel distribution* of each cluster is analyzed and abnormalities can then be identified.

A. Edge detection by Canny edge detector

Edge image is first derived by using Canny edge detector [1]. The standard deviation is chosen to be equal to 2.5 so that only strong edges are detected.

[1]Electrical and Computer Engineering Department, University of Tennessee, Knoxville, TN 37996, USA, Email: hqi@utk.edu

[2]Elliott Mastology Center, Baton Rouge, LA 70806, USA, Email: emcmri@iamerica.net

B. Feature curve extraction by Hough transform

There are four dominant curves appeared in the edge image which we called the feature curves: the left and right body boundaries, and two lower boundaries of the breasts. The body boundaries are easy to detect. Difficulties lie in the detection of the lower boundaries of the breasts. We observe that the breast boundaries are generally in parabolic shape. Therefore, Hough transform [4] is used to detect the parabola.

C. Segmentation

Segmentation is based on three key points: the two armpits (P_L, P_R) derived from the left and right body boundaries by picking up the point where the largest curvature occurs, and the intersection (O) of the two parabolic curves derived from the lower boundaries of the breasts. The vertical line that goes through point O and is perpendicular to line P_LP_R is the one used to separate the left and right breasts.

D. Unsupervised learning

Pixel values in a thermogram represent the thermal radiation resulting from the heat emanates from the human body. Different tissues, organs and vessels have different amount of radiation. Therefore, by observing the heat pattern, or in another word, the pattern of the pixel value, we should be able to discover the abnormalities if there are any.

Usually, in pattern classification algorithms, a set of training data are given to derive the decision rule. All the samples in the training set have been correctly classified. The decision rule is then applied to the testing data set where samples have not been classified yet. This classification technique is also called supervised learning. In unsupervised learning, however, data sets are not divided into training sets or testing sets. No *a-priori* knowledge is known about which class each sample belongs to.

In asymmetry analysis, none of the pixels in the segment knows its class in advance, thus there will be no training set or testing set. Therefore, this is an unsupervised learning problem. We use k-means algorithm to do the initial clustering. k-means algorithm is described as follows:

1. Begin with an arbitrary set of cluster centers and assign samples to nearest clusters;
2. Compute the sample mean of each cluster;
3. Reassign each sample to the cluster with the nearest mean;
4. If the classification of all samples has not changed, then stop, else go to step 2.

E. Within cluster pixel distribution

After each sample is relabeled to a certain cluster, the cluster mean can then be calculated. The segmented image can also be displayed in labeled format. From the difference of mean distribution, we can tell if there is any asymmetric abnormalities.

III. Experimental Results

Testing images are obtained using the Inframetrics 600M camera, with a thermal sensitivity of 0.05^0K. The image are collected at Elliott Mastology Center. Results from two testing images (lr, nb) are shown here.

Figure 2 shows the intermediate results from edge detection, feature curve extraction, to segmentation. From the figure, we can see that Hough transform can derive the parabola at the accurate location.

Figure 3 provides the histogram of pixel value from each segment with 10-bin setup. We can tell just from the shape of the histogram that lr shows a more apparent abnormalities than nb. However, histogram only reveals global information.

Figure 4 displays the classification results for each segment in its labeled format. Here, we choose to use four clusters. The figure also shows the mean difference of each cluster in each segmented image. From Fig. 4, we can clearly see the much bigger difference shown in the mean distribution or image lr which can also be observed from the labeled image.

IV. Conclusion

This paper describes an automatic approach for asymmetry analysis in thermograms to help identify abnormalities. It includes an automatic segmentation using Hough transform and an unsupervised pattern classification for segment comparison. From the experimental results, we can see that Hough transform can accurately extract the feature curves, and k-means algorithm provides useful information in the analysis of abnormalities.

References

[1] J. Canny. A computational approach to edge detection. *IEEE Trans. Pattern Anal. and Machine Intell.*, 6:679–698, 1995.

[2] W. F. Good, B. Zheng, Y. Chang, et al. Generalized procrustean image deformation for subtraction of mammograms. In *Proceeding of SPIE Medical Imaging - Image Processing*, volume 3661, pages 1562–1573. San Diego, CA, 1999. SPIE.

[3] J. F. Head, C. A. Lipari, and R. L. Elliott. Computerized image analysis of digitized infrared images of the breasts from a scanning infrared imaging system. In *Proceedings of the 1998 Conference on Infrared Technology and Applications XXIV, Part I*, volume 3436, pages 290–294. San Diego, CA, 1998. SPIE.

[4] M. Z. Jafri and F. Deravi. Efficient algorithm for the detection of parabolic curves. In *Vision Geometry III*, volume 2356, pages 53–62. SPIE, 1994.

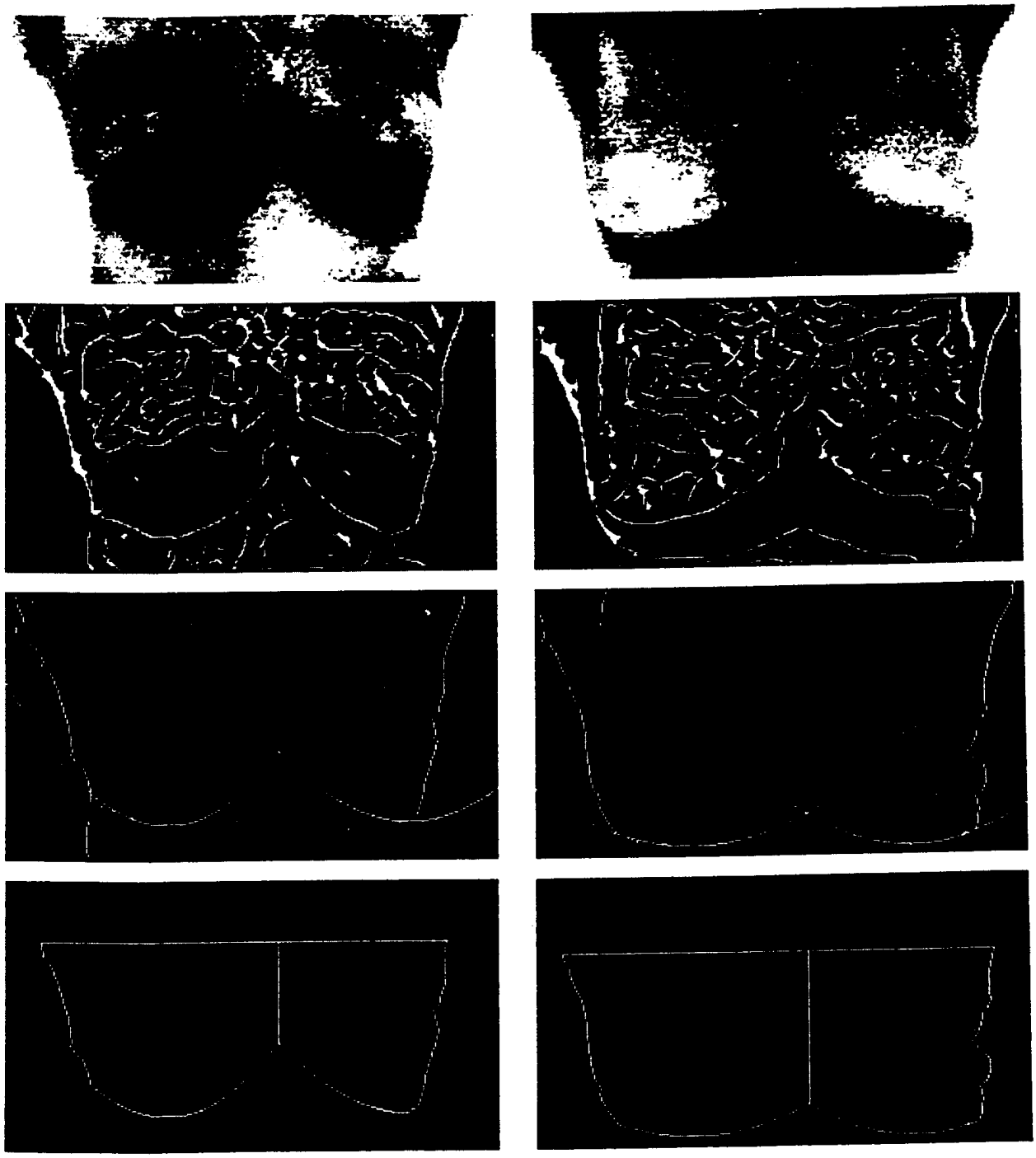

Fig. 2. Segmentation results of two images. Left: results from *lr*. Right: results from *nb*. From top to bottom: original image, edge image. four feature curves, segments.

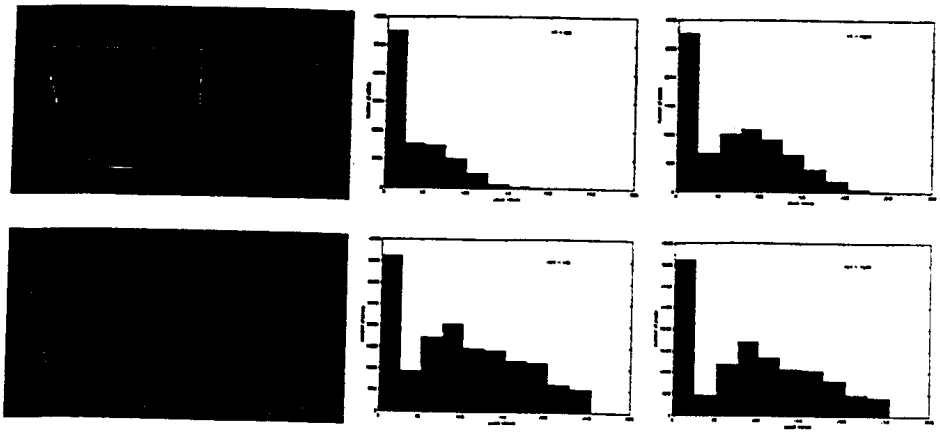

Fig. 3. Histogram of the left and right segments. Top: results from *lr*. Bottom: results from *nb*. From left to right: the segments, histogram of the left segment, histogram of the right segment.

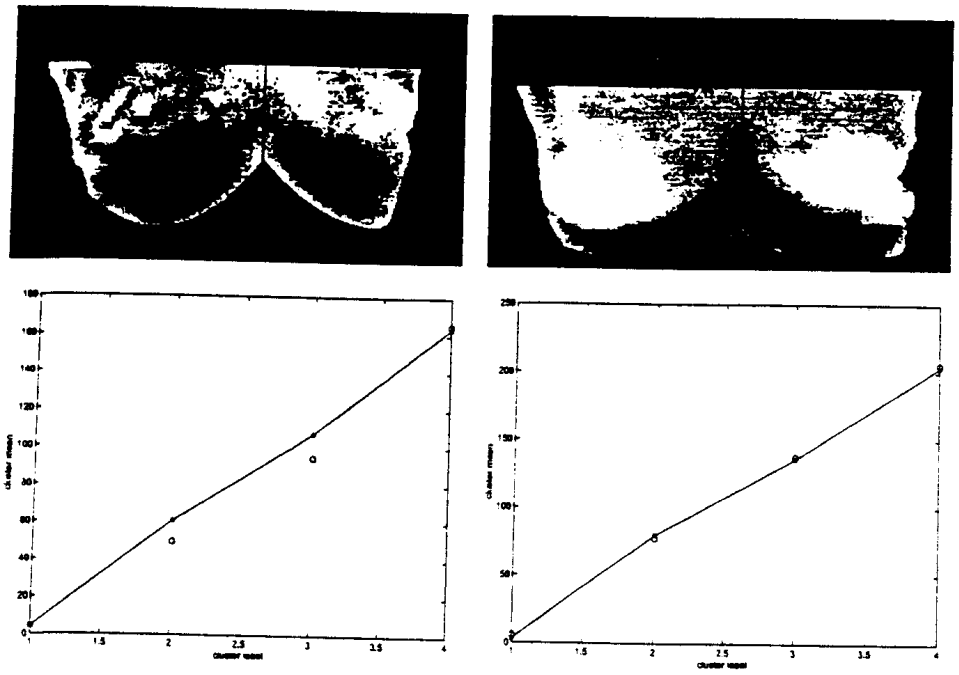

Fig. 4. Labeled image and the profile of mean for each cluster. Left: results from *lr*. Right: results from *nb*. Top: labeled image. Bottom: average pixel value profile of each cluster

[5] C. A. Lipari and J. F. Head. Advanced infrared image processing for breast cancer risk assessment. In *Proceedings for 19th International Conference of IEEE/EMBS*, pages 673–676, Chicago, IL, Oct. 30 - Nov. 2 1997. IEEE.

[6] H. Qi, W. E. Snyder, J. F. Head, and R. L. Elliott. Detecting breast cancer from infrared images by asymmetry analysis. In *World Congress on Medical Physics and Biomedical Engineering: Proceedings of the 22nd Annual Int. Conf. of the IEEE EMB Society*, Chicago, MI, July 2000.

[7] L. Shen, Y. P. Shen, R. M. Rangayyan, and Desautels. J. Measures of asymmetry in mammograms based upon the shape spectrum. In *Proceedings of the Annual Conf. on EMB*, volume 15, pages 48–49. San Diego, CA, 1993.

[8] F. F. Yin, M. L. Giger, K. Doi, et al. Computerized detection of masses in digital mammograms: analysis of bilateral subtraction images. *Med Phys*, 18:955–963, 1991.

[9] F. F. Yin, M. L. Giger, K. Doi, et al. Computerized detection of masses in digital mammograms: automated alignment of breast images and its effect on bilateral-subtraction technique. *Med Phys*, 21:445–452, 1994.

[10] F. F. Yin, M. L. Giger, C. J. Vyborny, et al. Comparison of bilateral-subtraction and single-image processing techniques in the computerized detection of mammographic masses. *Invest Radiol*, 6:473–481, 1993.

[11] B. Zheng, Y. H. Chang, and D. Gur. Computerized detection of masses from digitized mammograms: comparison of single-image segmentation and bilateral image subtraction. *Acad Radiol*, 2(12):1056–1061, Dec 1995.

COMPARISON OF MAMMOGRAPHY AND BREAST INFRARED IMAGING: SENSITIVITY, SPECIFICITY, FALSE NEGATIVES, FALSE POSITIVES, POSITIVE PREDICTIVE VALUE AND NEGATIVE PREDICTIVE VALUE

J.F. Head*, C.A. Lipari**, R.L. Elliott*
*Mastology Research Institute of The Elliott Mastology Center, Baton Rouge, LA
**Arizona State University East, Mesa, AZ
E-mail: emcmri@iamerica.net

ABSTRACT

Breast infrared imaging (IRI) for detection of breast cancer has been unfairly maligned as having unacceptably high false positive and false negative rates. IRI actually has statistical performance characteristics that are similar to mammography. The false positive rate of 14% is about twice as high as mammography but surgical intervention is not possible (no increase in invasive procedures). Also, the false negatives of IRI do not hinder the detection of breast cancer by physical exam, mammography and ultrasound. Finally, the ability of IRI to predict who will develop breast cancer is not appreciated and IRI results should be used to select patients for prevention trials.

KEY WORDS: breast cancer, thermography, infrared imaging, mammography, risk assessment, detection.

INTRODUCTION

Use of IRI of the breasts for detection of breast cancer has been criticized because of its presumed high false positive and false negative rates. However, few clinicians can enumerate the percentage of patients being screened for breast cancer that are false positive or false negative for either mammography or IRI. In this paper we are reporting the statistical performance characteristics of mammography and IRI found through a literature search.

METHODS. The sensitivity, specificity, false positives, false negatives, positive predictive value, and negative predictive value for mammography were found (1-7) in a Pubmed/medline search, and for breast IRI from a 10 year follow-up study on 11,240 women screened for breast cancer reported by Stark (8) in 1985.

RESULTS. The reported performance characteristics of mammography are: sensitivity from 69 to 94% (mean 86%, median 87%), specificity from 59 to 94% (mean 79%, median 84%), false positives of 18%, false negatives of 6%, positive predictive value from 15 to 40% (mean 28%, median 23%) and negative predictive value of 92%. From Stark's study (8) on IRI of the breasts with 10 years of follow-up the performance characteristics were: sensitivity of 86%, specificity of 89%, false positive rate of 11%, false negative rate of 14%, positive predictive value of 23%, and negative predictive value of 99.4%.

DISCUSSION. Sensitivity, specificity, false positive rate, positive predictive value and negative predictive value for breast IRI are as good as or better than those found for mammography. The approximately 2 times higher false negative rate for breast IRI than for mammography (14% vs 6%) might at first concern the physician. However the resulting clinical decisions are quite different: abnormal IRI results in only following the patient closer in their screening (noninvasive), whereas an abnormal mammogram often results in a surgical biopsy (invasive). Therefore the finding of the abnormal infrared image without localization by an abnormal mammogram or ultrasound, does not result in an increase in the number of invasive surgical procedures.

CONCLUSION. Infrared imaging has performance characteristics similar to mammography for detection of breast cancer. Therefore IRI should be re-evaluated for risk assessment and detection of breast cancer.

REFERENCES

1. Hindle WH, Chen EC. Accuracy of mammographic appearances after breast fine-needle aspiration. *Am J Obstet Gynecol* 17, 1286-1290 1997.

2. Ozdemir A, Oznur II, Vural G, Atasever T, Karabacak NI, Gokcora N, Isik S, Unlu M. TI-201 scintigraphy, mammography and ultrasonography in the evaluation of palpable and nonpalpable breast lesions: a correlative study. *Eur J Radiol* 24, 145-154 1997.

3. Neumann P, Romann D, Camara O, Riedel HH. Possibilities and limits of mammography with special reference to breast carcinoma--a comparison of clinical, mammography and histologic diagnoses. *Zentralbl Gynakol* 119, 154-159 1997.

4. Clifford EJ, Lugo-Zamudio C. Scintimammography in the diagnosis of breast cancer. *Am J Surg* 172, 483-486 1996.

5. Laya MB, Larson EB, Taplin SH, White E. Effect of estrogen replacement therapy on the specificity and sensitivity of screening mammography. *J Natl Cancer Inst* 15, 643-649 1996.

6. Khalkhali I, Cutrone J, Mena I, Diggles L, Venegas R, Vargas H, Jackson B, Klein S. Technetium-99m-sestamibi scintimammography of breast lesions: clinical and pathological follow-up. *J Nucl Med* 36, 1784-1789 1995.

7. Warren DL, Stelling CB. Sensitivity, specificity, predictive value and accuracy of film/screen mammography. A three-year experience. *J Ky Med Assoc* 87, 169-173 1989.

8. Stark, Agnes M. The value of risk factors in screening for breast cancer. *European Journal of Surgical Oncology* 11, 147-150 1985.

Computerized image analysis of digitized infrared images of the breasts from a scanning infrared imaging system

Jonathan F. Head, Charles A. Lipari, and Robert L. Elliott

Medical Thermal Diagnostics, LA Business & Technology Center,.Baton Rouge, LA 70803

ABSTRACT

Infrared imaging of the breasts has been shown to be of value in risk assessment, detection, diagnosis and prognosis of breast cancer. However, infrared imaging has not been widely accepted for a variety of reasons, including the lack of standardization of the subjective visual analysis method. The subjective nature of the standard visual analysis makes it difficult to achieve equivalent results with different equipment and different interpreters of the infrared patterns of the breasts. Therefore, this study was undertaken to develop more objective analysis methods for infrared images of the breasts by creating objective semiquantitative and quantitative analysis of computer assisted image analysis determined mean temperatures of whole breasts and quadrants of the breasts. When using objective quantitative data on whole breasts (comparing differences in means of left and right breasts), semiquantitative data on quadrants of the breast (determining an index by summation of scores for each quadrant), or summation of quantitative data on quadrants of the breasts there was a decrease in the number of abnormal patterns (positives) in patients being screen for breast cancer and an increases in the number of abnormal patterns (true positives) in the breast cancer patients. It is hoped that the decrease in positives in women being screened for breast cancer will translate into a decrease in the false positives but larger numbers of women with longer follow-up will be needed to clarify this. Also a much larger group of breast cancer patients will need to be studied in order to see if there is a true increase in the percentage of breast cancer patients presenting with abnormal infrared images of the breast with these objective image analysis methods.

Keywords: thermography, infrared imaging, breast, breast disease, breast neoplasms, risk assessment, image analysis

1. INTRODUCTION

Infrared imaging of the breast, usually referred to as thermography in medicine, has been shown to be efficacious in risk assessment[1,2,3] and prognostic determination in breast cancer[3,4]. Infrared imaging has also been shown to be a useful in conjunction with mammography and ultrasound for the detection and diagnosis of breast cancer. However, the subjective visual analysis of asymmetric abnormalities in infrared images of the breast for risk assessment, detection, diagnosis and prognosis in breast cancer has hindered acceptance of this technology as it has been very difficult to standardize and to learn the subjective analysis method. Therefore it has been very difficult to obtain reproducible results among investigators and clinicians, who are determining the presence or absence of asymmetric infrared abnormalities of the breasts. The introduction of digital output in a variety of both proprietary and standard formats has allowed image analysis by both proprietary image capturing cards and software, and also standard image capturing formats. Standard imaging formats that can export standard files are more useful as they can be submitted to a variety of commercially available image analysis software that are very good at target identification and for creating automated image analysis programs.

Although early attempts at standardizing the analysis procedure of analogue exported images by creating scoring systems by which patients could be categorized in term of risk, detection, diagnosis and prognosis were a great improvement that allowed highly trained thermographers to detect and semiquantitate the infrared abnormalities, they were still quite subjective. These semiquantitative results were quite reproducible by highly trained thermographers, but training was still quite an involved and time consuming experience. The present study is an attempt to totally automate the process so that thermographers can look at an infrared image of the breasts and combine the information that is subjectively processed by their minds with quantitative numerical data derived from image analysis of digitized images that were derived from the analogue output. Eventually we hope to develop an image analysis method that will eliminate the highly subjective nature of the present day infrared image

reading by thermographers with an automated procedure that will only require qualified thermographers to over-read the image analysis results.

2. MATERIALS AND METHODS

Infrared images from 13 patients (10 women without breast cancer, 5 with normal infrared patterns and 5 with abnormal infrared patterns, and 3 breast cancer patients, 2 with normal infrared patterns and 1 with an abnormal infrared pattern) were taken with a first generation, liquid nitrogen cooled, scanning mercury cadmium telluride detector, Inframetrics 500M infrared imaging system with an 8 bit dynamic range, 100 mK sensitivity@30° and a spectral range of 8-12 microns. Although there was proprietary software, we chose to export the digitized images in a TIF file and used customized image analysis software to derive quantitative data on infrared patterns that previously had been subjectively visually analyzed by an expert thermographer. For each patient the mean, standard deviation, minimum, median and maximum temperatures were determined for each breast and comparisons were made between the two breasts. Then, each breast was divided into upper outer, upper inner, lower outer and lower inner quadrants (Figure 1) by drawing lines on the infrared images from the chin of the patient

FIGURE 1
GUIDELINES FOR BREAST QUADRANTS

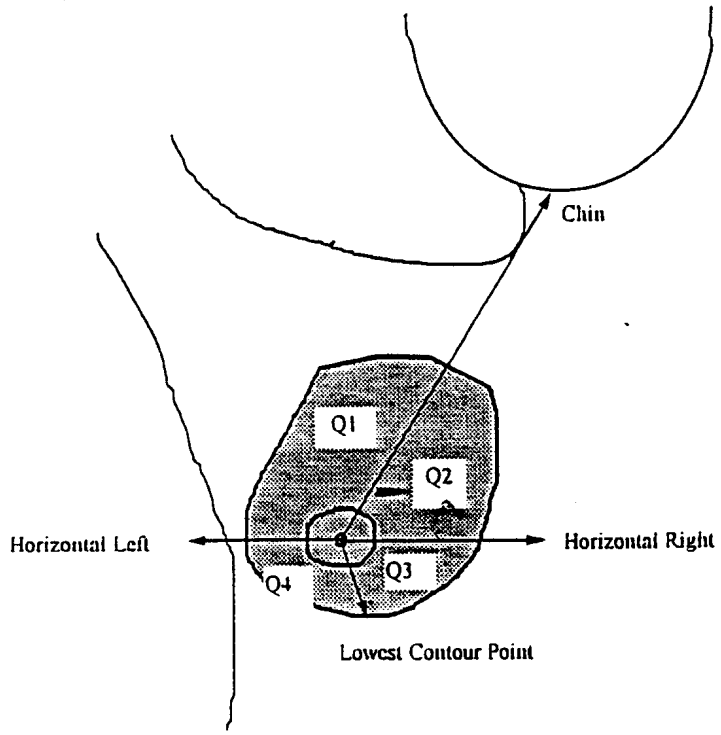

to each nipple and then two horizontal lines left and right to the edge of the breast and finally a forth line to the lowest contour of the breast. Again the mean, standard deviation, minimum, median and maximum temperatures were determined for each quadrant of both breasts, and comparative statistics were generated between the left and right breasts.

Three objective quantitative methods of determining asymmetric abnormalities of the breast were developed. The first method (Method 1) compared the difference in mean temperature between the right and left breasts and if this mean temperature was equal to or greater than 0.50°C then the patient was considered to have an abnormal asymmetric breast infrared heat pattern.

The second method (Method 2) involved calculating a score based on addition of scores to create an index, if the mean temperature of a quadrant was 0.50 to 1.00°C higher than the same quadrant of the opposite breast then a score of 0.5 is assigned, and when a quadrant has a mean temperature that is greater than 1.00°C higher then a score of 1.0 is assigned. An index is created by adding together the scores for the comparisons of all four quadrants and the index can have a value from 0.0 to 4.0. For purposes of this study patients with an index greater than 1.0 were considered to have.abnormal asymmetric breast infrared heat patterns. The third method was the simple addition of the mean differences of the quadrants comparing the left and right breasts and absolute differences greater than 1.00 were considered to represent abnormal asymmetric infrared patterns. Comparison of the results from these three objective determinations of asymmetry of infrared heat patterns of the breasts were then compared to the subjective results of an expert thermographer.

3. RESULTS

Figure 2 shows the quadrants of the breasts of a patient (patient #1 in Table 1) with a normal infrared heat pattern of the breasts and Figure 3 shows a patient (patient #2 in Table 1) with a highly abnormal asymmetric infrared heat pattern of the breasts. In both Figures 2 and 3 the quadrant lines have been overlaid on the actual digitized infrared images from the

FIGURE 2
NORMAL INFRARED PATTERN IN PATIENT BEING SCREENED FOR BREAST CANCER

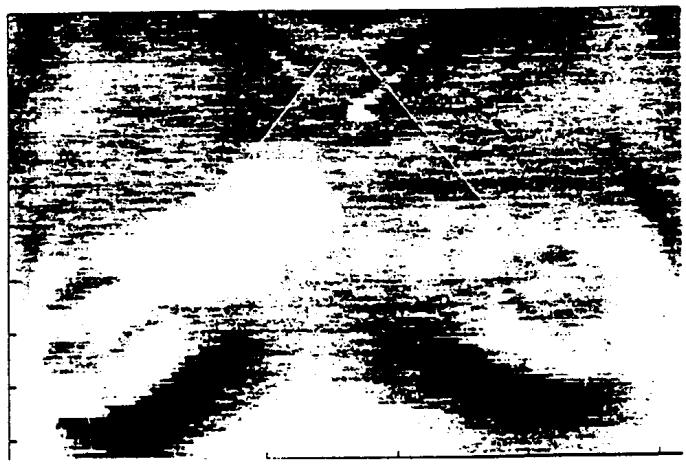

FIGURE 3
ABNORMAL INFRARED PATTERN IN PATIENT BEING SCREENED FOR BREAST CANCER

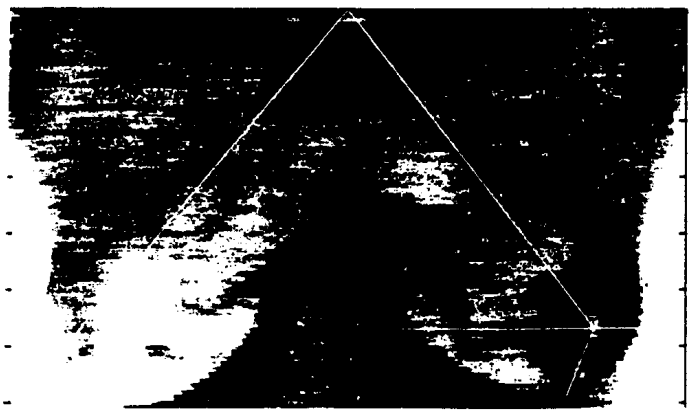

TABLE 1
SUBJECTIVE AND OBJECTIVE DETERMINATION OF ASYMMETRIC INFRARED ABNORMALITIES IN PATIENTS BEING SCREEN FOR BREAST CANCER

PATIENT #	SUBJECTIVE	METHOD 1 (°C)	METHOD 2 (INDEX)	METHOD 3 (°C)
1N[a]	N[b]	-0.42	1.0	-1.00
2N	L+	**-1.30**[c]	**3.5**	**-8.68**
3N	N	+0.33	1.0	+0.94
4N	N	+0.20	0.0	+0.74
5N	L+	+0.10	1.0	-0.46
6N	N	-0.26	0.0	-0.60
7N	L+	-0.24	0.5	-0.56
8N	L+	**-0.79**	**2.0**	**-2.95**
9N	N	-0.28	0.0	-0.87
10N	L+	-0.45	**1.5**	-0.88
11CA	N	+0.10	0.5	+0.36
12CA	R+	**+0.59**	**1.5**	**+1.99**
13CA	N	**+0.65**	**1.5**	**+2.60**

[a]N, normal patient; CA, breast cancer patient
[b]N, normal infrared breast pattern; L+, abnormal left infrared breast pattern; R+, abnormal right infrared breast pattern
[c]bold numbers signify abnormal values for infrared images

patients with normal and abnormal infrared images of their breasts. The patient in Figure 2 with the normal infrared heat pattern has vascularity demonstrated in both breasts but they are approximately equivalent, as there are no major asymmetries in either breast. The patient in Figure 3 has a generally hotter (black is hot) left breast with periareolar heat and a large hot spot on the outer quadrants, and vascular asymmetry on the inner quadrants.

Table 1 presents the results from the subjective whole breast analysis, quantitative whole breast analysis (Method 1), semiquantitative quadrant analysis (Method 2) and quantitative quadrant analysis (Method 3) of the 13 patients in this study. While doing the subjective analysis the thermographers were not sure if patient 9 had a normal or a slightly abnormal left breast and for patient 11 there was some uncertainty whether the right breast was abnormal. When the objective quantitative Method 1 was used, that compared the difference in mean temperature between the two breasts, there was a decrease from 50% abnormal infrared patterns in the 10 patients being screened for breast cancer (chosen to be half normal and half abnormal) by 3 so that only 20% (2 of 10) of the patients being screened for breast cancer had abnormal asymmetric heat patterns of the breasts. Both the objective semiquantitative Method 2 and quantitative Method 3, decreased the abnormal asymmetric infrared images in the patients being screened for breast cancer to 3 patients (a 20% decrease in the positive rate for this group of patients). In the 3 breast cancer patients one of the three patients with a normal infrared pattern by subjective analysis was found to have an abnormal infrared pattern by all three objective analysis methods.

4. DISCUSSION

The subjective method of determining whether an asymmetric infrared abnormality of the breasts is significant, that is presently being utilized by most physicians, is hard to learn, and not adequately reproducible. In a previous study[5] we attempted to use a semiquantitative method of determining when an asymmetric infrared heat pattern of the breasts was sufficiently different to be called abnormal. Although this method seemed to produce a greater continuum of abnormalities through the creation of an abnormality index from 1 to 8 (summation of scores that reflected the severity of hot spots, global heat, vascularity, areolar/periareolar heat and edge sign), it still had major shortcomings: The method required highly trained thermographers to rate the abnormalities and the exact cut-off index for abnormal was not obvious or easy to determine. Further it would be almost impossible to create a computer assisted analysis program that could do this analysis without subjective input by a highly qualified thermographer.

The present study used a computer assisted image analysis program that presently requires significant operator interaction but will be made operator independent. We believe that eventually whole breast or quadrant temperature differences will be inputed into one of the three methods of analyses presented in this paper, or some other method of analysis, and that the subjective methods presently used by thermographers will be replaced by an objective method of analysis. Initially the results from objective analysis will probably be used as another piece of information in the present subjective analysis, but, if successful, the results of the whole breast or quadrant image analysis should become the most important information used in determining whether patients, being screened for breast cancer or presenting with breast cancer, have abnormal asymmetric infrared patterns of their breasts.

Image analysis for determination of mean temperatures of the whole breast or quadrants of the breast, followed by a simple method of numerical analysis and finally the application of numerical cut-offs for a normal range of temperature difference was also undertaken in this study to determine if this type of analysis could decrease the high false positive rate found in women being screened for breast cancer with infrared imaging. The results from this study show that all three objective methods, based on image analysis for temperature differences in either whole breast or quadrant comparisons, significantly reduced the number of patients being screened for breast cancer with abnormal asymmetric infrared heat patterns. The two methods (Methods 1 and 3), where 0.50°C and 1.00°C are the normal cut-offs for whole breast and summation of quadrant differences, respectively, seem to be very promising methods of analysis and could easily transform the infrared pattern analysis from a subjective visual analysis into a purely objective quantitative analysis. One somewhat surprising finding in this study was the increase in the number of patients with breast cancer that had positive infrared patterns of the breast. Although these objective quantitative results suggest that their application will reduce the number of false positives in women being screened for breast cancer with infrared imaging, while also increasing the true positive rate for women found to have breast cancer during screening with infrared imaging, larger studies must be undertaken to better clarify if the objective methods are better than the subjective methods and, if the objective methods are better, then which objective method is the best.

5. ACKNOWLEDGEMENTS

Partial financial support was provided through a SBIR contract with the Army Night Vision Laboratory.

6. REFERENCES

1. M. Gautherie and C.M. Gros, "Breast thermography and cancer risk prediction", *Cancer* **45**, pp. 51-56, 1980.
2. A. M. Stark, "The value of risk factors in screening for breast cancer", *Eur. J. Cancer* **11**, pp. 147-150, 1985.
3. J. F. Head, F. Wang and R. L. Elliott, "Breast thermography is a noninvasive prognostic procedure that predicts tumor growth rate in breast cancer patients, *Ann. N. Y. Acad. Sci.* **698**, pp. 153-158, 1993.
4. H. J. Isard, C. J. Sweitzer and G. R. Edelstein, "Breast thermography: A prognostic indicator for breast cancer survival", *Cancer* **62**, pp. 484-488, 1988.
5. J. F. Head, C. A. Lipari, F. Wang and R. L. Elliott, "Cancer risk assessment with a second generation infrared imaging system", *Proc. Int. Soc. Optical Eng.* **3061**, pp. 300-307, 1997.

Further author information -
J.F.H.(correspondence): Email: emcmri@iamerica.net; Telephone: 504-927-2256; Fax: 504-927-3772

Thermography

Its Relation to Pathologic Characteristics, Vascularity, Proliferation Rate, and Survival of Patients with Invasive Ductal Carcinoma of the Breast

We were very surprised to see that Sterns et al.[1] had results that contradicted those presented by our group which demonstrated an association between three growth rate–related prognostic indicators for breast carcinoma and findings from infrared imaging.[2] Careful review of the Sterns et al. article[1] showed that they performed the infrared imaging with a different and outdated technology, did not quantitate actual growth rate with serial measurements from mammography, and looked at only one of the three growth rate–related parameters reported by our group[2] to be associated with abnormalities found in infrared images of the breast.

In reviewing the two articles by Sterns et al.[1,3] on contact thermography, we noted that they reported that 56% of the breast carcinoma patients from the initial 214 patients who were screened with thermography had an abnormal breast thermogram, whereas only 19% had abnormal breast thermography when 420 women were enrolled in the study. This inconsistency is due to the fact that in the initial study the patients with equivocal thermal patterns were considered abnormal, whereas in the recent expanded study equivocal patients were considered normal. This clearly demonstrates that the authors are not sure what level of abnormality is really significant when attempting to relate infrared images to growth rate and growth rate–related parameters. In our study,[2] in which telethermography was used, 65% of the breast carcinoma patients had abnormal thermograms (including both the small number of patients with slightly abnormal thermograms and all the patients with definitely abnormal thermograms), and Isard et al.[4] found that 54% of their patients had either PF2- or PF3-level abnormalities. In both of these studies, the presence of an abnormal breast thermogram had a significant impact on survival.

It is not appropriate to compare contact thermography results, produced by a technology that is over 20 years old and was not used in either our study or that of Isard et al.,[2,4] with the results from infrared telethermography (a newer, more sensitive technology with much better image quality). It appears that the superior image quality of infrared telethermography may be necessary to demonstrate that abnormal infrared images of the breast (asymmetric hot spots, global

heat, vascularity, areolar/periareolar heat, or edge sign) are related to survival and growth rate–related prognostic indicators. Our emphasis at present is to improve our sensitivity and image quality further by using second-generation infrared imaging technology, which has previously been used only by the military. The second-generation infrared imaging system that we have been evaluating is more sensitive than scanning telethermography units and produces a better image, with a 256 × 256 element focal plane array sensor. In addition, we are currently developing methods of analyzing the infrared images of the breast with computerized image analysis software that compares the heat pattern of one breast with that of the other to delineate the asymmetric infrared abnormalities. This computer analysis is an attempt to automate the process, but it will initially only be used to aide the image reader by pointing out possible asymmetric areas. Eventually, we hope to quantitate different parameters of the infrared abnormalities in order to define the significance of the different abnormalities better, partly in terms of their presence and partly to allow for the assignment of a numerical value to each abnormality in an attempt to create an infrared abnormality index by adding together the numerical results. None of this computer-assisted image analysis can be done with the images from contact thermography, as the images from contact thermography cannot be easily digitized for image analysis.

Reevaluation of the authors' data with the chi-square test, comparing the three levels of thermographic abnormality (normal, equivocal, and abnormal) to the levels of previously demonstrated prognostic indicators, showed that there were significant associations of thermographic results with a patient's age ($P = 0.0113$), tumor size ($P = 0.0078$), lymph node involvement ($P = 0.0023$), stage ($P = 0.0001$), histologic grade ($P = 0.0028$), and estrogen receptor status ($P = 0.0429$), but there was only a trend toward association with ultrasound vascularity ($P = 0.0663$) and no association with Ki67 ($P = 0.2898$). It seems that if thermographic abnormalities are so strongly associated with so many known prognostic indicators, then it is unlikely that thermographic results of the breasts would not have prognostic significance and not be a predictor of disease free and overall survival. The number of patients that were actually followed in the study to determine 5-year disease free and overall survival was not given in the article, but infrared imaging results were very significantly correlated with 5-year disease free survival ($P = 0.0009$) as well as tumor size ($P = 0.0001$), lymph node status ($P = 0.0001$), stage ($P = 0.0001$), and grade ($P = 0.0001$). Overall survival was not significantly related to thermographic abnormality but again was strongly associated with tumor size, lymph node status, stage, and grade. However, disease free and overall survival were quite different between the groups of breast carcinoma patients with normal and abnormal infrared images of the breast, with differences in disease free and overall survival of 21% and 9%, respectively. Establishing a significant difference in survival may require a larger follow-up study, with more patients enrolled and followed for 5 years. It may even be necessary to follow the patients for a longer period of time, as it is common for differences in disease free survival to predate significant differences in overall survival, and thus significant differences in overall survival are often only reached when the study groups are followed for a few extra years beyond the point at which significant differences are found in disease free survival.

The first analysis suggesting that the results from breast thermography were related to the growth rate of breast carcinomas was reported in a paper by Gautherie and Gros.[5] That analysis clearly showed that tumors classified as T1 and T2 (with diameters between 0.9 and 3.7 cm) had greater heat production than normal breast tissue and that the heat production correlated with the growth rate of the tumor. We have recently provided further evidence[2] that the thermographic results are related to the growth rate of a breast carcinoma by showing that the result of three growth rate–related prognostic indicators (biochemical assay of tumor ferritin concentration, immunocytochemical analysis of Ki67, and determination of S-phase/growth fraction by flow cytometry) are strongly associated with thermographic results. Sterns et al.[1] compared one of these prognostic indicators, Ki67, to results from contact thermography and concluded that thermographic results are not related to the growth rate of breast tumors. However, they did not attempt to make an actual clinical determination of growth rate with serial measurements, nor did they semiquantitate or quantitate the two other prognostic indicators that have been related to thermographic results from telethermography.

Additional studies will be needed either to confirm or disprove a relationship between the results of breast thermography and survival and/or the growth rate of breast carcinomas. These studies must attempt to repeat the original studies and not rely on outdated technology, such as contact thermography, that was not even state of the art at the time of the original publications,[1–5] let alone today. Future investigators should not do any more studies on single growth-related prognostic indicators, as this will only further confuse the issue. It would be best to undertake large prospective studies that look at thermographic abnormalities determined with state-of-the-art telethermography and then compare the results to the growth rate of

tumors, determined by direct measurement of doubling time, and growth rate–related prognostic indicators (tumor ferritin concentration, S-phase determined by flow cytometry, and growth fraction of the tumor determined by Ki67 immunocytochemical analysis).

REFERENCES

1. Sterns EE, Zee B, SenGupta S, Saunders FW. Thermography: its relation to pathological characteristics, vascularity, proliferation rate, and survival of patients with invasive ductal carcinoma of the breast. *Cancer* 1996;77:1324–8.
2. Head JF, Wang F, Elliott RL. Breast thermography is a noninvasive prognostic procedure that predicts tumor growth rate in breast cancer patients. *Ann N Y Acad Sci* 1993;698:153–8.
3. Sterns EE, Zee B. Thermography as a predictor of prognosis in cancer of the breast. *Cancer* 1991;67:1678–80.
4. Isard HJ, Sweitzer CJ, Edelstein GR. Breast thermography: a prognostic indicator for breast cancer survival. *Cancer* 1988;62:484–8.
5. Gautherie M, Gros CM. Breast thermography and cancer risk prediction. *Cancer* 1980;45:51–6.

Jonathan F. Head, Ph.D.
Robert L. Elliott, M.D., Ph.D.
The Elliott Mastology Center
Baton Rouge, Louisiana

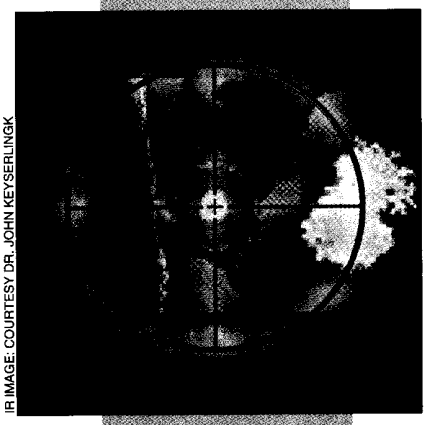

IR IMAGE: COURTESY DR. JOHN KEYSERLINGK

Infrared Imaging: Making Progress in Fulfilling Its Medical Promise

Past, Present, and Future Applications of Infrared Imaging in Medicine

Jonathan F. Head and Robert L. Elliott
Elliott-Hailey-Head Breast Cancer Research and Treatment Center

Infrared imaging in medicine has been around since the early 1970s, but its utility for any medical application has not been clearly demonstrated. Therefore, infrared technology is not widely accepted in medicine. Over the past ten years improvements in infrared systems (including staring array sensors, true digital output, sophisticated image processing, and analysis using target recognition software) have allowed objective analysis of digital radiometric information for a variety of medical applications.

Current medical applications that have supporting documentation in the peer-reviewed medical literature include breast cancer risk assessment and prognosis, analysis of burn trauma, and battlefield application of a helmet-mounted infrared imager for use by medics. Other promising areas for medical application of infrared imaging in medicine include coronary artery bypass surgery, diabetes, deep vein thrombosis, and areas involving angiogenesis (wound healing and microsurgery). However, some classic uses of infrared imaging that have achieved some amount of widespread use, such as pain management, probably will not survive rigorous scientific scrutiny. This article looks at where current applications of medical imaging started and promising future uses as the technology improves.

Applications

Breast Cancer

Initial studies of the application of infrared imaging to breast cancer concentrated on trying to use breast infrared imaging (contact or telethermography) as a stand-alone technology for the detection of breast cancer in a screening environment. The early Breast Cancer Detection and Demonstration Projects (BCDDP), which were done between 1973 and 1981 by the American Cancer Society and National Cancer Institute of the United States, clearly demonstrated the shortcomings of both mammography and infrared imaging of the breast but also showed that mammography was a superior stand-alone detection technology, if only because it localized a lesion that could be then surgically resected and examined by the pathologist to determine if the patient had breast cancer. In other words, even if infrared imaging was able to tell the surgeon that the patient was very likely to have breast cancer, its inability to tell the surgeon where the lesion was, because it is a physiological measurement and not a physical view as in mammography, made it unacceptable as a stand-alone detection device.

The ability of infrared imaging to be used in a multimodality-screening environment has not received the attention that it deserves. Although physical exam and ultrasound examination are widely accepted as techniques that complement mammography and are routinely used in the differential detection/diagnosis of breast cancer, this has not happened with breast infrared imaging. This is despite support for this concept by physicians who routinely use infrared technology. Recently Keyserlingk et al. [1] have shown that in their hands infrared imaging can help confirm the diagnosis of breast cancer, but larger studies are needed to determine if the false positive rate of 66 to 80% in the present clinical setting (physical exam, mammography and/or ultrasound) [2] can be reduced by integrating routine infrared imaging into breast cancer screening programs.

 0739-5175/02/$17.00©2002IEEE

An application of infrared imaging in breast cancer that has been extensively studied with very positive results is the use of breast infrared imaging in risk assessment (determining whether a female is at average or high risk of getting breast cancer during her lifetime). Other imaging technologies (such as mammography, breast ultrasound, magnetic resonance imaging (MRI), and positron emission tomography (PET) scans) have not been found to be useful for predicting whether a woman will develop breast cancer in her lifetime. In addition, infrared imaging was not studied during the Breast Cancer Detection and Demonstration Projects to determine its ability to define a subgroup of women at increased risk of developing breast cancer, as this was not considered important. However, in more recent times intervention or prevention trials have become a reality, specifically the use of the anti-estrogen tamoxifen in patients who have not been diagnosed with breast cancer but are believed to be at a higher than normal risk of getting breast cancer due to their genetic makeup and/or environmental factors. Presently, the Gail Model is used to determine if a woman is at increased risk of getting breast cancer. This model uses age, age at first menstrual period, number of first-degree relatives who have had breast cancer, whether the woman had a previous breast biopsy (number and presence of atypical hyperplasia), and race to determine the risk of getting breast cancer for a woman who has received regular clinical breast exams and screening mammography. This risk assessment model does not apply to genetically predisposed women or women who have previously had a biopsy that contained DCIS (ductal carcinoma in situ) or LCIS (lobular carcinoma in situ). However, even by combining all these factors, less than half of the women at risk of getting breast cancer can be identified, and the women at increased risk only have about a two- to four-fold increase.

Several studies have shown that infrared imaging is a good, and perhaps the best, method for risk assessment in breast cancer. Gautherie and Gros [3] demonstrated in a prospective study of 58,000 women being screened for breast cancer that there were 784 patients that had an abnormal asymmetric infrared image of their breasts with normal physical exams, mammograms, and ultrasounds, and that 298 (38%) of these 784 patients were diagnosed with breast cancer within four years. This is in contrast to expecting only 1-2% of women from the general population being diagnosed with breast cancer in a four-year period, and thus the presence of an abnormal asymmetric infrared heat pattern of the breasts probably increases a woman's risk of getting breast cancer at least ten-fold. In a second study Stark [4] followed 11,249 women who were being screened for breast cancer and found that 1,499, or about 15%, of the women had abnormal asymmetric heat patterns of their breasts. Stark further found that in the next ten years 346, or 23%, of the women with abnormal asymmetric infrared images of their breasts were diagnosed with breast cancer. Stark further found that only 8.1% of women who had not had any children and 8.6% of women with one or two first-degree relatives who had breast cancer (family history) developed breast cancer during the same period of time. Therefore, two of the major criteria used to enroll patients in the tamoxifen prevention trial were poorer risk assessment tools than the presence of an abnormal asymmetric breast infrared image. The presence of atypical hyperplasia in a biopsy sample was found by Stark to result in 30 to 50% of these patients being diagnosed with breast cancer, but only 34 women had this risk marker, and this is too small a proportion of the overall population to be a significant risk assessment tool. In our own studies [5]-[10], we have found that approximately 28% of women have abnormal asymmetric breast infrared patterns (Figure 1) and are therefore at increased risk of getting breast cancer, and this is supported by the fact that a much higher proportion (65%) of breast cancer patients at presentation have an abnormal asymmetric breast infrared pattern (Table 1).

Although these studies support the use of breast infrared imaging in breast cancer risk assessment, it will be necessary for the

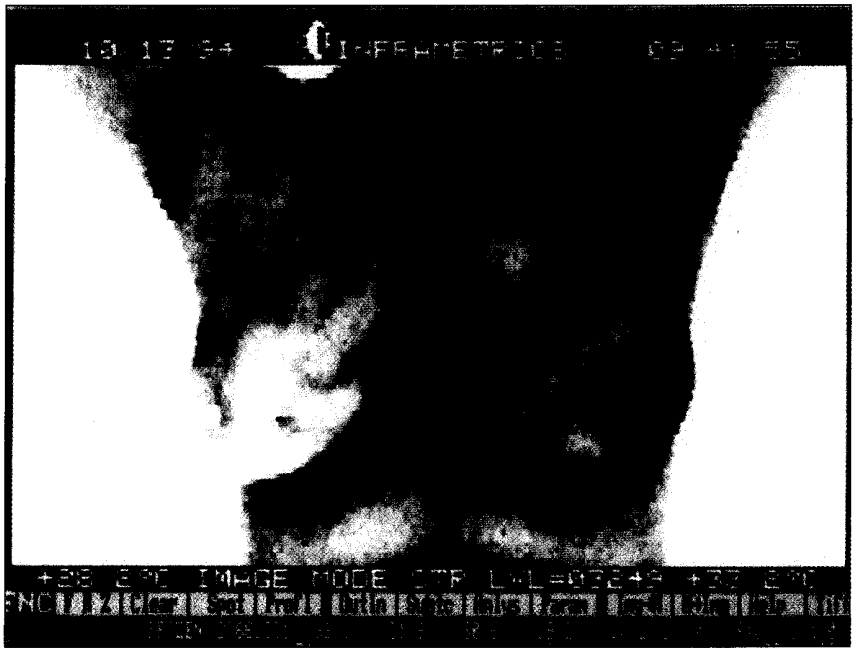

1. A patient with an abnormal asymmetric breast infrared image.

Table 1. Infrared results from normal, cancer, and deceased cancer patients.

Infrared Results	Patients		
	Normal	Cancer	Deceased
Normal	72 72%	35 35%	15 12%
Abnormal	28 28%	65 65%	111 88%
$p < 0.0001$, chi-square analysis for independence			

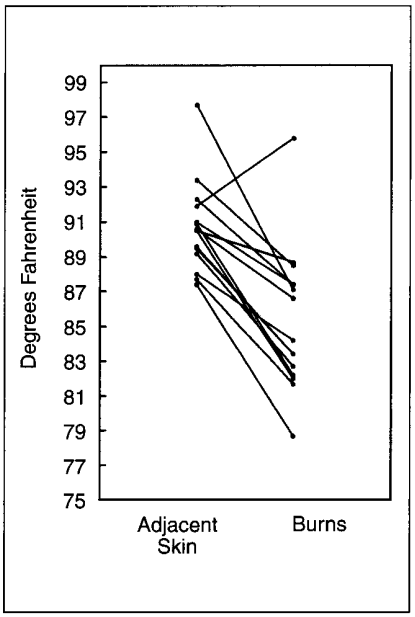

2. Normal adjacent skin and burn temperatures.

results to be confirmed in large multi-institutional studies done in the United States in order to obtain FDA and HCFA approval. This approval is necessary in order for any new technology to be reimbursed by both Medicare and private insurance, and without reimbursement no new technology can achieve wide acceptance. Also, if infrared imaging is determined to be a viable tool for risk assessment, then further multi-institutional studies will be needed to see if the subset of patients being screened for breast cancer, which have an abnormal asymmetric infrared image of their breasts, are better candidates for the tamoxifen prevention/intervention trial or any other prevention/intervention trial. It will be necessary to show that the group containing the higher proportion of women at increased risk of getting breast cancer (those with abnormal breast infrared images) respond to tamoxifen prevention/intervention. Hopefully, this will allow less women to be treated with tamoxifen in order to reach the women that will be prevented from getting breast cancer by the prevention/intervention strategy.

Another application of infrared imaging in breast cancer is for predicting prognosis. Isard [11] has shown by following 70 breast cancer patients for five years that breast cancer patients presenting with abnormal asymmetric breast infrared images had only a 30% chance of surviving the five years, whereas breast cancer patients presenting with normal symmetric breast infrared images had an 80% survival at five years. Head et al. [5], [6] provided additional evidence that the results of infrared imaging have prognostic significance when they found that 65% of breast cancer patients at diagnosis had abnormal asymmetric breast infrared images but 88% of breast cancer patients that succumbed to breast cancer had abnormal asymmetric breast infrared images. Thus, breast cancer patients with abnormal asymmetric breast infrared images are more likely to die of breast cancer, and they therefore have a poorer prognosis at diagnosis.

Gautherie [12] was the first to show that breast cancer patients with abnormal asymmetric breast infrared images had tumors with faster growth rates. Head et al. [13] further showed that the results from three growth-rate-related clinical laboratory tests were associated with the findings from breast infrared imaging. Higher tumor ferritin concentrations were found in breast tumors from patients with abnormal asymmetric infrared breast images and tumors with faster growth rates had previously been shown to have greater concentrations of ferritin. Also, the percentage of cells in S-phase (DNA synthesis) and G_2M (mitosis/cell division) were also greater in breast tumors from patients with abnormal asymmetric infrared images of the breasts, thus showing that tumors with greater cell proliferation are more likely to occur in patients with abnormal asymmetric breast infrared images. Finally, the proliferation-associated antigen Ki-67 was higher in tumors from women with abnormal asymmetric breast infrared images. Therefore, the results from two studies by different investigators have shown that four growth-rate and proliferation-rate associated parameters were related to breast infrared image results. This supports the use of infrared imaging results in determining prognosis, as growth rate is one of the few documented and accepted prognostic indicators in breast cancer.

Helmet-Mounted Infrared for Battlefield Medical Application

Military medical personnel, specifically the forward battlefield medics, have not seen any significant improvement in nighttime visual assistance since the advent of the flashlight. Thus, medics during night operations or when medical assistance to wounded military personnel extends into the night, always expose themselves to enemy identification when they illuminate the battlefield with light from their flashlights to find wounded military personnel, make triage decisions, or treat the wounded personnel in need of immediate care. Of course after the enemy spots and identifies the medic, the medic is immediately subjected to enemy gunfire, which hinders and often curtails battlefield medical treatment. Further, the spotting and identification of the medic by the enemy requires only the use of a free, always available, very high tech sensing device—the human eye.

Since the 21st century warrior concept for the United States military envisions every military helmet on the battlefield being equipped with an infrared imager, we became interested in the possibility of using this infrared capability to the benefit of the medic and wounded on the battlefield [14]-[16]. It immediately became apparent that the optics on the prototype models of the 21st century warrior helmets were inadequate for battlefield medical applications. The major limitation was that the infrared imagers were not required or able to be focused any closer than 5 feet, a distance that would allow combat personnel to see from their feet to infinity but not allow them to work with their hands. Thus either the optics had to be altered or new optics made. We found that we were able to modify our prototype in order to focus down to 18 inches and then proceeded to determine if the helmet-mounted infrared imager would be useful for medical applications.

We found that variations in heat patterns were associated with a wide range of medical conditions. Living wounded military personnel can be found on the battlefield in complete darkness due to their much higher body temperature compared to their surroundings. Infrared can also be used to distinguish between an unconscious and dead battlefield casualty, for if the person is only wounded the infrared image of the nostrils will alternate between hot and cold as the person breathes in and out. Also, living individuals have a mottled infrared pattern on their skin that becomes a smoother, more consistent pattern with death due to the lack of movement of the blood and its associated heat to the surface of the body. Bleeding associated with sharp trauma can easily be found because of the higher temperature of the blood than the surface of the body, and arterial bleeding can be distinguished from venous by its higher temperature. Blunt trauma can be distinguished by an increase in heat associ-

ated with inflammation. First- and second-degree burns can be detected and the area determined by the increase in temperature at the site, and third-degree burns are visualized as areas with significantly decreased temperature (see next section for an in-depth discussion). This is not an exhaustive list of what can be seen, but it does help one envision the possibilities.

Helmet-mounted infrared imagers can also be used to allow medics to see their hands and the instruments necessary to do the initial first aid in the dark. Therefore, the medic can perform the necessary first aid that the wounded individual needs to survive removal from the battlefield, without being spotted by the enemy and being subjected to enemy fire.

Burns

In 1990 Cole et al. [17] reported on infrared assessment of hand burns in an attempt to stage the burns with temperature measurements. Although they thought that infrared imaging had great potential for differentiating a second-degree burn from a third-degree burn at presentation, they were not able to clearly demonstrate its efficacy. Thus, the problem has remained that many burn patients for whom the physician cannot initially determine whether the burn is a second- or third-degree burn have to wait 5 to 7 days before a decision on grafting can be made. If infrared imaging could be used to differentiate third-degree burns at presentation, then average hospital time for burn patients could be significantly reduced. Problems of evaporation and the associated cooling of badly burned areas, which could possibly lower the temperature of a second-degree burn to that of a third-degree burn, were addressed by Cole et al. [18] by using a sterile nonpermeable plastic wrap to cover the wound before infrared imaging. The same group of investigators [19] has also followed the infrared signature of burns over time.

In 1999 Hargroder et al. [20] performed infrared imaging on the burns of ten patients (Figure 2) with burns that could not be staged by visual analysis; that is, the burns could be either second- or third-degree. They found that in third-degree burns the area of the burn had reduced temperatures compared to the surrounding normal unburned skin, but that an obvious second-degree burn had an increased temperature, probably due to inflammation (Figure 2). They also concluded that the surface temperature of the body, arms, and legs of patients were quite constant, whereas normal surface temperature of the feet, hands, and face were quite variable. They concluded that the temperature decreases occurring with third-degree burns are due to the destruction of the vasculature below the skin, and that a 2 °C (4 °F in the study) decrease in temperature at presentation, which is within the first 24 hours, was a good diagnostic characteristic of a third-degree burn. This suggested that any burn area greater than one square inch in area with a greater than 2 °C decrease in temperature will require grafting and can be grafted immediately without waiting until a definite visual diagnosis can be made. Further study is needed on a much larger population of burn patients in order to confirm these findings and to refine the distinctions between true second- and third-degree burns in terms of their infrared images.

Other Promising Applications

Other promising areas of medicine for which infrared imaging may have significant applications include any disease in which there is a vascular component. The diabetic foot has complications that infrared imaging might be able to detect, such as the subtle decrease in blood flow, which is the harbinger of serious problems that too often lead to amputation of the foot. Also, the use of infrared imaging in surgery is under utilized, as it is obvious that blood flow can easily be monitored with infrared imaging. Therefore, infrared imaging should be available to the coronary bypass surgeon and the microsurgeon, so that the quality of the vascular connections can be monitored and checked during the surgery by the quantity of heat being brought to the newly attached blood vessels or reattached appendage. Deep leg thrombosis also appears to be able to be diagnosed with infrared imaging. One exciting new area of study that has recently arisen is the ability to detect angiogenesis with infrared imaging [21] and the possible application of infrared imaging to monitoring the response of breast cancer or skin cancer patients to anti-angiogenic drugs. This is far from a complete list of promising medical applications but does point out some of the major areas into which medical infrared imaging may grow.

Image Analysis and Algorithm Development

State-of the-art infrared imaging instruments and the associated computers and software for analysis have not been adequately used in or applied to medicine. Even today, the instrumentation used in medical applications is almost exclusively first-generation (Table 2). Thus, most of the published research with infrared imaging used scanning instrumentation with visual analysis of a very poor quality infrared image. The use of visual analysis has hindered the acceptance of infrared imaging in medicine because it requires that there be a pool of experts that are willing to set standards (agree on diagnostic standards) and to train other individuals in the art of visual analysis.

The most obvious way to improve infrared imaging would be to bring the instrumentation at least to the level of second-generation instrumentation. This would mean that the sensitivity would be increased to 50 mK or below at 37 °C, and the output would be digitized. True digital output from a focal plane staring array in-

Table 2. Comparison of features between first and second generation infrared systems.

First Generation	Second Generation
Scanning Mercury Cadmium Telluride Detector	Indium Antimonide Focal Plane Array
Liquid Nitrogen Cooler	Stirling Cycle Cooler
175 Elements/Line@Line Rate: 7866 Hz RTS-170/NTSC	256 × 256 Elements/Staring Array
Dynamic Rating: 8 Bits/Element	Dynamic Rating: 12 Bits/Element
Thermal Sensitivity: 100 mK@30 °C	Thermal Sensitivity: 25 mK@30 °C
Spectral Range: 8-12 Microns	Spectral Range: 3-5 Microns
External Calibration	Internal Calibration
Video Output: Analog	Video Output: Either Digital or Analog

frared imaging system would eliminate the necessity of improving scanned images by the manipulation of the multi-image scans that are pieced together to form one image [22], [23].

Today's focal plane staring array digital imagers are able to assign temperatures to every point in the pictorial array. State-of-the art radiometric infrared imaging instruments can now save images on flash cards so that they can be imported into personal computers for image analysis using a variety of mainly proprietary software. The inability to access and interpret the radiometric information that is encoded in the image file is one of the shortcomings of the present-day systems, and standardization of the encoded image will be necessary for the information to be analyzed by a wide variety of already developed algorithms, such as algorithms developed by the military for target recognition. Therefore, one of the most pressing problems in infrared image analysis is that the radiometric information, which is saved and exported, is done in a proprietary format that is not easily, if at all, imported into already developed (or under development) computer analysis programs. This means that already-developed algorithms cannot be tested on radiometric infrared image data sets from state-of-the-art infrared instrumentation.

When investigators have been allowed to access proprietary radiometric information, they have been able to develop image analysis software to analyze the infrared images. Using test infrared image data sets, they have developed algorithms for infrared medical applications. Head et al. [24]-[28] have been able to export the radiometric information from digitized infrared images of the breast and to perform image analysis on them. The analysis involved the dividing of each of the two semi-spherical breasts into four quadrants (Figure 3) and then deriving numerical parameters for the quadrants (mean temperature, median temperature, highest temperature, lowest temperature, etc.). They then compared the four quadrants from the two breasts looking for higher temperatures in a quadrant that would signal that the patient being screened for breast cancer was at increased risk of getting breast cancer or, if she has breast cancer, that she has a poorer prognosis. Anbar et al. [29] have developed dynamic area telethermometry (DAT), which is an image analysis system that integrates radiometric information from a series of infrared images. DAT has been applied to a variety of medical applications but seems to be most promising in the area of diagnosis of breast cancer.

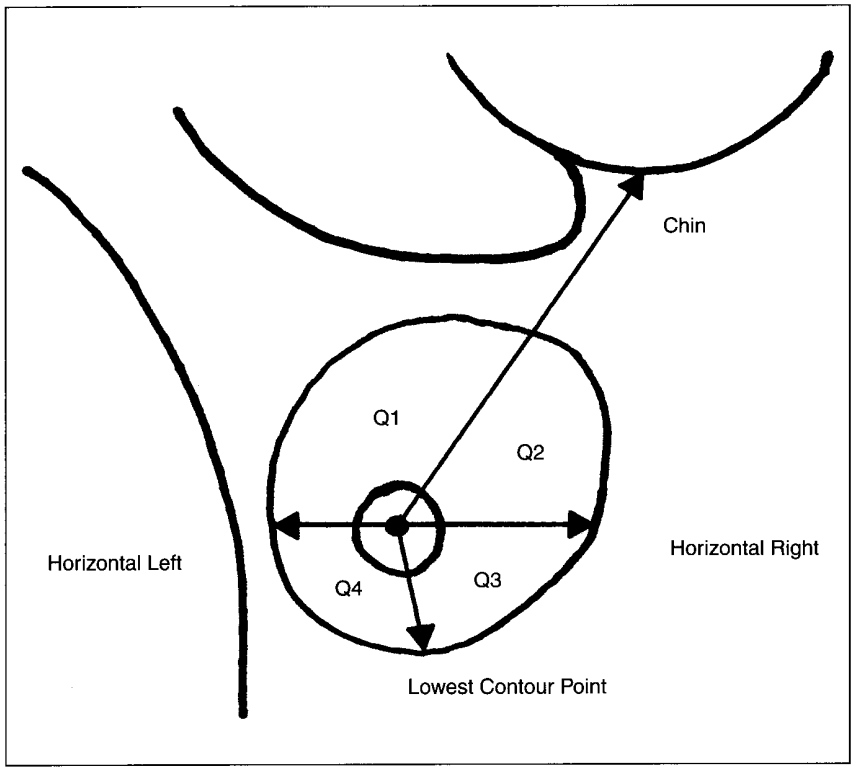

3. Quadrants used for analysis of breast temperatures.

The future of infrared imaging in medicine will be dependent on the ability of the engineering and medical research community to integrate infrared imaging instruments with computer-assisted image processing and then to create dedicated infrared imaging systems that will be applicable to specific applications in medicine. This will require the development of algorithms that can be tested in standard clinical trials to determine the efficacy of infrared imaging in any specific medical application.

Conclusions

Infrared imaging was introduced into medicine in the second half of the 20th century. Early studies using contact thermography (infrared imaging) and scanning thermography produced results that suggested there were applications of the technology in areas as diverse as detection of breast cancer and malfunctions of the nervous system. However, the early instrumentation was not sensitive enough to detect the subtle changes in temperature needed to accurately detect and monitor disease.

In recent years the military has greatly improved the sensitivity of infrared instruments so that it now approaches 0.025 °C, a level at which 0.50 °C to 1.00 °C differences or changes in temperature can now be reliably measured. The further development of focal plane staring array infrared sensors has allowed very high quality imaging as well as the export of digital temperature measurements amiable to computer-assisted image analysis and algorithm development.

The medical community has only recently acquired the new state-of-the-art focal plane staring array instrumentation and is now beginning to investigate the applications of this state-of-the-art instrumentation and computer-assisted image analysis to today's most difficult medical problems. These applications include breast cancer (risk assessment, detection, prognosis and therapeutic monitoring), burn trauma (staging), diabetes, vascular problems, and neurological problems. The future is here and promises to produce new algorithms for the use of infrared imaging in prevention, diagnosis, and treatment of many diseases.

Acknowledgments

Funding for this project was provided by The Breast Foundation, Baton Rouge, Louisiana, USA.

Jonathan F. Head is the director of research at the Mastology Research Institute of the Elliott-Hailey-Head Breast Cancer Research and Treatment Center, Baton Rouge, Louisiana. He obtained his B.S. in zoology from Syracuse University, an M.A. in biology from Brooklyn College of CUNY, and a Ph.D. in biology from Fordham University. He was with the Division of Cell Biology of the Naylor Dana Institute for Disease Prevention of The American Health Foundation, New York (1974-1978); the Department of Immunology at Cornell University Medical School, New York (1978); the Department of Pediatrics at Mt. Sinai Medical School, New York (1978-1987); and was the director/department head of tumor cell biology at The Center for Clinical Sciences, International Clinical Laboratories, Tennessee (1986-1988). In 1988, he moved to Baton Rouge, Louisiana, to become president of the Mastology Research Institute and is both the director of research and director of the clinical laboratory. He has appointments in the Department of Biochemistry at Tulane University School Medicine and the Departments of Biology and Physical Sciences at Delta State University.

Robert L. Elliott received his M.D. from the University of Mississippi School of Medicine in 1961. He did a residency in general and thoracic surgery from 1961 to 1967 at the University of Mississippi School of Medicine and did a traineeship in electron microscopy at Washington University during his residency. He was in private practice of general and thoracic surgery from 1967 to 1973 in Anniston, Alabama. In 1974, he moved to Baton Rouge, Louisiana, and founded the Elliott-Hailey-Head Breast Cancer Research and Treatment Center, which consists of the Breast Clinic and the Mastology Research Institute. He received his Ph.D. from LaSalle University in 1994. He limits his practice to the areas of prevention, early diagnosis, treatment, and research of diseases and cancer of the breast.

Address for Correspondence: Dr. Jonathan F. Head, Mastology Research Institute, 17050 Medical Center Drive, 4th Floor, Baton Rouge, LA USA 70816. Tel.: 1 225 755 3070; National Toll Free: 1 800 762 5313; Fax: 1 225 755 3085. E-mail: jhead @ehhbreastca.com.

References

[1] J.R. Keyserlingk, P.D. Ahlgren, E. Yu, N. Belliveau, and M. Yassa, "Functional infrared imaging of the breast," *IEEE Eng. Med. Biol. Mag.*, vol. 19, pp. 30-41, 2000.

[2] J.F. Head, C.A. Lipari, and R.L. Elliott, "Comparison of mammography and breast infrared imaging: Sensitivity, specificity, false negatives, false positives, positive predictive value and negative predictive value," in *Proc. 21st Ann. Int. Conf. IEEE Eng. Med. Biol. Soc.*, CDROM, 1999.

[3] M. Gautherie and C.M. Gros, "Breast thermography and cancer risk prediction," *Cancer,* vol. 45, pp. 51-56, 1990.

[4] A.M. Stark, "The value of risk factors in screening for breast cancer," *Eur. J. Cancer,* vol. 11, pp. 147-150, 1985.

[5] R.L. Elliott, J.F. Head, and D.K. Werneke, "Thermography in breast cancer: Comparison with patient survival, TNM classification and tissue ferritin concentration," in *Proc. Amer. Soc. Clin. Oncol.*, vol. 9, pp. 99, 1990.

[6] J.F. Head, U. Shah, M.C. Elliott, and R.L. Elliott, "Breast thermography and cancer patient survival," *Thermology,* vol. 3, pp. 277, 1991.

[7] J.F. Head, F. Wang, C.A. Lipari, and R.L. Elliott, "Breast cancer risk assessment with an advanced infrared imaging system," *Proc. Amer. Soc. Clin. Oncol.*, vol. 16, pp. 172, 1997.

[8] J.F. Head, C.A. Lipari, F. Wang, and R.L. Elliott, "Cancer risk assessment with a second generation infrared imaging system," *S.P.I.E. 3061*, pp. 300-307, 1997.

[9] R.L. Elliott, F. Wang, C.A. Lipari, and J.F. Head, "Application of second generation infrared imaging to breast cancer risk assessment," *Southeastern Surg. Conf.,* vol. 65, pp. 16, 1997.

[10] J.F. Head, F. Wang, C.A. Lipari, and R.L. Elliott, "The important role of infrared imaging in breast cancer: New technology improves applications in risk assessment, detection, diagnosis and prognosis," *IEEE Eng. Med. Biol. Mag.*, vol. 19, pp. 52-57, 2000.

[11] H.J. Isard, C.J. Sweitzer, and G.R. Edelstein, "Breast thermography: A prognostic indicator for breast cancer survival," *Cancer,* vol. 62, pp. 484-488, 1988.

[12] M. Gautherie, "Thermography of breast cancer: Measurement and analysis of *in vivo* temperature and blood flow," *Ann. N.Y. Acad. Sci.,* vol. 335, pp. 383-413, 1980.

[13] J.F. Head, F. Wang, and R.L. Elliott, "Breast thermography is a noninvasive prognostic procedure that predicts tumor growth rate in breast cancer patients," *Ann. New York Acad. Sci.,* vol. 698, pp. 153-158, 1993.

[14] D.G. Luther, J.E. Davidson, and J.F. Head, "Helmet mounted infrared imaging combat casualty system," *Adv. Tech. Applicat. Combat Casualty Care* CDROM, 1997.

[15] D. Luther, J. Davidson, R. Cromer, and J. Head, "A head mounted infrared imager for treating the wounded on the battlefield," in *Proc. 21st Ann. Int. Conf. IEEE Eng. Med. Biol. Soc.*, vol. 19, pp. 722-724, 1997.

[16] D.G. Luther, J.F. Head, J.E. Davidson, M. Grenn, A.G. Hargroder, and K. Hubble, "A head mounted thermal imaging system for the medic," *Adv. Tech. Applicat. Combat Casualty Care,* CDROM, 1998.

[17] R.P. Cole, S.G. Jones, and P.G. Shakespeare, "Thermographic assessment of hand burns," *Burns,* vol. 16, pp. 60-63, 1990.

[18] R.P. Cole, P.G. Shakespeare, H.G. Chissell, and S.G. Jones, "Thermographic assessment of burns using a nonpermeable membrane as wound covering," *Burns,* vol. 17, pp. 117-122, 1991.

[19] M.I. Liddington and P.G. Shakespeare, "Timing of the thermographic assessment of burns," *Burns,* vol. 22, pp. 26-28, 1996.

[20] A.G. Hargroder, J.E. Davidson, D.G. Luther, and J.F. Head, "Infrared imaging of burn wounds to determine burn depth," *S.P.I.E.* 3698, pp. 103-108, 1999.

[21] W. Li and J. Head, "Infrared imaging in the detection and evaluation of tumor angiogenesis," in *Proc. 22nd Ann. Int. Conf. IEEE Eng. Med. Biol. Soc.*, CDROM, 2000.

[22] W. Snyder, C. Wang, F. Wang, R. Elliott, and J. Head, "Improving the resolution of infrared images of the breast," in *Proc. 18th Ann. Int. Conf. IEEE Eng. Med. Biol. Soc.*, pp. 1058-1059, 1996.

[23] W.E. Snyder, H. Qi, R.L. Elliott, J.F. Head, and C.X. Wang, "Increasing the effective resolution of thermal images: An algorithm based on mean-field annealing that also removes noise and preserves image edges," *IEEE Eng. Med. Biol. Mag.*, vol. 19, pp. 63-70, 2000.

[24] J.F. Head, C.A. Lipari, F. Wang, J.E. Davidson, and R.L. Elliott, "Application of second generation infrared imaging and computerized image analysis to breast cancer risk assessment," in *Proc. 18th Ann. Int. Conf. IEEE Eng. Med. Biol. Soc.*, pp. 1019-1021, 1996.

[25] J. Head, C. Lipari, F. Wang, and R. Elliott, "Image analysis of digitized infrared images of the breasts from a first generation infrared imaging system," in *Proc. 19th Ann. Int. Conf. IEEE Eng. Med. Biol. Soc.*, pp. 681-684, 1997.

[26] C. Lipari and J. Head, "Advanced infrared image processing for breast cancer risk assessment," in *Proc. 19th Ann. Int. Conf. IEEE Eng. Med. Biol. Soc.*, pp. 673-676, 1997.

[27] J.F. Head, C.A. Lipari, and R.L. Elliott, "Computerized image analysis of digitized infrared images of the breasts from a scanning infrared imaging system," *S.P.I.E.* 3436, pp. 290-294, 1998.

[28] H. Qi, W.E. Synder, J.F. Head, and R.L. Elliott, "Detecting breast cancer from infrared images by asymmetry analysis," in *Proc. 22nd Ann. Int. Conf. IEEE Eng. Med. Biol. Soc.*, CDROM, 2000.

[29] M. Anbar, C. Brown, L. Milescu, J. Babalola, and L. Gentner, "The potential of dynamic area telethermometry in assessing breast cancer," *IEEE Eng. Med. Biol. Mag.*, vol. 19, pp. 58-62, 2000.

Detecting Breast Cancer from Infrared Images by Asymmetry Analysis

Hairong Qi[1], Wesley E. Snyder[2], Jonathan F. Head[3], Robert L. Elliott[3]

Abstract—**Infrared imaging of the breast (also called thermography) has shown effective results in both risk assessment and prognostic determination of breast cancer. This paper proposes an automated approach to detect asymmetric abnormalities in thermograms. Canny edge detector is first used to derive the edges from the original image. Hough transform is then applied to the edge image to recognize the four feature curves, which include the left and the right body boundary curves, and the two parabolic curves indicating the lower boundaries of the breasts. Segmentation is conducted based on the intersection of the two parabolic curves and the body boundaries. Bézier histogram is then derived from each segment. Curvature information is finally computed from the histogram to be used to easily indicate the asymmetry.**

Keywords— **asymmetry analysis, thermography, Hough transform, Bézier histogram, curvature analysis**

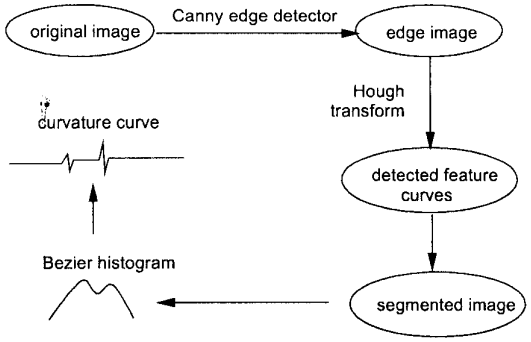

Fig. 1. Procedure of automatic asymmetry analysis of thermogram.

I. Introduction

MAKING comparisons between contralateral images are routinely done by radiologists. When the images are relatively symmetrical, small asymmetries may indicate a suspicious region. This is the underlying philosophy in the use of asymmetry analysis for mass detection [1].

There have been a few papers addressing techniques for asymmetry analysis of mammograms [1], [2], [3], [4], [5]. [6] also proposed an interesting approach which used computer-generated mammogram-like images to compare images from two viewing modalities. [7], [8] recently analyzed the asymmetric abnormalities in infrared images. In their approach, the thermograms are segmented first by operator. Then breast quadrants are derived automatically based on unique point of reference, i.e. the chin, the lowest, rightmost and leftmost points of the breast.

In this paper, we propose an automated asymmetry analysis technique on thermograms, which include automated segmentation and automated asymmetric abnormality detection. It involves 5 steps: (1) Edges are first detected by Canny edge detector. (2) Four feature curves in the edge image are distinguished: the left and right body boundary curves, and the two lower boundaries of the breasts. Hough transform is used to detect the parabolic shaped lower breast boundaries. (3) Segmentation is based on a line and an intersection. The line is formed by the two armpits which can be obtained by curvature analysis of the left and right body boundaries. The intersection is the point that intersects the two parabolic curves. (4) After segmentation, Bézier histogram is derived from each segment. (5) Curvature can then be computed from the two histograms which can easily indicate the asymmetric hot pattern if there are any.

Testing images are obtained using the Inframetrics 600M camera, with a thermal sensitivity of 0.05^0K.

[1]Electrical and Computer Engineering Department, University of Tennessee, Knoxville, TN 37996, USA, hqi@utk.edu

[2]Center for Advanced Computing and Communication, North Carolina State University, Raleigh, NC 27695, USA, wes@eos.ncsu.edu

[3]Elliott Mastology Center, Baton Rouge, LA 70806, USA, emcmri@iamerica.net

II. Approach

Figure 1 is a system guideline of the steps involved in the proposed approach: *edge image* obtained by Canny edge detector, *feature curves* detected by Hough transform, *segmentation* based on the feature curves, *Bézier histogram* derived from the segments, and *curvature curve* computed from the histograms.

A. Edge detection by Canny edge detector

Edge image is first derived by using Canny edge detector [9]. The standard deviation is chosen to be equal to 2.5 so that only strong edges can be detected.

B. Feature curve detection by Hough transform

There are four most important curves appeared in the edge image which we called the feature curves: the left and right body boundaries, and two lower boundaries of

0-7803-6468-6/00/$10.00 (c)2000 IEEE

the breasts. The body boundaries are easy to detect. Difficulties lie in the detection of the lower boundaries of the breasts. We observe that the breast boundaries are generally in parabolic shape. Therefore, Hough transform [10] is used to detect the parabola.

C. Segmentation

Segmentation is based on three key points: the two armpits (P_L, P_R) derived from the left and right body boundaries by picking up the point where the largest curvature occurs, and the intersection (O) of the two parabolic curves derived from the lower boundaries of the breasts. The line goes through point O and is perpendicular to line $P_L P_R$ is the line to separate the left and right breasts.

D. Bézier histogram of segments

Histogram provides us a view of brightness distribution. But pure histogram would not help us much in asymmetry analysis because the curve usually zig-zags a lot. To make it smoother, we use Bézier splines [11].

We have 256 rounded brightness levels, and the histogram values of these levels are used as the control-point positions: $\mathbf{p}_k = (x_k, y_k)$, with k and x_k varying from 0 to 255. These coordinate points are blended to produce the position vector $\mathbf{P}(u)$ (Eq. 1), which describes the path of an approximating Bézier polynomial function between $\mathbf{p}_0$ and $\mathbf{p}_{255}$.

$$\mathbf{P}(u) = \sum_{k=0}^{255} \mathbf{p}_k BEZ_{k,255}(u). \tag{1}$$

Here $0 \leq u \leq 1$. The Bézier blending functions $BEZ_{k,255}(u)$ are the Bernstein polynomials (Eq. 2):

$$BEZ_{k,255}(u) = C(255,k)u^k(1-u)^{n-k} \tag{2}$$

and the $C(255,k)$ are the binomial coefficients (Eq. 3):

$$C(255,k) = \frac{255!}{k!(255-k)!} \tag{3}$$

E. Curvature curve of Bézier histogram

The vector equation in Eq. 1 represents a set of two parametric equations for the individual curve coordinates, as shown in Eq. 4,

$$\begin{aligned} x(u) &= \textstyle\sum_{k=0}^{255} x_k BEZ_{k,255}(u) \\ y(u) &= \textstyle\sum_{k=0}^{255} y_k BEZ_{k,255}(u) \end{aligned} \tag{4}$$

Once the Bézier histogram is represented as the form of $x(u)$ and $y(u)$, local curvature (κ) can then be computed by Eq. 5,

$$\kappa = \frac{\dot{x}(u)\ddot{y}(u) - \dot{y}(u)\ddot{x}(u)}{(\dot{x}(u)^2 + \dot{y}(u)^2)^{3/2}} \tag{5}$$

where $\dot{x}(u)$ and $\dot{y}(u)$ represents the first derivatives, and $\ddot{x}(u)$ and $\ddot{y}(u)$ represents the second derivatives.

The two curvature curves from the two histograms are compared. A threshold is chosen based on testing images which can be used to decide if a difference is large enough to indicate the abnormality.

References

[1] W. F. Good, B. Zheng, Y. Chang, et al., "Generalized procrustean image deformation for subtraction of mammograms," in *Proceeding of SPIE Medical Imaging - Image Processing*, San Diego, CA, 1999, SPIE, vol. 3661, pp. 1562–1573.

[2] F. F. Yin, M. L. Giger, K. Doi, et al., "Computerized detection of masses in digital mammograms: analysis of bilateral subtraction images," *Med Phys*, vol. 18, pp. 955–963, 1991.

[3] F. F. Yin, M. L. Giger, C. J. Vyborny, et al., "Comparison of bilateral-subtraction and single-image processing techniques in the computerized detection of mammographic masses," *Invest Radiol*, vol. 6, pp. 473–481, 1993.

[4] F. F. Yin, M. L. Giger, K. Doi, et al., "Computerized detection of masses in digital mammograms: automated alignment of breast images and its effect on bilateral-subtraction technique," *Med Phys*, vol. 21, pp. 445–452, 1994.

[5] B. Zheng, Y. H. Chang, and D. Gur, "Computerized detection of masses from digitized mammograms: comparison of single-image segmentation and bilateral image subtraction," *Acad Radiol*, vol. 2, no. 12, pp. 1056–1061, Dec 1995.

[6] J. Hsu, D. M. Chelberg, C. F. Babbs, et al., "Preclinical roc studies of digital stereomammography," *IEEE Transactions on Medical Imaging*, vol. 14, no. 2, pp. 318–327, June 1995.

[7] C. A. Lipari and J. F. Head, "Advanced infrared image processing for breast cancer risk assessment," in *Proceedings for 19th International Conference of IEEE/EMBS*, Chicago, IL, Oct. 30 - Nov. 2 1997, IEEE, pp. 673–676.

[8] J. F. Head, C. A. Lipari, and R. L. Elliott, "Computerized image analysis of digitized infrared images of the breasts from a scanning infrared imaging system," in *Proceedings of the 1998 Conference on Infrared Technology and Applications XXIV, Part I*, San Diego, CA, 1998, SPIE, vol. 3436, pp. 290–294.

[9] J. Canny, "A computational approach to edge detection," *IEEE Trans. Pattern Anal. and Machine Intell.*, vol. 6, pp. 679–698, 1995.

[10] M. Z. Jafri and F. Deravi, "Efficient algorithm for the detection of parabolic curves," in *Vision Geometry III*. SPIE, 1994, vol. 2356, pp. 53–62.

[11] D. Hearn and M.P. Baker, *Computer Graphics, C Version*, Prentice Hall, 2nd edition, 1997.

World Congress 2000 Abstract - William W. Li, M.D. January 13, 2000

Infrared Imaging in the Detection and Evaluation of Tumor Angiogenesis

William W. Li, M.D.
Institute for Advanced Studies, MEDIRIM Program, the Angiogenesis Foundation, Cambridge, MA

Jonathan F. Head, Ph.D.
Mastology Research Institute, Baton Rouge, LA

It is now well-recognized that angiogenesis, the growth of new blood vessels, is a turn-key event for the growth, invasion and metastases of solid tumors. Over the past three decades, major cellular and molecular pathways of tumor angiogenesis have been elucidated. Clinical studies have further correlated disease severity and patient outcome (prognosis) with several histological and serum markers of angiogenesis for a wide variety of cancer types. More than forty antiangiogenic agents have been developed by the biopharmaceutical industry and are now in human clinical trials. Emerging from these efforts is a new requirement for imaging technologies for detecting, quantifying and evaluating the angiogenic process for the purposes of conducting basic research, preclinical studies and human clinical trials. Ultimately, such technologies will find primary clinical use in assessing the antiangiogenic treatment of cancer.

Infrared (IR) sensing is a highly-sensitive imaging modality with present-day applications in the aerospace and military sectors. Early IR medical applications (in the 1960s) were limited by: 1) lack of commercially-available, sufficiently sensitive sensors; 2) little to no knowledge of the molecular and physiological basis for diseases (such as cancer); and 3) the development of alternative imaging techniques (x-ray, ultrasound, computed tomography, magnetic resonance) which were globally adopted by radiologists. Recently, we have re-examined the potential for adapting high sensitivity IR imaging techniques to detect pathological features of disease (tumor angiogenesis), in order to fulfill an unmet scientific and

0-7803-6468-6/00/$10.00 (c)2000 IEEE

clinical need in cancer research and therapy. Data from early preclinical studies will be presented and discussed.

A significant body of clinical work, employing IR imaging for breast cancer risk assessment, detection and as a prognostic indicator, further supports the rational of investigating the application of IR imaging to tumor angiogenesis. Comparison of older scanning IR technology with state of the art focal plane staring array technology has demonstrated that focal plane technology has greater ability to image the vasculature of the breasts, and to demonstrate the vascular asymmetry that is associated with both an increased risk as well as presence of breast cancer, and poor prognosis. Data from clinical studies of breast cancer will be presented and discussed.

In summary, the infrared sensor is an a important new research tool for exploring the biological and clinical correlates of tumor angiogenesis. Advances can be made by integrating the current knowledge and efforts of specialists in the multiple disciplines of engineering, molecular and cellular biology, oncology, radiology, and biotechnology.